Integrated anaerobic digestion and UV photocatalytic treatment of industrial wastewater in fluidized bed reactors

Thesis submitted for the degree of Doctor of Philosophy in Chemical Engineering

Seth Otieno Apollo

Vaal University of Technology

Supervisor: Prof. Ochieng Aoyi

Co-Supervisor: Prof. Maurice S. Onyango

Dedication

To my lovely wife, Linda and loving daughter Angela

Declaration

I, Seth Otieno Apollo, declare that the material in this dissertation is my work, except where it is otherwise stated. This work has not been submitted to another university for any other degree.

Signed……

S.O Apollo

Student number: 211029696

Date: 28/03/2017

Place: Vanderbjilpark.

Acknowledgement

During my entire study, I needed much guidance and support. I thank God for the ability and patience He gave me during this time. I also humbly express my sincere gratitude to the following people for their support in the completion of this Thesis:

- My supervisors, Prof. Ochieng Aoyi and Prof. Maurice S. Onyango, for their expert advice and guidance, and helping me complete this work in time.
- Dr L. Shoko, Senior Laboratory Technologist in the Department of Chemical Engineering, for helping me with instrumentation and analysis.
- My colleagues, Mr J. Akach, Mr O. Benton and L. Koech for their assistance and encouragements.
- My family members for their support, prayers and encouragements

List of publications

1. Apollo, S., Onyango, M. S., and Ochieng, A., (2016). Modelling energy efficiency of an integrated anaerobic digestion and photodegradation of distillery effluent using response surface methodology. *Environmental Technology*, 37, (19) 2016.

2. Apollo, S. and Ochieng, A., (2016). Combined anaerobic digestion and photocatalytic treatment of distillery effluent in fluidized bed reactors focusing on energy conservation. *Environmental Technology*, 37 (17) 2243-2251.

3. Apollo, S., Akach, J., Ochieng, A., Synergistic effects between photodegradation and biodegradation. *The International Conference on Pure and Applied Chemistry*, Mauritius 18^{th} – 22^{nd} July 2016.

Abstract

Anaerobic digestion (AD) is usually applied in the treatment of distillery effluent due to the fact that it is effective in chemical oxygen demand (COD) reduction and bioenergy recovery. However, due to the presence of biorecalcitrant melanoidins present in distillery effluent, AD is ineffective in colour reduction. For this reason, ultraviolet (UV) photodegradation, which is effective in melanoidins' degradation, can be integrated with AD to achieve high efficiency in colour and COD reduction. However, the UV process is energy intensive, majorly due to the electricity requirement of the UV lamp. In contrast, the AD process has high potential of renewable energy production in the form of biomethane, which can be transformed into electrical energy and applied to supplement the energy requirement of the UV process. The aim of this study was to evaluate the efficiency of a combined AD-UV system in colour and COD reduction for the treatment of distillery effluent in fluidised bed reactors. The potential of the application of the bioenergy produced by the AD process to supplement the energy intensive UV process was evaluated and modelled using response surface methodology.

In the first place, the optimal hydrodynamic conditions of the fluidised bed reactors were determined using optical attenuation technique. The best homogeneity in the bioreactor, in which zeolite was used as microbial support, was found to be at a superficial liquid velocity of 0.6 cm/s while the best catalyst and gas hold up in the photoreactor were found to be 0.077 and 0.003, respectively. At these conditions, it was found that the initial biological step removed about 90% of COD and only about 50% of the colour while photodegradation post-treatment removed 98% of the remaining colour. Kinetic analysis of the bioreactor showed that ~ 9% of the feed total organic carbon (TOC) was non-biodegradable and this was attributed to the biorecalcitrant melanoidins. Photodegradation post-treatment mineralized the biorecalcitrant melanoidins via a reductive pathway as was indicated by the formation of NH_4^+ in large quantity compared to NO_3^-. Kinetic analysis further showed that the rate of substrate utilization in the bioreactor increased with an increase in organic loading rate and it was inversely proportional to the rate of photodegradation post-treatment. Modeling using response surface methodology (RSM) was applied to predict the effects of the operating parameters of the initial AD step on the performance of the photodegradation post-treatment process and the energy efficiency. Energy analysis of the integrated system showed that the AD process could produce 59 kWh/m^3 of electricity which could supplement the electricity demand of the UV lamp by 30% leading to operation cost reduction of about USD 4.8/m^3. This led to a presumed carbon dioxide emission reduction (CER) of 28.8 kg CO_2e/m^3.

Contents

Table of Figures

List of Tables

Symbols

A_c	Reactor cross sectional area (cm^2).
A_o	Initial absorbance.
A_t	Absorbance at time t.
A_T	Attenuation.
D_p	Particle diameter (mm).
E_{bio}	Bioenergy production (kWh/m^3).
E_{COD}	COD removal efficiency.
EL_{bio}	Electricity from bioenergy (kWh/m^3).
E_p	Power consumption of the pump (W).
E_{UV}	Energy consumption of UV lamp (kWh/m^3).
E_{AOP}	Energy consumption of advanced oxidation process (kWh/m^3)
H	Fluidised bed height.
I	Signal for particle free liquid.
I_o	Signal in a liquid with particles or bubbles.
K	Maximum substrate utilization rate (g sTOC/gVSSd).
K_d	Endogenous decay coefficient (d^{-1}).
K_s	Michaelis Constant (g sTOC/L).
L	Path length travelled by the signals (cm).
m	Particle mass (g)
n	Bed expansion index.
P	Power rating of UV lamp (kW).

Q	Feed flow rate (L/d).
Qc	Recycle flow rate (m^3/s).
r	Substrate utilization rate (g sTOC/gVSSd).
S	Feed concentration (g/L).
S_b	Concentration of biodegradable feed (g/L).
U_g	Superficial gas velocity (cm/s).
U_L	Superficial liquid velocity (cm/s).
U_t	Particle Terminal velocity (cm/s)
V	Reactor volume (L).
V_e	Volume of effluent (L).
V_w	Volume of Water (L).
X	Biomass concentration (g/L).
Y	Microbial growth yield.
Y_p	Methane yield coefficient (L/g).

Greek symbols

$\emptyset_s$	Volume fraction of solids.
ε_g	Gas Hold up.
ε_s	Solid hold up.
η	Methane production rate (L/d).
Θ	Mean cell residence time (d).
μ	Specific micro-organisms growth rate (d^{-1}).

μ_{max}	Maximum micro-organisms growth rate (d^{-1}).
ρ_p	Particle density (g/cm^3).
β	Energy ratio.
ω	Pump efficiency.

Abbreviations

AD:	Anaerobic digestion.
AFBR	Anaerobic fluidised bed reactor.
AOPs	Advanced oxidation processes.
ATDE	Anaerobically treated distillery effluent.
BOD_5	Five days biochemical oxygen demand.
CER	Carbon emission reduction.
COD	Chemical oxygen demand.
DF	Dilution factor.
EE/O	Electrical energy per order.
F:M	Feed to micro-organisms ratio.
FBP	Fluidised bed photoreactor.
FBR	Fluidised bed reactor.
GDM	Green development mechanism.
GEF	Grid emission factor.
HMW	High molecular weight.
HRT	Hydraulic retention time (d).
LCVFAs	Long chain volatile fatty acids.
LED	Light emitting diode.
LHV_{CH4}	Low heating value of methane (kWh/m^3).
LMW	Low molecule weight
MCRT	Mean cell residence time (d).

MR	Millard reaction.
MRPs	Millard reaction products
OAT	Optical attenuation technique.
OLR	Organic loading rate (kg/m^3d).
SRB	Sulphate reducing bacteria.
SS	Suspended solids.
sTOC	Soluble total organic carbon.
TOC	Total Organic carbon.
UV	Ultra-Violet
VFA	Volatile fatty acids.
VSS	Volatile suspended solids.

Chapter 1

1. Introduction

1.1 Background

Treatment of municipal or industrial wastewater has become a complex procedure due to the stringent environmental policies on waste discharge and the need to recycle water as a result of water scarcity. In particular, distillery industries are major environmental pollutants due to their large discharge volumes of wastewater which contain high amount of organic pollutants among others. The distillery effluent is characterised by high chemical oxygen demand (COD) which ranges between 80,000 mg/l and 120,000 mg/l and biochemical oxygen demand (BOD) in the range of 50,000 mg/l to 75,000 mg/l (Acharya et al., 2008). The effluent also contains melanoidins, which are biorecalcitrant organic compounds formed by Millard reaction between glucose and amino acids (Satyawali & Balakrishnan, 2008). Despite the fact that melanoidins form only about 2% of distillery effluent, they impart an intense dark brown colour to the effluent (Kalavathi et al., 2001). Anaerobic digestion (AD) has been widely considered as the most attractive first step treatment technique for the distillery effluent due to its reputation as a low cost and environmentally friendly technique, besides its biomethane generation potential (Oller et al., 2011). Moreover, AD treatment is preferred due to the fact that a great component of distillery effluent is biodegradable (Sankaran et al., 2014). The anaerobic digestion is reported to remove about 75-90% COD and 80-90% BOD (Satyawali & Balakrishnan, 2008). This means that anaerobically treated distillery effluent (ATDE) still contains some organic load and is not safe for discharge (Chaudhari et al., 2007). Moreover, the effluent still has a dark brown colour imparted by the biorecalcitrant melanoidins (Satyawali & Balakrishnan, 2008). In many instances, industries dilute the anaerobically treated distillery effluent by mixing with raw water before discharge in order to meet the set waste disposal standards. This dilution, even though accepted in some regions, is of great environmental concern as it does not reduce the absolute pollution load of the effluent (Chaudhari et al., 2007; Satyawali & Balakrishnan, 2008). Therefore, different post-treatment methods for biomethanated distillery effluent have been proposed for colour removal (Sankaran et al., 2014; Satyawali & Balakrishnan, 2008).

Coagulation technique using aluminium salts such as alum, sodium aluminate and aluminium chloride has been widely applied to reduce colour and COD in BMDW. However, recent studies have pointed out drawbacks, such as Alzheimer's disease, of using aluminium salts (Chaudhari et al., 2007). Moreover, alum reacts with the natural alkalinity of water leading to

a pH reduction (Prasad, 2009). Besides, other coagulants such as $FeCl_3$ perform better at very low pH and this may require neutralization of the treated effluent. Further, coagulation leads to high sludge generation which may require secondary treatment. Other methods such as wet oxidation and catalytic thermolysis have also been applied in the treatment of ATDE. However, high pressure and temperature employed during wet oxidation and catalytic thermolysis lead to high operational cost, which hinders the application of these processes (Chaudhari et al., 2007). Treatment by adsorption using cost effective adsorbents such as natural zeolites has huge potential for colour removal in ATDE (Onyango et al., 2011). However, adsorption is considered as a non-destructive technique since it merely transfers pollutants from liquid to solid surface and it also generates sludge (Al-Momani et al., 2002).

Recently, studies have established that advanced oxidation processes (AOPs) such as photodegradation are effective in the degradation of biorecalcitrant organic compounds (Vineetha et al., 2013). For this reason, AOPs can be combined with AD for the effective removal of both biodegradable and biorecalcitrant components of distillery effluent (Apollo et al., 2013). Among the AOPs, UV photodegradation has an advantage in that it can rapidly degrade organic contaminants to mineralization without producing sludge. Despite the fact that UV photodegradation is effective in mineralization of organic pollutants, the electrical consumption of the UV lamp makes this process costly for wastewater treatment. Oller et al. (2011) reported that electrical energy represents about 60% of the total cost of operating a UV photocatalytic reactor. In contrast, distillery effluent has a high renewable energy production potential (Yasar et al., 2015). This is evidenced by the fact that biomethane potential of distillery effluent is about 0.4 L CH_4/g COD with energy production potential of about 15.2 kJ/g COD (Zupancic et al., 2007). Consequently, the application of an integrated AD-UV photodegradation technique for distillery effluent treatment can lead to energy conservation if the bioenergy produced by the AD is used to supplement the energy demand of the UV photodegradation process.

To improve the performance of the integrated AD-UV process robust reactors such as fluidised bed reactors can be employed for both the processes. Application of fluidised bed reactors in a combined AD and photodegradation can result in better pollution removal due to the well mixing attained by fluidised bed reactors, which promotes mass transfer thereby increasing reaction rate (Andalib et al., 2012). Due to the achievable fast reaction rates, energy requirement by the UV photodegradation could be reduced while the bioenergy production by

the AD process could be enhanced. Incorporating the bioenergy produced in the AD-UV system could lead to the implementation of the green development mechanism (GDM). As a result, a reduction in greenhouse gases emission (GHG) could be realized compared to the case where electricity generated from fossil fuels was applied to power the UV lamp.

In this study, the efficiency of fluidised bed reactors in a combined anaerobic and photodegradation system was investigated for pollution removal and energy utilisation when treating distillery effluent. The kinetics of the integrated process was evaluated and the effect of organic loading rate and hydraulic retention time on system performance was analysed. The energy produced by the anaerobic process was compared to that required by the UV lamp in the photodegradation process. Lastly, modelling of the energy efficiency of the integrated system based on potential renewable energy application was carried out using response surface methodology.

1.2 Problem statement

Alcohol distilling industries produce huge amounts of wastewater with high organic load. Distillery industries produce about 10-15 L wastewater per litre of alcohol produced (Moraes et al., 2015). The wastewater is significantly biodegradable and often anaerobic digestion is applied to treat the wastewater with methane production potential of about 0.4 L CH_4/g COD resulting in energy production potential of 15.2 kJ/g COD. However, distillery effluent contains traces of biorecalcitrant melanoidins which cannot be removed by anaerobic digestion, as a result, anaerobically digested effluent still has a very dark brown colour imparted by the melanoidins. Usually various post-treatment techniques are employed to remove the colour and residual COD. Among them coagulation and adsorption have been widely studied due to their simplicity. However, they do not destroy the pollutants but transfer them from the wastewater to the adsorbent or coagulant resulting in enormous sludge production, which in turn requires appropriate handling techniques.

Due to the aforementioned shortcomings, AOPs have been proposed for post-anaerobic treatment of distillery effluent due to their ability to achieve total mineralization of the organic compounds leading to no or minimal sludge production. Of the AOPs, UV photodegradation is considered as a rapid technique for wastewater treatment. However, just like all other AOPs, this method is energy intensive and therefore costly. Electrical energy requirement of the UV lamp is singled out as the major expense of running a UV photodegradation process (Oller et al., 2011). For the post-treatment of anaerobically treated distillery effluent, perhaps the energy

production by the AD unit can supplement the energy requirement of the UV photodegradation, therefore making an integrated AD-UV photodegradation process cost effective. More significant in such a scenario is to determine the relationship between the AD and UV photodegradation dependent factors on energy production and energy utilization in the AD and UV process, respectively. Further, the development of a model correlating these factors with system performance can be of high significance for wastewater treatment engineering, for it can be applied for process optimization. Fluidised bed reactors (FBRs), which are considered as robust due to effective mixing, could be used to improve the performance of the integrated process. For high efficiency of FBR, an appropriate method such as optical attenuation technique should be employed to determine the best hydrodynamic conditions.

1.3 Main objective

The main objective was to determine the efficiency of an integrated anaerobic digestion and photocatalysis in the treatment of distillery wastewater applying anaerobic fluidised bed (AFBR) reactor and fluidised bed photoreactor (FBP).

Specific objectives

a) To determine the optimal hydrodynamic conditions of the fluidised bed bioreactor and photoreactor.
b) To apply kinetic modelling to define the best operating conditions of the anaerobic digestion process.
c) To evaluate the bioenergy production potential of the anaerobic digestion process and energy demand of the photodegradation.
d) To analyse the performance of the integrated anaerobic digestion-photodegradation process in colour, TOC, COD and sulphate reduction.
e) To determine carbon dioxide emission reduction potential of the integrated system based on renewable energy application.
f) To model the energy efficiency of the integrated system using response surface methodology.

1.4 Thesis Layout

Chapter one of the thesis gives background information on the integration of anaerobic digestion and photodegradation for distillery effluent treatment. In this Chapter, motivation for the study is outlined and the research objectives are set. Chapter two reviews literature on the new trends in the application of AD and photodegradation on wastewater treatment. Chapter

three covers experimental methods and data interpretation for hydrodynamic studies while Chapter four examines kinetics of anaerobic digestion in fluidised bed reactors. In Chapter five, batch studies on combined AD and UV photodegradation are presented while in Chapter six, a study on a continuous operation of the combined AD and photodegradation process is covered with focus on modelling the combined system using response surface methodology. Finally, Chapter seven concludes on the research findings.

References

ACHARYA, B.K., MOHANA, S. & MADAMWAR, D. (2008). Anaerobic treatment of distillery spent wash - a study on upflow anaerobic fixed film bioreactor. *Bioresour. Technol*. 99. p.4621–6.

AL-MOMANI, F., TOURAUD, E., DEGORCE-DUMAS, J., ROUSSY, J. & THOMAS, O. (2002). Biodegradability enhancement of textile dyes and textile wastewater by VUV photolysis. *J. Photochem. Photobiol. A Chem*. 153. p.191–197.

ANDALIB, M., HAFEZ, H., ELBESHBISHY, E., NAKHLA, G. & ZHU, J. (2012). Treatment of thin stillage in a high-rate anaerobic fluidized bed bioreactor (AFBR). *Bioresour. Technol*. 121. 411–8.

APOLLO, S., ONYANGO, M.S. & OCHIENG, A. (2013). An integrated anaerobic digestion and UV photocatalytic treatment of distillery wastewater. *J. Hazard. Mater*. 261. p.435–42.

CHAUDHARI, P.K., MISHRA, I.M. & CHAND, S. (2007). Decolourization and removal of chemical oxygen demand (COD) with energy recovery: Treatment of biodigester effluent of a molasses-based alcohol distillery using inorganic coagulants. Colloids Surfaces A. *Physicochem. Eng. Asp*. 296. p.238–247.

KALAVATHI, D., UMA, L. & SUBRAMANIAN, G. (2001). Degradation and metabolization of the pigment—melanoidin in distillery effluent by the marine cyanobacterium Oscillatoria boryana BDU 92181. *Enzyme Microb. Technol*. 29. p.246–251.

MORAES, B.S., ZAIAT, M. & BONOMI, A. (2015). Anaerobic digestion of vinasse from sugarcane ethanol production in Brazil: Challenges and perspectives. Renew. Sustain. *Energy Rev*. 44. p.888–903.

OLLER, I., MALATO, S. & SÁNCHEZ-PÉREZ, J.A. (2011). Combination of Advanced Oxidation Processes and biological treatments for wastewater decontamination--a review. *Sci. Total Environ*. 409. p.4141–66.

ONYANGO, M., KITTINYA, J., HADEBE, N., OJIJO, V. & OCHIENG, A. (2011). Sorption of melanoidin onto surfactant modified zeolite. *Chem. Ind. Chem. Eng. Q*. 17. p.385–395.

PRASAD, R.K. (2009). Color removal from distillery spent wash through coagulation using Moringa oleifera seeds: use of optimum response surface methodology. *J. Hazard. Mater*. 165. p.804–11.

SANKARAN, K., PREMALATHA, M., VIJAYASEKARAN, M. & SOMASUNDARAM, V.T. (2014). DEPHY project: Distillery wastewater treatment through anaerobic digestion and phycoremediation - A green industrial approach. Renew. Sustain. *Energy Rev.* 37.

p.634–643.

SATYAWALI, Y. & BALAKRISHNAN, M. (2008). Wastewater treatment in molasses-based alcohol distilleries for COD and color removal: a review. *J. Environ. Manage*. 86. p.481–97.

VINEETHA, M.N., MATHESWARAN, M. & SHEEBA, K.N. (2013). Photocatalytic colour and COD removal in the distillery effluent by solar radiation. *Sol. Energy.* 91. p.368–373.

YASAR, A., ALI, A., TABINDA, A.B. & TAHIR, A. (2015). Waste to energy analysis of shakarganj sugar mills; biogas production from the spent wash for electricity generation. *Renew. Sustain. Energy Rev*. 43. p.126–132.

ZUPANCIC, G.D., STRAZISCAR, M. & ROS, M. (2007). Treatment of brewery slurry in thermophilic anaerobic sequencing batch reactor. *Bioresour. Technol*. 98. p.2714–22.

Chapter 2

2 Literature review

2.1 Distillery effluent generation and characteristics

The major steps in ethanol production from cane molasses are feed preparation, fermentation, distillation and packaging. In the first place, molasses is diluted until the desired sucrose level is attained; it is then supplemented with various nutrients like ammonium sulphate before fermentation using active yeast culture. Sludge from the fermenter is discharged as waste and the supernatant is fed into the distillation column where it is distilled, fractionated and rectified (Satyawali & Balakrishnan, 2008). It is the residue of the fermented mash which comes out as distillery spent wash (Sankaran et al., 2014). Figure 2-1 shows the processes involved in alcohol production and waste generation.

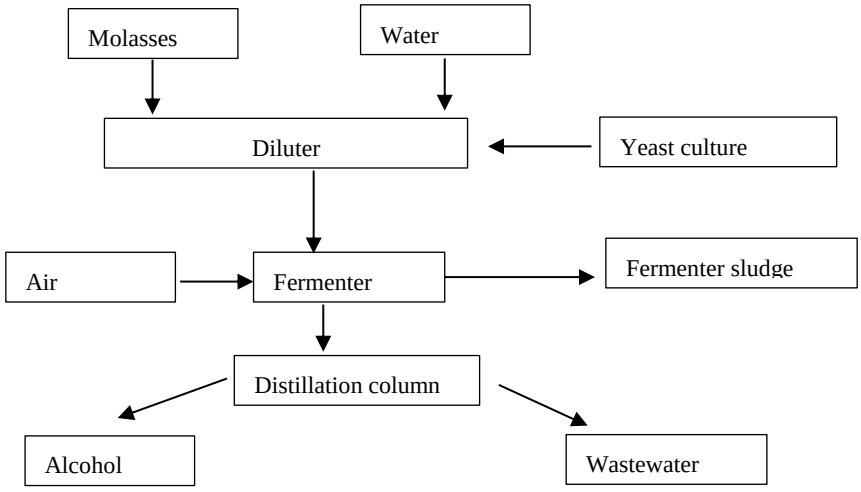

Figure 2-1: Operations in distillery plant and wastewater generation (Sankaran et al., 2014)

Process factors such as the quality of molasses used, unit operation procedures applied during the alcohol production process and process recovery of alcohol determine the pollution load of the distillery effluent (Satyawali & Balakrishnan, 2008). Sankaran et al. (2014) reported that for every litre of alcohol produced 10 - 15 litres of effluent is generated. Moreover, the increase in the demand for alcohol due to wide spread application of alcohol as fuel, in food and pharmaceuticals, has led to the rise in distillery industries resulting in a corresponding increase in wastewater discharge (Mohana et al., 2009). As shown in Table 2-1, the wastewater from distillery plant has a high organic load and dark brown colour.

Table 2-1: Characteristics of distillery effluent.

Parameter	(Sankaran et al., 2014)	(Siles et al., 2011)	(Satyawali & Balakrishnan, 2008)
Colour	Dark brown	-	Dark brown
Temperature (°C)	80-90	-	-
pH	4-4.6	3.75 -3.83	3.0 - 5.4
Conductivity (mS/cm)	26-31	-	-
Total suspended solids (TSS) (mg/l)	4,500-7,000	-	350
COD (mg/l)	85,000-110,000	68,560 -76,600	65,000 - 130,000
BOD (mg/l)	25,000-35,000	29,700 - 29,800	30,000 - 70,000
Volatile acids/Acidity (mg/l)	5,200-8,000	1,500 -1,600	-
Sulphate (mg/l)	13,100-13,800	-	2,000 - 6, 000
Total nitrogen (mg/l)	4,200-4,800	-	1,000 - 2,000
Chlorides (mg/l)	4,500-8,400	-	-
Phosphates (mg/l)	1,500-2,200	-	800 - 1,200
Phenols (mg/l)	3,000-4,000	450 - 460	-

Poorly treated distillery wastewater poses a serious threat to water quality in several regions around the world (Mohana et al., 2009). It has been observed that discharge of distillery effluent into water bodies interferes with the respiration in fish due to the presence of inorganic and organic salts in the effluent (Ramakritinan et al., 2005). These pollutants lead to coagulation in gill mucous of the fish, resulting in a decrease in dissolved oxygen consumption which causes asphyxiation (Mohana et al., 2009). In addition to that, the effect of uncontrolled disposal of distillery spent wash on land surface has also been studied and it was found that these wastes are equally harmful to vegetation. Fuess & Garcia (2014) reported that this waste inhibits seed germination since it alters soil alkalinity and reduces manganese availability to plants. Distillery effluent contains biorecalcitrant melanoidins which are responsible for its dark brown colour.

2.2 Melanoidins in distillery effluent

Distillery effluent has a characteristic dark brown colour imparted by melanoidins. Melanoidins are heterogeneous nitrogen containing organic compounds, with brown pigments, produced by Millard reaction (Wang et al., 2011). Discharge of wastewater containing melanoidins to water bodies is harmful as they block light penetration into aquatic systems thus hampering the growth of aquatic photosynthetic plants. This in turn leads to reduction in dissolved oxygen in such water bodies. Moreover, melanoidins are reported to have antioxidant properties that make them harmful to aquatic life (Sankaran et al., 2014).

Melanoidins are formed through a complex pathway which involves the reaction between reducing sugars and amino acids through Millard reaction (MR) during cane juice processing (Satyawali & Balakrishnan, 2008). The structure of melanoidin produced in the MR heavily depends on the specific reducing sugars and amino acids involved in the reaction and reaction conditions such as temperature, reaction time, pH and solvent used (Wang et al., 2011). The complex reactions leading to the formation of melanoidins during MR are cyclization, dehydration, retroadolization, rearrangement, isomerization and condensation of intermediates produced in the MR process (Wang et al., 2011). Due to the complexity of the products that are generated in the MR, it is not easy to elucidate melanoidins and determine their definite structure, therefore the definite structure of melanoidin is not well understood (Wang et al., 2011; Sankaran et al., 2014; Satyawali & Balakrishnan, 2008). Determining the structure of natural melanoidins is even more complicated by the fact that the elemental composition of melanoidin polymer depends on the type and molar concentrations of the parent reactants which are amino acids and reducing sugars (Chandra et al., 2008). In nature multiple amino acids and reducing sugars can simultaneously react in a given setup to produce melanoidin polymers with varying elemental composition.

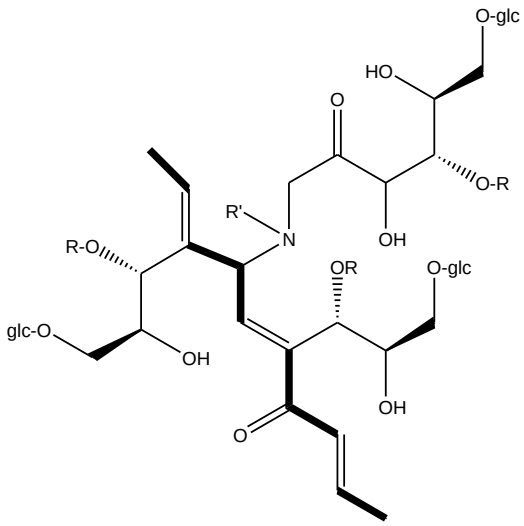

Figure 2-2: Structure of basic melanoidin formed from 3-deoxyhexosuloses and amadori reaction products (Sankaran et al., 2014)

However, researchers have suggested the basic melanoidin structure (Figure 2-2) which is produced by reacting model reducing sugars with model amino acids under specific reaction conditions (Sankaran et al., 2014). Still, this does not give any reliable information on

melanoidins formed in industrial processes as it is not easy to simulate the natural reaction conditions, and there exist multiple precursors in industrial processes which possibly are simultaneously involved in the Millard reaction.

Researchers are in agreement that functional groups of melanoidins can vary widely due to variation in reaction conditions and type of carbohydrate (sugars) or amino acids present in particular melanoidin (Sankaran et al., 2014; Wang et al., 2011). The melanoidins in distillery effluent are generated during high temperature processing of cane juice. Under this condition reducing sugars and amino acids present in cane juice react to form melanoidins. Proposed reactions leading to the formation of melanoidin is shown in Figure 2-3.

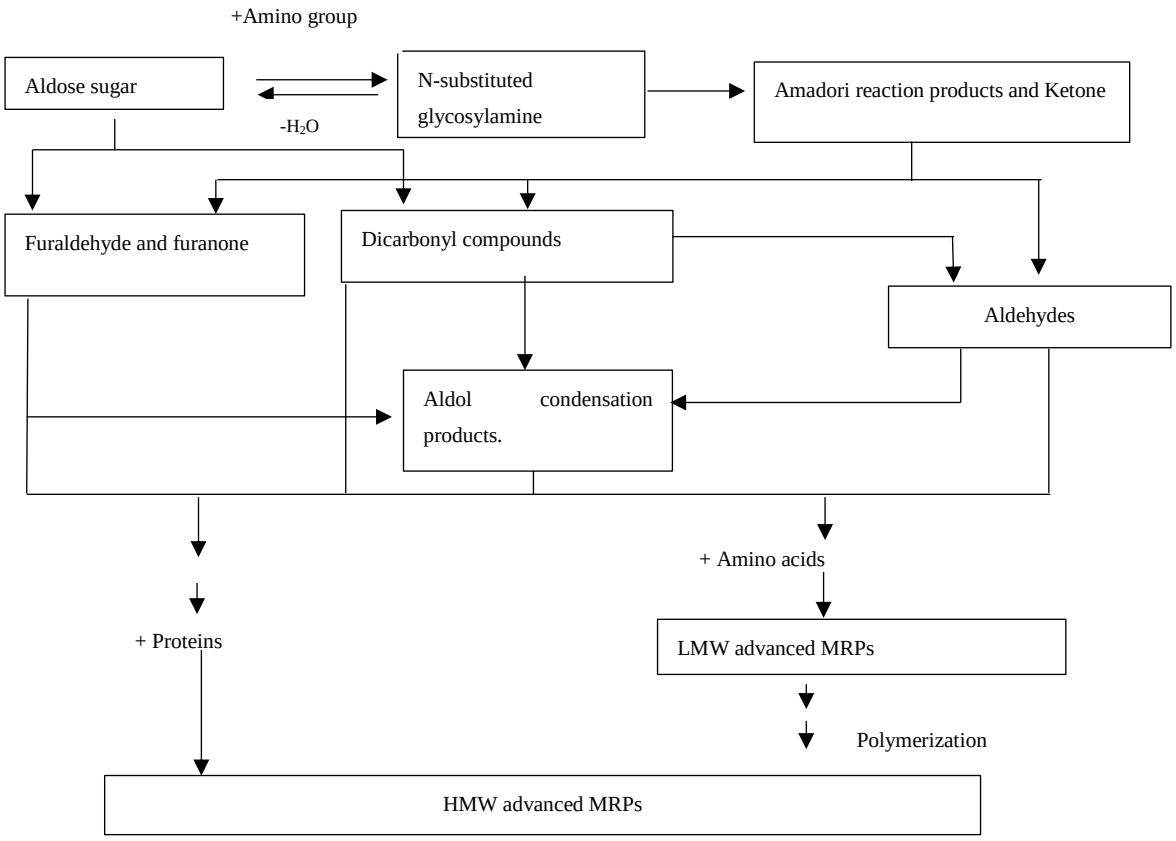

Figure 2-3: Formation of advance low molecular weight (LMW) and high molecular weight Millard reaction products (MRPs) from the Millard reaction (Wang et al., 2011).

Melanoidins have antioxidant property (Wang et al., 2011); due to this, they are not degraded by biological treatment (AD) of distillery effluent. Even though melanoidin imparts a dark brown colour to the distillery effluent, it is reported to constitute only about 2% of distillery effluent (Kalavathi et al., 2001). The remaining proportion of distillery effluent is fairly biodegradable (Sankaran et al., 2014). As a result, distillery effluent is a viable source of

renewable energy source if anaerobically digested (Satyawali & Balakrishnan, 2008). Therefore, anaerobic digestion is the most preferred method for the treatment of distillery effluent (Sankaran et al., 2014; Satyawali & Balakrishnan, 2008; Yasar et al., 2015)

2.3 Anaerobic digestion

Anaerobic digestion is widely applied in the treatment of industrial effluent with biodegradable organic content. This is due to its numerous advantages such as ability to operate at high organic loading rates at low retention time, low sludge production, high nutrient removal and production of biogas which is a renewable energy source (Yasar & Tabinda, 2010). The dual advantage of reducing pollution load while producing biogas has made anaerobic digestion (AD) to be of research interest. Moreover, the application of biogas, which is a renewable energy source, helps in conserving the depleting natural energy sources and mitigating the environmental problems such as global warming. In some industries, the biogas produced by anaerobic digestion has been used to supplement the energy requirement of the plant (Sankaran et al., 2014). However, one major challenge of AD is that it is complex as it occurs in a unique environment in which consortia of bacteria break down complex organic compounds to methane and carbon dioxide. For successful AD treatment of industrial wastewater, the anaerobic process and condition under which different bacterial groups operate optimally must be understood.

2.3.1 Anaerobic digestion process

A set of sequential complex metabolic processes occur during AD. The AD process involves three major distinct and interdependent groups of bacteria operating within a self-regulating fermentation process. These bacterial groups are acidogenic bacteria, acetogenic bacteria and methanogenic bacteria. The participation of different classes of bacteria existing in the anaerobic digester is shown in Figure 2-4. Acidogenic bacteria convert products of hydrolysis of complex organic matter into volatile fatty acids (VFAs), alcohols, ketones, carbon dioxide and hydrogen. Acetogens convert long chain VFAs (LCVFAs), alcohol and ketones into acetate, H_2 and CO_2. Methanogens then convert acetate, H_2 and CO_2 into methane and CO_2 via two pathways. In the first pathway, acetoclastic methanogens convert acetates into methane and carbon dioxide while in the second pathway hydrogentrophic methanogens convert H_2 and CO_2 into methane. About 70% of methane is produced via the acetate route (Yasar & Tabinda, 2010). If sulphate is present in wastewater, then sulphate reducing bacteria (SRB) will also be involved in the process as they will be responsible for the reduction of sulphates to sulphides,

dissolved in effluent as $HS^-/S^{-2}/H_2S$ or to H_2S in biogas (O'Flay et al., 2006; Acharya et al., 2008).

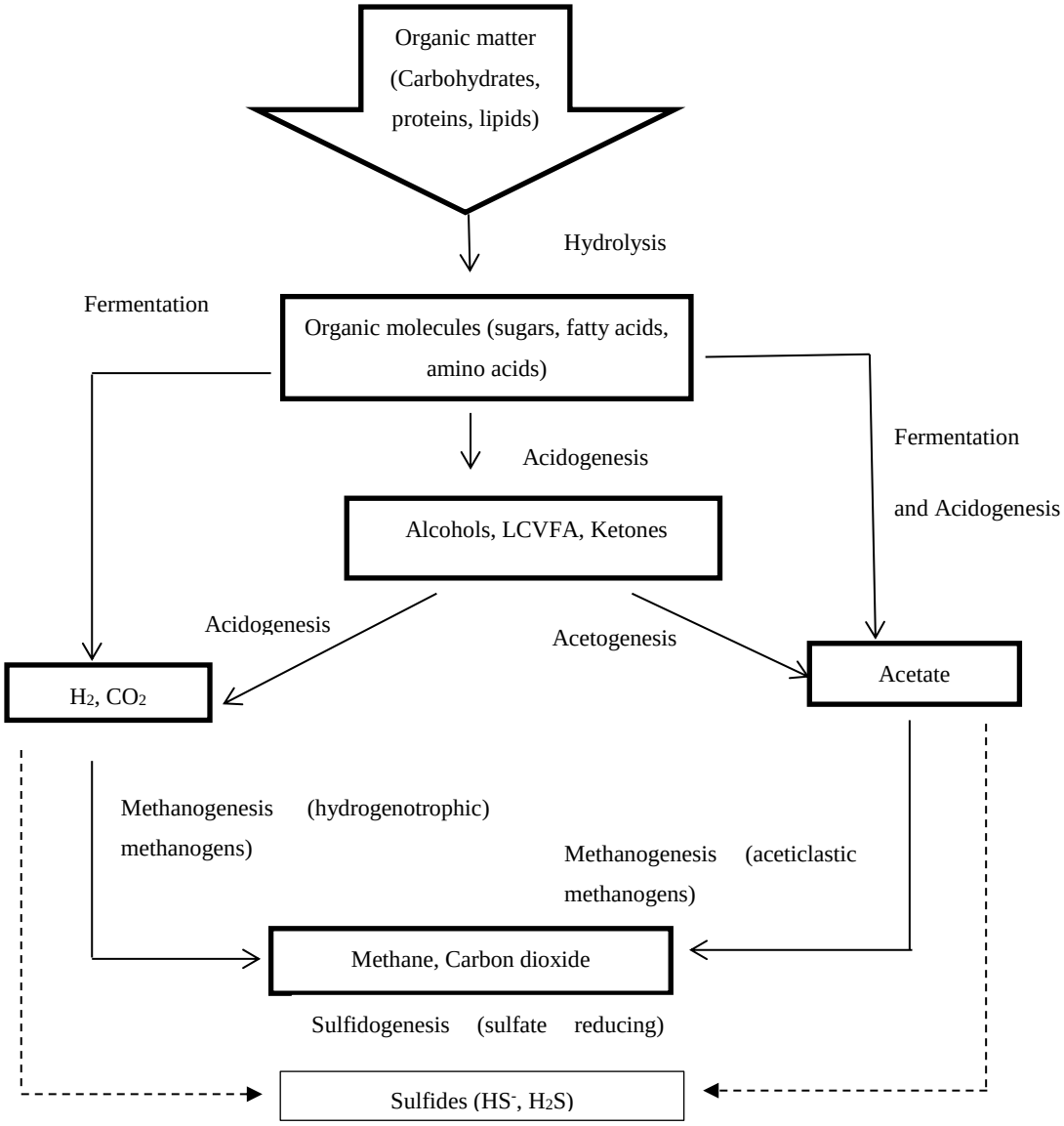

Figure 2-4: Metabolic steps involved in the complete anaerobic degradation of organic matter to methane and carbon dioxide, adopted with modification from (Aiyuk et al., 2006; Moraes et al., 2015).

2.3.2 Stability of anaerobic process

Quite often, anaerobic digesters fail due to imbalances in the reactor. The major causes of imbalances are organic overloading, presence of biorecalcitrant substrates, fluctuations in pH and temperature and microbial washout. The pH fluctuation is an indication of the inability of the system to buffer itself. This means that the rate of VFAs production is not matched by the

rate at which they are consumed (Acharya et al., 2008). In the anaerobic digestion, acidogenesis and acetogenesis reactions are acidifying while methanogenesis is alkalizing (Acharya et al., 2008). For a stable operation, there should be a state of equilibrium between the acidifying and alkalizing reactions in the digester. In a case where the stability is not achieved more acids will be generated leading to pH reduction of the system and eventually resulting in a digester failure. This is due to the fact that acidogenesis reactions are more thermodynamically favourable than methanogenesis (Table 2-2). Subsequently, the acidogens have the highest growth rates due to the fact that they have the highest substrate uptake rate compared to methanogens (Moraes et al., 2015).

Table 2-2: Some of the basic reactions during anaerobic process and their Gibbs free energies.

Step	**Reaction**	**Δ G^o (kJ/reaction)**
Acidogenesis	$C_6H_{12}O_6 + 2H_2O \rightarrow 2CH_3COO^- + 2CO_2 + 2H^+ + 4H_2$	-206
	$C_6H_{12}O_6 + 2H_2 \rightarrow 2CH_3CH_2COO^- + 2H_2O + 2H^+$	-358
	$C_6H_{12}O_6 \rightarrow CH_3CH_2CH_2COO^- + 2CO_2 + H^+ + 2H_2$	-255
Acetogenesis	$CH_3CH_2COO^- + 3H_2O \rightarrow CH_3COO^- + HCO_3^- + H^+ + 3H_2$	+76.1
	$CH_3CH_2COO^- + 2HCO_3^- \rightarrow CH_3COO^- + H^+ + 3HCOO^-$	+72.2
	$CH_3CH_2COO^- + 2H_2O \rightarrow 2CH_3COO^- + H^+ + 2H_2$	+48.1
Methanogenesis	$CH_3COO^- + H_2O \rightarrow CH_4 + HCO_3^- + H_2$	-31.0
	$H_2 + 1/4HCO_3^- + 1/4H^+ \rightarrow 1/4CH_4 + 3/4H_2O$	-33.9
	$HCOO^- + 1/4H_2O + 1/4H^+ \rightarrow 1/4CH_4 + 3/4HCO_3^-$	-32.6

Acidogenesis can only be a limiting step in an AD system if the substrate to be degraded is not easy to hydrolyse (Moraes et al., 2015). Contrary to the acidogenesis, acetogenesis is thermodynamically unfavourable in standard conditions as indicated by the difference in Gibbs free energy in Table 2-2. However, the possibility of acetogenesis reactions occurring in an AD system depends on the interaction between the acidogenesis and methanogenesis. Acetogenesis occurs favourably if the products of the acidogenesis are maintained at low concentration. This is achieved when methanogenesis consumes the products of acidogenesis and this ensures that the complex self-regulating process in the digester is stable. There are various factors that affect the stability of an anaerobic digester.

2.3.3 Factors affecting anaerobic digestion

For anaerobic digestion to occur successfully, it is significant for a favourable environmental condition to be maintained in the reactor. The various environmental conditions which heavily affect anaerobic digestion process are: temperature, pH/alkalinity, mixing, organic loading rate hydraulic retention time and availability of nutrients.

Temperature

Anaerobic digestion is reported to be more effective in two different temperature ranges, namely, mesophilic and thermophilic conditions (Yasar & Tabinda, 2010). The optimal temperature for mesophilic conditions is about 37 ^{o}C while for thermophilic it is about 55 ^{o}C. The variation in optimal temperature in the AD system is due to the existence of many classes of bacteria that have different responses to temperature (Moraes et al., 2015). Failure to maintain temperature within the optimal range may affect the balance between production of intermediates and their consumption leading to inhibition or reduction in digester efficiency (Moraes et al., 2015).

pH/Alkalinity

Anaerobic digestion is pH sensitive and the favourable pH condition is reported to be between 6.0 and 8.0, with optimum value at 7.0 (Acharya et al., 2008; Yasar & Tabinda, 2010). Acidogenesis and acetogenesis are acidifying steps as they produce acids and hydrogen while the methanogenesis is an alkalizing step as it consumes hydrogen and H_3O^+ ions (Acharya et al., 2008). Further, hydrolysis of proteins that releases ammonia and salts of weak acids is also an alkalizing step (Moraes et al., 2015). In a stable condition the balance between the acidifying and alkalizing steps maintains the pH within the required range. However, depending on the characteristics of the wastewater being treated, alkalizing agents can be added in small amounts to improve the buffering capacity of the system. Mild alkalizing agents such as $NaHCO_3$ or $Ca(HCO_3)_2$ are more recommended than strong agents such as NaOH and KOH.

Even though monitoring of pH is necessary, it is also necessary to monitor alkalinity alongside pH. Monitoring of alkalinity is more efficient than that of pH. This is due to the fact that pH is expressed in logarithmic scale while alkalinity is expressed in linear scale. It implies that a slight decrease in pH may result in consumption of a large amount of alkalinity leading to substantial reduction in buffering capacity (Moraes et al., 2015).

Availability of nutrients

For faster reactor start up and reactor stability, the nutrients for biodegradation which are majorly carbon (C), nitrogen (N) and phosphorus, must be in a specific optimum ratio. An optimum ratio which exists in literature varies considerably. A COD:N:P ratio of 300:5:1or 350:7:1 has been reported for a rapid and efficient start up and reactor stability (Aiyuk et al., 2006; Farhadian et al., 2007). A C:N:P ratio of 400:5:1 and 100:28:6 has also been reported and it was also reported that a COD:SO_4 ratio of less than 10:1 causes H_2S inhibition, odour, corrosion and deteriorated biogas quantity and quality (Aiyuk et al., 2006).

Organic loading rate and hydraulic retention time

Organic loading rate (OLR) is the amount of organics which is fed into the reactor per given period of time; it is expressed as mass of organic per volume of digester per day (kg/L.d). The performance of anaerobic digesters depends on OLR applied and there exists an OLR value at which the performance is optimum. At OLR above the optimum, the reactor experiences organic overloading which is indicated by accumulation of volatile fatty acids (Borja et al., 2004). This in turn leads to reduction in pH and high consumption of alkalinity in the reactor. Organic loading rate is related to hydraulic retention (HRT) as:

$$OLR = \frac{Q.S}{V} = \frac{S}{HRT} \quad (1)$$

where Q is the feed flow rate (m^3/day), S is the feed COD (kg/m^3) and V is the digester volume (m^3).

A digester which is capable of achieving high efficiency at short HRT is economical as high volumes of wastewater can be treated within a short period. Moreover, robust anaerobic digesters such as fluidised bed and up-flow anaerobic sludge blanket reactors have been devised and they are able to reduce HRT from conventional ~30 days to a few days or hours (Singh & Prerna, 2009).

Mixing

The performance of anaerobic digestion, just like any other biochemical reaction, depends on the degree of mixing. Proper mixing ensures efficient contact between the microbes and the substrate and it prevents local accumulation of VFAs in various parts of the reactor. However, a very high mixing speed can create shear stress which may interfere with bacterial colonies. Mixing in a reactor can be achieved by an installed stirrer or by recirculation of the effluent. In the case of recirculation, the velocity of the fluid needs to be regulated and it should be high

enough to provide good contact between biomass and substrate as well as being able to disturb the gas trapped on the biomass to facilitate separation of gas bubbles from biomass surface (Yasar & Tabinda, 2010). Different types of reactor configurations achieve mixing in various ways and thus vary in performance.

2.4 Reactor configuration

The type of reactor employed in an AD system influences the overall efficiency of the treatment process. The two major distinguishing aspects in efficiency of reactor types is the ability to achieve a desired degree of mixing and ability to retain microbial colonies in the reactor (Singh & Prerna, 2009; Melidis et al., 2003). These two qualities will determine the OLR, HRT and gas production potential of a given reactor type. Initially, AD treatment of industrial effluent was carried out in suspended growth systems such as covered lagoons, complete mix digesters and plug flow digesters. These digesters were not efficient as they operated under long HRT ranging from 30 to 45 days due to microbial wash out (Singh & Prerna, 2009). This was due to the fact that in these reactors the microbes were floating or suspended in liquid and a fraction of these actively growing microbes was always continuously discharged with the effluent.

The efficiency of the AD process has been greatly improved by applying reactors containing microbial carrier materials. In these reactors, the carrier materials are colonized by the microbial mass thus the microbial population in the reactor is always maintained by avoiding wash out. The microbial carrier can either be an inert material or granular sludge formed by dead biomass. The reactors with carrier material can further be classified as fixed bed anaerobic reactor, up-flow anaerobic sludge blanket reactor (UASB) and fluidised bed reactor (FBR). In fixed bed reactors, the packed bed does not move and the microbes colonise the stationary bed. This reactor type can withstand high organic loading without experiencing shock due to its ability to retain large amounts of microbial mass. The fixed bed also acts like a filter which removes suspended solids from the treated effluent, therefore installing a clarifier after the AD unit may not be necessary. However, since the bed is stationary, poor mixing is achieved and VFAs may accumulate in some parts of the reactor leading to relatively lower efficiency. Also bed clogging is very common in fixed bed reactors therefore high energy is required to pump the effluent across the bed. Furthermore, the working volume of a fixed bed reactor is small as a large part is occupied by the stationary bed of packed material.

In the UASB reactor, granular sludge is allowed to grow and mixing is achieved by upward flow of recycled effluent thereby achieving good mixing. This reactor type is more efficient

than fixed bed but it is relatively complex to construct and operate. Anaerobic fluidised bed reactor shares in the good attributes of fixed bed reactor and UASB. This is due to the fact that the bed is made up of inert biomass carrier material, like in fixed bed, however fluidization, which results in mixing, is achieved by recirculating the effluent through the bed like in the case of UASB. The mixing enables the bed to expand and therefore very little biomass carrier material is used unlike in fixed bed reactors. The advantage of FBR over UASB is that the granulation process in the UASB during start up takes a long time and needs special conditions, unlike in FBR in which there is inert material for microbial colonization. Due to this advantage, this work will focus on fluidised bed reactor. The performance of various packed reactors is shown in Table 2-3.

Table 2-3: Performance of different packed anaerobic digesters treating distillery effluent.

Reactor type	HRT (d)	OLR (kg COD/m^3d	COD removal %	Reference
UASB	2.1	5.5 – 20	70-90	
	2	6.1 - 18	>90	
	2.2	5.1 - 10.1	90	(Melamane et al., 2007)
Fluidised bed reactor				
Perlite	0.19 - 2	35	84	(Sowmeyan & Swaminathan, 2008)
Perlite	0.35	17	75-95	(Garcia-Calderon et al., 1998)
Zeolite	0.45	3.0 - 20.0	>80	(Andalib et al., 2012)
Zeolite	0.45	3.0 - 20.0	>80	(Fernández et al., 2008)
Fixed bed reactors				
Charcoal	10 - 30	6.2 - 18.6	80	(Acharya et al., 2008)
Coconut coir	8 - 30	6.2-23.3	80	
Nylon fibre	20 - 30	6.2-9.3	60	
Zeolite (batch)	25	5.7 g/l	75	(Apollo et al., 2013)

2.5 Fluidised bed reactor

A wide application of fluidized bed reactors in biochemical processes such as enzyme production, fermentation and bioconversions have been reported due to its high efficiency. The major advantages of fluidised bed bioreactors are as follows. In the first place, due to the fact that the FBR can operate at high biomass concentration, there is a high mass transfer area. This, coupled with efficient mixing capacity, results in high conversion. Subsequently, much smaller reactor volumes are required than in suspended growth systems such as covered lagoons, plug flow reactors and continuously stirred tank reactors. Secondly, the use of FBR leads to low sludge generation due to biomass retention by the support materials leading to reduction in sludge management cost. Finally, fluidization is able to solve the operating problems like bed clogging and high pressure drop associated with fixed bed reactors (Andalib et al., 2012). The type of carrier material used in an FBR affects its efficiency in biogas production and waste removal.

2.5.1 Carrier Material

Various types of materials have been used as support for microbial growth in several fluidised bed reactors in biological processes. The major properties which affect fluidisation of microbial support materials are particle density, size, shape and total mass in the FBR. Apart from low density, another desirable quality for a carrier material is high total surface area to mass ratio which enables high microbial attachment. Materials used in FBR treating wastewater can be classified as those with density higher than that of water and those with density lower than that of water (Papirio et al., 2013). Some of the widely used materials with density higher than that of water are porous glass beads, zeolites, granular activated carbon, sand and celite particles, among others. The applied materials with density lower than that of water are majorly polymers such as polyethylene, polypropylene and polystyrene and other materials such as perlite and cork (García-Calderón et al., 1998; Papirio et al., 2013). The higher density materials are applied in up-flow fluidization while those of low density are applied in down-flow fluidization processes. Both of these materials have been applied with varied biomass attachment capacities reported (Papirio et al., 2013).

A study on the suitability of spherical glass beads as biomass carrier material in FBR has been reported (Nagpal et al., 2000). The particles were found to be very suitable due to their porosity and roughness which increased their surface area for biomass attachment. The surface of the particles had pores of 10-30 µm in diameter and 5 µm deep. The availability of pores on biomass carrier is an advantage in that they do not only increase the surface area but also

provide shelter for the micro-organisms. This protects the micro-organism colonies on carrier surface from fluid shear forces and attrition between particles during fluidisation (Voice et al., 1992).

The biofilm thickness which was observed when sand was used as biomass carrier material in an FBR was exceedingly high. It was 200 µm compared to the reported optimum value of 100 µm (Papirio et al., 2013). The exceedingly high biofilm thickness is not favourable for the biochemical process as it hinders mass transfer to the microbes beneath the thick layer. Consequently, thick biofilm leads to starvation of the underlying microbes leading to their death. The excessive biomass thickness on the carrier material can be reduced or controlled by increasing superficial fluid velocity, which leads to an increase in liquid shear force which subsequently dislodges the excess biofilm (Papirio et al., 2013). Table 2-4 summarises application of various support materials in FBR in biochemical wastewater treatment processes.

Table 2-4: Application of various carrier materials in FBR.

Carrier	Size (mm)	Superficial velocity (m/min)	Application	Reference
Granular activated and non-activated carbon	0.75	0.29 - 0.61	Treatment of volatile aromatic hydrocarbons	(Voice et al., 1992)
Sand particles	0.86	0.28 - 0.93	Denitrification	(Papirio et al., 2013)
Polyethylene spheres	3.6	0.14 - 0.22	Hydrodynamic study	(Garcia-Calderon et al., 1998b)
Polyethylene	10	0.02 – 0.48	Biological wastewater treatment	(Ochieng et al., 2003)
Glass beads	0.255	0.1 - 0.48	Hydrodynamic study	(Doroodchi et al., 2012)
Perlite particles	0.968	0.033	Anaerobic digestion of wine distillery wastewater	(Garcia-Calderon et al., 1998b)
Spherical granular silica particles	0.175	0.09	Anaerobic digestion of dairy wastewater	(Arnaiz et al., 2003)
Zeolite particles	0.4 - 0.6	0.852	Anaerobic digestion of thin stillage	(Andalib et al., 2012)
Zeolite particles	0.7 – 2.2	1.5 – 1.8	Hydrodynamic and sorption studies	(Jovanovic et al., 2014)
Polyvinyl chloride particles	2	0.5 – 1	Anaerobic digestion of wastewater	(Jaafari et al., 2014)

Generally, a good carrier material in the FBR should have a large surface area and should integrate its ability to accommodate high microbial density with its ability to attract the pollutants to its surface through adsorption so that there is intimacy between the feed and the attached microbes (Montalvo et al., 2012). Zeolites have been widely considered as biomass

support material due to the fact that they are naturally occurring, they have good adsorption capacity and have the ability to hold high microbial density (Fernández et al., 2008).

2.5.2 Zeolite as a suitable biomass carrier material

The surface area of zeolite is reported to be in the region of 24.9-26.5 m^2/g (Montalvo et al., 2012; Andalib et al., 2012), with adsorption capacity of about 23.3 mg/g (Jovanovic et al., 2014) and ion exchange capacity of 2 meq/g (Montalvo et al., 2012). These properties lead to high performance when zeolite is used as biomass carrier in anaerobic wastewater treatment. In the first place, the high surface area makes zeolites to hold high microbial population density while the adsorptive property helps bring the substrate in close proximity to the microbial colonies on the zeolite surface (Fernández et al., 2008). Moreover, the good ion exchange capacity enables zeolite to simultaneously remove cations in wastewater during AD treatment. Typically, zeolite is very effective in the removal of ammonium produced during anaerobic digestion of nitrogen rich organic compounds thus reducing the inhibitory effect of high ammonium concentration (Montalvo et al., 2012; Tada et al., 2005).

Colonization of zeolite particles by micro-organisms in anaerobic digester has been confirmed using scanning electron microscopy (SEM) and single strand conformation polymorphism (SSCP) analysis based on amplification of bacterial and archaeal 16s rRNA fragments (Weiß et al., 2011). The studies revealed that distinct species of the micro-organisms involved in the AD process preferred zeolite surface, probably due to a favourable environment for microbial growth. Colonization of zeolite was found to be more favoured by methanogens. Methanogens are considered to be a more delicate class of microbes than acidogens and due to their sensitivity to pH, organic load and VFAs their inactivity leads to digester failure and very low methane production. Therefore, application of zeolite in the biodigester has massive advantages as it ensures that methanogen population is maintained in the reactor. Methanogens were found to colonize zeolite surface in the order: *Methanococcaceae* > *Methanosarcina* > *Methanosaeta* (Montalvo et al., 2012). It was further observed that the application of zeolite in the digester doubled the specific methane productivity rate compared to a case where zeolite was not used (Montalvo et al., 2012). This further showed the significance of zeolite in maintaining the methanogens' population.

2.5.3 Hydrodynamic properties of zeolite in fluidised bed reactor (FBR)

The efficiency of an FBR depends on the hydrodynamic conditions of the reactor which is affected by physical properties of the fluidised particles. Fluidization of particles in an FBR occurs as the superficial liquid velocity is increased from minimum fluidization velocity to terminal velocity of the particles (Loranger et al., 2010). At a superficial velocity above the particle terminal velocity, transportation of the particles which leads to entrainment occurs (Galvin & Nguyentranlam, 2002). The optimal superficial velocity depends on the particle's density, size, shape, amount and the reactor design. The amount of particles and their size should be appropriately selected since large particle size and large amounts of particles require high fluidisation velocity that increases the operating cost. The effect of zeolite particle size and amount on minimum fluidization velocity and bed expansion characteristics, which is an indication of homogeneity, is shown in Table 2-5.

Table 2-5: Hydrodynamic characteristics of zeolite particles.

Zeolite size (mm)	Reactor size (L)	[Static bed height]/[Reactor height]	*n* value	U_{mf} (cm/min)	U_t (cm/min)	Reference
0.7	0.08	0.3	0.3	13.8	792	(Jovanovic et al., 2014)
2.2	0.08	0.4	0.3	336	336	(Jovanovic et al., 2014)
0.25 - 0.315	0.6	0.35	8.6			(Inglezakis et al., 2010)
0.315 - 0.5	0.6	0.35	11.3			(Inglezakis et al., 2010)
0.9	16	0.1	3.7	19.2		(Gallant et al., 2011)

The values were calculated from experimental data using the expression (Jovanovic et al., 2014):

$$U_L = U_t(1 - \emptyset_s)^n \quad (2)$$

where U_L (cm/s) is the superficial liquid velocity, U_t is the terminal velocity of the particles (cm/s) and *n* is the bed expansion index. The volume fraction of solids ($\emptyset_s$) at any bed height is calculated as:

$$\emptyset_s = \frac{m}{\rho_p A_c H} \quad (3)$$

where m is the mass (g) of the particles in the reactor, ρ_p is the density of the particles (g/cm^3), A_c is the cross sectional area of the reactor (cm^2) and H is the fluidised bed height (cm) at any U_L. The bed expansion index and the terminal velocity can be determined from a linear

regression of the plot of log (U_L) against log (1- $\emptyset_s$) from equation (2) as explained in various studies (Gallant et al., 2011; Jovanovic et al., 2014).

2.5.4 Performance of zeolite in FBR

Various studies have been conducted in FBR to evaluate the performance of zeolite in wastewater treatment under various hydrodynamic conditions. A study on the effects of bed expansion and particle size (D_p) was carried out (Fernández et al., 2008). The D_p studied was 0.2-0.5 mm and 0.5-0.8 mm while bed expansion was 20% and 40% at varying OLRs. The bed expansion was found to have a slight effect on COD removal efficiency while it had a significant effect on methane production rate. A slightly higher methane production was obtained at bed expansion of 40% than that of 20%. This was due to improved contact between micro-organisms on the carriers and substrate at bed expansion of 40%. However, both the bed expansion and D_p did not have any effect on reactor stability. The large zeolite particles had slightly higher COD reduction (<5%) compared to the smaller particles while methane production was almost similar for the two particle size ranges studied. Even though larger particles achieved about 5% more COD reduction than the smaller particles, it is costly to fluidize larger particles. However, taking the advantage of the improved biogas production, Andalib et al. (2012) used the biogas to supplement liquid in fluidisation, thereby reducing the operation cost.

Fernández et al. (2007) found that the biomass attached on zeolite (D_p = 0.25-5mm and 0.5-0.8 mm) in an FBR treating distillery wastewater was in the range of 40-45 gVS/L. The predominant colonies on zeolite were determined using fluorescent in situ hybridization (FISH) and they were found to be majorly methanogens of species *Methanosaeta* and *Methanosarcinaceae* while there was a reduction in sulphate reducing bacteria. The methane yield coefficient was found to be 0.29 L CH_4/g COD removed while COD reduction was 90% at OLR of up to 20 gCOD/m^3d. Almost a similar observation was reported by Montalvo et al. (2008) when treating winery wastewater using zeolite in FBR. The attached biomass concentration was found to be 40-46 gVS/L after 90 days of digestion with a COD reduction efficiency of 86%. The improved biogas production due to the application of zeolite is very significant considering the fact that biogas from anaerobic digestion of organic wastes has become an attractive source of renewable energy. This is due to the depletion of fossil fuels and the environmental concern associated with the application of energy from fossil fuels.

2.6 Energy potential of anaerobic digestion of distillery effluent

Research on replacement of fossil fuels by biofuels has intensified of late. Various economic sectors are encouraged to use renewable energy sources due to the fact that they are sustainable. This has triggered a growth in the exploitation of the renewable energy sources in most parts of the world (Moraes et al., 2015). Biogas production from various wastes and its conversion into energy has been reported in various parts of the world. Currently, Europe has recorded an increase of 18.4% in electricity production from biogas, which corresponds to actual electricity production of 35.9 tWh (Moraes et al., 2015).

Taping biogas produced from anaerobic digestion of distillery spent wash for energy generation is a growing trend in major parts of the world (Moraes et al., 2015; Yasar et al., 2015). The main form of energy recovery is through co-generation, which involves simultaneous electricity and heat generation. Heat generated from biogas can be applied in the anaerobic digestion plant for maintaining digester temperature or can be used to generate steam in boilers in the distillery plant (Sankaran et al., 2014). The heat can also be used to dry sludge while the electricity can be used in the plant (Moraes et al., 2015; Yasar et al., 2015).

Various studies have been conducted to evaluate the energy production potential of biomethanation plant treating distillery effluent. Recently, Yasar et al. (2015) conducted a study to evaluate the potential of a biomethanation plant treating distillery effluent in Shakarganj in Pakistan. In their work, a cleaned biogas was used to operate an engine of 8 MW installed capacity to generate electricity. Consequently, the exhaust gases from the engine, with temperatures of about 500-550 ^{o}C, was used to produce steam in boilers. The study found that the biogas plant could generate electricity and heat sufficient for its operation. The spent wash treated had COD of 24-32 g/l with an average spent wash volume of 1394 m^3/d which produced 55760 m^3/d of biogas, resulting in the production of 103 MWh of power and 77 t of steam per day. The variation in venasse volume, power generated and steam production of one year during the study period is shown in Table 2-6. High spent wash volume was recorded between the months of January and April since sugar cane is a seasonal crop with high production reported in these months.

Moraes et al. (2014) estimated that the biogas produced from distillery effluent treatment can generate approximately 7 MW of energy per season, if the methane content of biogas produced is 60%. Elsewhere, a case study of energy production from a biogas plant treating spent wash in Bordeaux, France is reported (Moraes et al., 2015). In a season, it received average effluent

volume of about 550000 m^3 with organic load of about 22 kg COD/m^3 and its biogas produced energy of about 20000 MWh. The energy was converted into heat and electricity of about 8000 MWh and 3300 MWh annually, respectively. Despite high energy production and good organic load removal of the anaerobic digestion of distillery effluent, the process is faced with some challenges.

Table 2-6: A comparison of monthly production of energy from spent wash (Yasar et al., 2015).

Month	Distillery units	Spent wash (m^3/d)	Biogas production (m^3/d)	Power generation (MWh)	Steam production (Ton/d)
Oct	2	946	37840	2102	53
Nov	2	946	37840	2102	53
Dec	3	1435.5	57420	3190	80
Jan	4	1980	79200	4400	110
Feb	4	1980	79200	4400	110
March	4	1980	79200	4400	110
April	4	1980	79200	4400	110
May	3	1435.5	57420	3190	80
Jun	3	1435.5	57420	3190	80
Jul	2	946	37840	2102	53
Aug	2	946	37840	2102	53
Sept	2	946	37840	2102	53
Average/day		**1394**	**55760**	**103**	**77**

2.7 Challenges of AD treatment of distillery effluent.

Application of robust anaerobic reactors such as FBR has been reported to result in high COD reduction and improved biogas production efficiency. However, due to the presence of the biorecalcitrant melanoidins, which forms about 2% of the effluent (Kalavathi et al., 2001), the biomethanated effluent still has an intense dark brown colour and residual COD. The characteristic of raw and anaerobically digested distillery effluent is shown in Table 2-7. Thus,

even though, anaerobic digestion is applied as major technology for distillery effluent treatment, it cannot be applied as single technology (Satyawali and Balakrishnan, 2008). For this reason, various treatment techniques are usually applied as post-treatment to the AD to further remove the biorecalcitrant compounds. Various methods which have been applied in the post-treatment of anaerobically treated distillery effluent (ATDE) include coagulation-flocculation, adsorption, membrane filtration and advanced oxidation process.

Table 2-7: Comparison of the characteristics of raw distillery effluent and anaerobically treated distillery effluent.

	Raw distillery effluent	**Anaerobically digested effluent**	
Parameter	(Sankaran et al., 2014)	(Sankaran et al., 2014)	(Chaudhari et al., 2007)
Colour	Dark brown	Dark brown	Blackish brown
Temperature ^{o}C	80 - 90	35 - 40	-
pH	4 - 4.6	7.5 - 8	8
Conductivity (mS/cm)	26 - 31	31 - 36	-
Total suspended solids (TSS) (mg/l)	4,500 – 7,000	-	-
COD (mg/l)	85,000 - 110,000	25,000 - 40,000	38,750
BOD (mg/l)	25,000 - 35,000	7,000 - 10,000	7,200
Volatile acids (mg/l as acetic acid)	5,200 - 8,000	-	-
Sulphate (mg/l)	13,100 - 13,800	4,000 - 4,500	-
Total nitrogen (mg/l)	4,200 - 4,800	350 - 400	-
Chlorides (mg/l)	4,500 - 8,400	8,400 - 8,600	3,000
Phosphates (mg/l)	1,500 - 2,200	400	38
Phenols (mg/l)	3,000 - 4,000	-	-

2.8 Post-treatment of anaerobically treated distillery effluent (ATDE)

2.8.1 Anaerobic digestion and coagulation/flocculation

Coagulation and flocculation (CF) using aluminium salts such as alum, sodium aluminate and aluminium chloride has been widely applied to reduce colour and COD in anaerobically treated distillery effluent (ATDE). These salts are able to rapidly destabilize the negatively charged melanoidins in wastewater and enhance their removal by sedimentation or flotation. Colour removal of up to > 95% has been reported when the conventional coagulant was applied in treating diluted ATDE (Satyawali & Balakrishnan, 2008). The CF, however, needs to be applied to wastewater with low pollution load as a high pollution load leads to high coagulant dosage which increases the operation cost (Fuess & Garcia, 2014). Moreover, concentrated effluent leads to the generation of a high volume of sludge which may be difficult to handle.

Concerns have been raised about the safety of some of the chemicals used for coagulation; recent studies have pointed out that application of aluminium salts can cause Alzheimer's disease (Chaudhari et al., 2007). In addition to that, alum reacts with the natural alkalinity of water leading to a pH reduction. Besides, other coagulants such as $FeCl_3$ perform better at very low pH and this may require neutralization of the treated effluent (Chaudhari et al., 2007). Alternative to using the inorganic salts, natural coagulants like seeds of *Moringa oleifera* can be used but their application on large scale has not been adequately explored. Prasad (2009) studied optimization of distillery effluent treatment using *Moringa oleifera* and found the highest colour removal efficiency of 64%.

2.8.2 Anaerobic digestion and adsorption

Treatment by adsorption has huge potential for ATDE. Decolourization of ATDE by adsorption on commercial activated packed bed reactors was found to achieve almost complete decolourization. However, the high cost of commercial activated carbon prohibits its application (Satyawali & Balakrishnan, 2008). In order to reduce dependency on activated carbon as a sole adsorbent, researchers have developed low cost adsorbents by modifying some natural materials such as zeolites (Onyango et al., 2011), bagasse (Mane et al., 2006), pyorchar (activated carbon prepared form paper mill sludge) and other plant materials (Satyawali & Balakrishnan, 2008). *A*pplication of modified bagasse on ATDE resulted in 50% colour reduction after 4 h contact time when treating 100 ml of diluted effluent (Mane et al., 2006), while colour removal of up to 98% with pyorchar was obtained (Satyawali & Balakrishnan, 2008). A study was carried out to compare the dosage of commercial activated carbon and pyorchar required in removing colour to similar levels and it was found that a higher dosage was required for pyorchar than for commercial activated carbon (Satyawali & Balakrishnan, 2008). Similarly, 30 g/l of modified bagasse could remove 58% colour while 20 g/l commercial activated carbon could remove 81% of the colour (Satyawali & Balakrishnan, 2008). Therefore, as much as adsorbents from modified natural materials are more cost effective than commercial activated carbon, they generate more sludge which is costly to handle. Generally, high sludge generation, when adsorption is applied in treating effluent with high pollution load like ATDE, still remains its major challenge.

2.8.3 Anaerobic digestion and membrane filtration

Membrane filtration and reverse osmosis (RO) has also been widely applied in the treatment of ATDE. An RO treated effluent has a high quality and in some instances can be recycled for molasses dilution in the distillery industry (Satyawali & Balakrishnan, 2008). To improve the

quality of the RO treated effluent to ensure its recycling, the RO effluent is diluted with fresh water in a 50% v/v basis before recycling to the industry. Recently Nano Filtration (NF) has been introduced for post-treatment of anaerobically digested distillery effluent. The NF process is reported to remove all the colour besides attaining 95% removal of colloidal particles. However, RO and NF are costly as they operate at pressures of 30-50 bars (Satyawali & Balakrishnan, 2008). Moreover, frequent membrane clogging calls for regular maintenance which increases operation cost. An energy analysis based on the energy consumed to provide the necessary pressure and that produced by the AD process in relation to attainable effluent quality, needs to be studied. This can give an insight into the actual cost of running the membrane process.

2.8.4 Anaerobic digestion and aerobic digestion

As a post-treatment aerobic digestion has been widely applied in the treatment of ATDE, and it led to a significant reduction in COD which remained after the anaerobic process. The colour removal by conventional aerobic post-treatment is however, very low (Satyawali & Balakrishnan, 2008). To achieve high colour reduction, specific classes of micro-organisms such as fungi or bacteria with the ability to remove colour have been isolated and applied (Fuess & Garcia, 2014). The specific micro-organisms are able to remove the colour up to above 90%. However, high sludge generation coupled with a high demand for aeration limits the application of aerobic digestion as post-treatment technique. It is reported that sludge generation of aerobic digestion is about 0.55 kg COD microbial biomass/kg feed COD (Fuess & Garcia, 2014). The high sludge generation rate leads to high sludge handling cost which makes the whole treatment process to be costly. The electricity demand for aeration can reach up to 2 kWh/kg COD while anaerobic digestion produces about 2.6-2.8 kWh/kg COD (Fuess & Garcia, 2014; Cheng et al., 2012). Performance of various methods integrated with the anaerobic process in treating distillery effluent is shown in Table 2-8. Recently, studies on the application of advanced oxidation processes (AOPs) for post-treatment of ATDE have been carried out. This is due to the fact that these technologies are considered to be rapid and are able to mineralize the pollutants.

Table 2-8: Performance of anaerobic digestion integrated with various technologies in treating distillery effluent

Combined Technology	Efficiency		Reference
	COD removal %	Colour removal, %	
AD+Coagulation/Flocculation	65	98.4	(Zayas et al., 2007)
	80	88	(Ryan et al., 2008)
	89	98	(Fuess and Garcia, 2014)
Anaerobic digestion+aerobic digestion			
	66	60	(Ghosh et al., 2002)
	88	80	(Tondee et al., 2008)
Anaerobic digestion+UV photodegaradation	85.4	88	(Apollo et al., 2013)
UV photodegradation + Anaerobic digestion	70	79	(Apollo et al., 2013)
Ozonation + electrocoagulation	83	100	(Asaithambi et al., 2012)
Ozonation + anaerobic digestion + ozonation	79	100	(Sangave et al., 2007)

2.9 Advanced oxidation processes for post-treatment of ATDE

Application of AOPs in post-treatment of anaerobically digested wastewater has been widely considered on laboratory scale (Yasar et al., 2006; Apollo et al., 2013). Common AOPs are UV irradiation, O_3, H_2O_2, UV/H_2O_2/, UV/TiO_2 and photophenton (UV/H_2O_2/Fe^{2+}). The AOPs operate by generating highly reactive hydroxyl radicals in solution which attack and break down the organic molecules. The AOPs have become popular due to the fact that they are rapid and can mineralize the organic contaminant with little or no sludge generation. Some AOPs involving UV radiation or ozone also have the combined effect of organic removal and water disinfection (Rizzo, 2011). The fact that AOPs are rapid means that they require less space than that of slower processes like biodegradation. The efficiency of various AOPs such as UV, O_3, H_2O_2, UV/H_2O_2 and UV/H_2O_2/Fe^{2+} was tested in post-treatment of effluent from a biological UASB reactor treating mixed industrial wastewater, and the order of efficiency was found to be UV/H_2O_2/Fe^{2+} > O3 > UV/H_2O_2 > UV (Yasar et al., 2006).

Despite photo Fenton showing the best efficiency, it operates best at extreme pH conditions. Ozonation was found to depend on temperature; at high temperatures there is compromise between high mass transfer (particle collision) and low solubility. Just like photo Fenton,

ozonation attains high efficiency at elevated pH (Yasar & Tabinda, 2010). In some studies, ozonation was reported to enhance biodegradability of most wastewaters including that of distillery effluent (Siles et al., 2011; Robles-González et al., 2012). However, according to Yasar et al. (2007), application of ozone in post-treatment leads to consumption of less energy than if applied in pre-treatment. This could be as a result of the indiscriminative nature of ozone in pre-treatment where it degrades both recalcitrant and biodegradable constituents leading to high energy consumption, unlike if used in post-treatment when most biodegradable constituents have been eliminated.

Apollo et al. (2014) compared various AOPs in the treatment of molasses wastewater, and the performance was in the following order: $TiO_2/H_2O_2/UV > TiO_2/UV < UV/H_2O_2/ > UV$. In another study treatment (Apollo et al., 2013), no increase in biodegradability was observed when UV phocatalytic degradation was used as pre-treatment for distillery effluent. However, the application of UV phocatalytic degradation in post-treatment was more efficient in colour reduction than when applied in pre-treatment. Evaluation of the performance of AOPs based on pollution removal alone may not be very accurate as the AOPs are energy intensive. Therefore, energy efficiency of AOPs needs to be considered when calculating their efficiency.

2.10 Electrical energy requirement for AOPs

The electrical energy efficiency for the AOPs process is analysed using electrical energy per order (E_{AOP}). The E_{AOP} is defined as the electrical energy (kWh) required to degrade a contaminant by one order of magnitude in 1.0 m^3 water (Shu et al., 2013). The EE/O is calculated as:

$$E_{AOP} = \frac{P\,t}{V \log(\frac{C_i}{C_f})} \ (kWhm^{-3}order^{-1}) \qquad (4)$$

where P is the power (kW), t is the irradiation time (hrs), V is the volume (m^3) of water treated, C_i and C_f are the initial and final concentrations of the target contaminant. The energy calculation for AOPs involving UV irradiation is based on the power consumption of the UV lamp while for ozonation the power consumption of the ozone generator is considered (Yasar & Tabinda, 2010). A study on the comparison of electrical energy consumption of some AOPs treating mixed industrial wastewater after anaerobic digestion has been reported and results shown in Table 2-9 (Yasar et al., 2006).

Table 2-9: Table comparison of electrical energy requirement of different AOPs in colour and COD reduction (Yasar et al., 2006)**.**

	Colour		COD	
Process	EE/O	Removal,%	EE/O	Removal,%
Ozone	8	96	12.5	89
UV	160	79	295	57
UV/H_2O_2	86	91	120	82
$UV/H_2O_2/Fe^{2+}$	6	100	11.8	97

Energy consumption for AOPs treating molasses wastewater in conical flasks by Apollo et al. (2014b) was calculated and found to be in the order: $TiO_2/H_2O_2/UV > TiO_2/UV < UV/H_2O_2 >$ UV. The use of photocatalyst (TiO_2) irradiated with UV led to remarkable reduction in energy consumption compared to cases where photocatalyst was not applied (i.e UV/H_2O_2 and UV). This is due to high photoactivity of TiO_2 and its ability to generate high amounts of hydroxyl radicles that rapidly degrade the organic contaminants. Therefore, photocatalytic degradation is considered as an appropriate AOP technology in this work.

2.11 Photocatalytic degradation.

Photocatalytic degradation is an advanced wastewater treatment technique that is employed to destroy highly toxic and biorecalcitrant compounds such as aromatic chlorophenols and dyes in wastewater stream. Photacatalytic degradation involves the use of a semi-conductor (photocatalyst) in the presence of a light source to degrade such complex hydrocarbon compounds into simpler organic compounds. The semi-conductors that can be used as photocatalyst are TiO_2, WO, FeTiO and SrTiO. Compared to other semiconductors, TiO_2 has been used extensively due to its high photocatalytic activity, non-toxicity, low cost and chemical as well as thermal stability (Huang et al., 2008), while sunlight or UV irradiation have been used as the source of light.

2.12 Application of photocatalysis in wastewater treatment

Industrial wastewater can be characterized by very high and recalcitrant COD. However, photocatalysis can be suitably used for the treatment of industrial effluent with relatively low COD (< 5, 000 mg/l), since high COD values will require the consumption of large amounts of costly reactants and energy required to power the UV source (Andreozzi et al., 1999). This therefore limits the application of photocatalysis to either low strength wastewater or for removal of targeted biorecalcitrant components of otherwise high strength effluent. In this

context, photocatalysis is suitable for removing the biorecalcitrant components of effluent after primary biological treatment or it can be applied to improve the biodegradability of the biorecalcitrant components before the final biological treatment step is applied. Due to this, photocatalysis can therefore be applied in wastewater treatment in order to improve the quality of biological wastewater treatment plant effluent by removing residual xenobiotics in order to decrease final toxicity and make final wastewater reusable (Rizzo, 2011). Also, it can be used to disinfect biologically treated wastewater to be reused. In this case, it is used as an alternative to conventional chemical disinfectants such as chlorine, chlorine dioxide and ozone.

2.12.1 Challenges of photocatalytic wastewater treatment

Photodegradation performs well in mineralization of toxic and recalcitrant organic compounds which cannot be easily biodegraded, however, it is faced with some challenges. In the first place, the major challenge of this process is high energy requirement in cases where artificial irradiation such as UV light is used (Oller et al., 2011). In this case, the associated cost can often be prohibitive for wastewater treatment. Another problem is encountered in the treatment of wastewater with high colour intensity. In this case, the high colour intensity hinders the penetration of light rays thus lowering the performance of the process. It therefore means that to improve photocatalytic degradation in the treatment of such wastewater, high dilutions are required. This again is not economical as a larger reactor volume is required.

2.12.2 Need for integration of photodegradation and anaerobic degradation

In this work, it is proposed that the solution to the challenges facing both the anaerobic degradation and photocatalytic degradation of organic pollutants lies in the integration of the two processes. This is based on the possibility that photocatalytic pre-treatment of toxic pollutants can increase their biodegradability before conducting the anaerobic process. This means that the photodegradation process can be carried out for a shorter period since complete mineralization is not required. Moreover, the cost of energy required by the photodegradation process can be offset by the energy generated by the anaerobic process. Alternatively, photodegradation can be employed for the final polishing of the anaerobically treated effluent. Used in this manner, the resulting effluent may not only be safe for discharge but can be clean enough for re-use.

2.13 Energy analysis of integrated AD-UV system

The economic viability of an integrated anaerobic digestion and UV photodegradation process depends on its energy consumption. This is due to the fact that UV photodegaradtion is an energy intensive process. However, the advantage of such an integration in treatment of

distillery effluent is that the anaerobic step has high energy production potential of 74 – 248 kWh/m^3 (Sankaran et al., 2014; Yasar et al., 2015), depending on the wastewater strength, which can supplement the energy requirement of the UV process. What is not clear is the energy consumption rate of the UV photodegradation (kWh/COD removed) and the associated colour removal per KWh of energy utilized when treating distillery effluent. Moreover, how factors such as OLR and HRT can impact on the energy consumption of the integrated process and pollution removal efficiency is of interest.

The energy potential of biogas from distillery effluent cannot be underestimated as it has been reported that if used as an alternative fuel, biogas can offset up to 40% of diesel requirement of agricultural operations of sugarcane biorefinery and still produce 14 MWh of electricity annually (Moraes et al., 2014). In relation to this fact, the supplementation of the UV process energy requirement by that from biogas produced in the AD process needs to be studied. Application of this technology can lead to the implementation of the clean development mechanism under Kyoto protocol which encourages the use of renewable energy in production.

2.14 Clean development mechanism (CDM)

Clean development mechanism (CDM) was developed under Kyoto protocol and it entails environmental management and climate change monitoring by reducing greenhouse gases emissions, particularly CO_2, to the environment. It encourages efficient use and conservation of energy or adopting the use of renewable energy to replace energy from fossil fuels. Application of renewable energy is one of the strongest CDM projects as it leads to the reduction in CO_2 emission. The application of bioenergy in powering the UV process can lead to a remarkable reduction in CO_2 emission than in a case where electricity from national grid is applied. In order to evaluate the efficiency of the application of renewable energy in CO_2 reduction, it is important to first determine the standard/baseline grid emission factor. The baseline grid emission is expressed as mass of CO_2 equivalent emitted per amount of electricity generated (t CO_2e/MWh). The baseline grid emission factor in South Africa is reported as 0.957 tCO_2e/MWh (Spalding-Fecher, 2011) while Yasar et al. (2015) applied baseline grid emission factor of 0.4829 tCO_2e/MWh in Pakistan. A study on the potential of an integrated AD-UV system in CO_2 emission reduction is therefore very necessary.

References

ACHARYA, B.K., MOHANA, S. & MADAMWAR, D. (2008). Anaerobic treatment of distillery spent wash - a study on upflow anaerobic fixed film bioreactor. *Bioresour. Technol.* 99. p.4621–6.

AIYUK, S., FORREZ, I., LIEVEN, D.K., VAN HAANDEL, A. & VERSTRAETE, W. (2006). Anaerobic and complementary treatment of domestic sewage in regions with hot climates--a review. *Bioresour. Technol.* 97. p.2225–41.

ANDALIB, M., HAFEZ, H., ELBESHBISHY, E., NAKHLA, G. & ZHU, J. (2012). Treatment of thin stillage in a high-rate anaerobic fluidized bed bioreactor (AFBR). *Bioresour. Technol.* 121. p.411–8.

ANDREOZZI, R., CAPRIO, V., INSOLA, A. & MAROTTA, R. (1999). Advanced oxidation processes (AOP) for water purification and recovery. *Catal. Today*. 53. p.51–59.

APOLLO, S., ONYANGO, M.S. & OCHIENG, A. (2013). An integrated anaerobic digestion and UV photocatalytic treatment of distillery wastewater. *J. Hazard. Mater*. 261. p.435–42.

APOLLO, S., ONYANGO, S. & OCHIENG, A. (2014). UV / H 2 O 2 / TiO 2 / Zeolite Hybrid System for Treatment of Molasses Wastewater. *Iran. J. Chem. Chem. engineering.* 33. p.107–117.

ARNAIZ, C., BUFFIERE, P., ELMALEH, S., LEBRATO, J. & MOLETTA, R. (2003). Anaerobic digestion of dairy wastewater by inverse fluidization: the inverse fluidized bed and the inverse turbulent bed reactors. *Environ. Technol*. 24. p.1431–1443.

ASAITHAMBI, P., SUSREE, M., SARAVANATHAMIZHAN, R. & MATHESWARAN, M. (2012). Ozone assisted electrocoagulation for the treatment of distillery effluent. *Desalination.* 297. p.1–7.

BORJA, R., RINCÓN, B., RAPOSO, F., DOMÍNGUEZ, J.R., MILLÁN, F. & MARTÍN, A. (2004). Mesophilic anaerobic digestion in a fluidised-bed reactor of wastewater from the production of protein isolates from chickpea flour. *Process Biochem*. 39. p.1913–1921.

CHANDRA, R., NARESH, R. & RAI, V. (2008). Melanoidins as major colourant in sugarcane molasses based distillery effluent and its degradation. 99. p.4648–4660.

CHAUDHARI, P.K., MISHRA, I.M. & CHAND, S. (2007). Decolourization and removal of chemical oxygen demand (COD) with energy recovery: Treatment of biodigester effluent of a molasses-based alcohol distillery using inorganic coagulants. Colloids Surfaces A. *Physicochem. Eng. Asp*. 296. p.238–247.

CHENG, K.Y., HO, G. & CORD-RUWISCH, R. (2012). Energy-efficient treatment of organic wastewater streams using a rotatable bioelectrochemical contactor (RBEC). *Bioresour. Technol*. 126. p.31–436.

DOROODCHI, E., PENG, Z., SATHE, M., ABBASI-SHAVAZI, E. & EVANS, G.M. (2012). Fluidisation and packed bed behaviour in capillary tubes. *Powder Technol*. 223. p.131–136.

FARHADIAN, M., BORGHEI, M. & UMRANIA, V. V. (2007). Treatment of beet sugar wastewater by UAFB bioprocess. *Bioresour. Technol*. 98. p.3080–3.

FERNÁNDEZ, N., MONTALVO, S., BORJA, R., GUERRERO, L., SÁNCHEZ, E., CORTÉS, I., COLMENAREJO, M.F., TRAVIESO, L. & RAPOSO, F. (2008). Performance evaluation of an anaerobic fluidized bed reactor with natural zeolite as support material when treating high-strength distillery wastewater. *Renew. Energy.* 33. p.2458–2466.

FERNÁNDEZ, N., MONTALVO, S., FERNÁNDEZ-POLANCO, F., GUERRERO, L., CORTÉS, I., BORJA, R., SÁNCHEZ, E. & TRAVIESO, L. (2007). Real evidence about zeolite as microorganisms immobilizer in anaerobic fluidized bed reactors. *Process Biochem*. 42. p.21–728.

FUESS, L.T. & GARCIA, M.L. (2014). Implications of stillage land disposal: A critical review on the impacts of fertigation. *J. Environ. Manage*. 145. p.210–229.

GALLANT, J., PRAKASH, A. & HOGG, L.E.W. (2011). Fluidization and hydraulic behaviour of natural zeolite particles used for removal of contaminants from wastewater. *Can. J. Chem. Eng*. 89. p.159–165.

GALVIN, K.P. & NGUYENTRANLAM, G. (2002). Influence of parallel inclined plates in a liquid fluidized bed system. *Chemical Engineering Science*.

GARCÍA-CALDERÓN, D., BUFFIÈRE, P. & ELMALEH, S. (1998). Influence of Biomass Accumulation on Fluidized-Bed Reactor. *Biotechnol. Bioeng.* 57. p.136–144.

GARCIA-CALDERON, D., BUFFIERE, P., MOLETTA, R. & ELMALEH, S. (1998b). Anaerobic digestion of wine distillery wastewater in down-flow fluidized bed. *Water Res*. 32. p.3593–3600.

GHOSH, M., GANGULI, A. & TRIPATHI, A.K. (2002). Treatment of anaerobically digested distillery spentwash in a two-stage bioreactor using *Pseudomonas putida* and *Aeromonas* sp. *Process Biochem*. 37. p.857–862.

HUANG, M., XU, C., WU, Z., HUANG, Y., LIN, J. & WU, J. (2008). Photocatalytic discolorization of methyl orange solution by Pt modified TiO2 loaded on natural zeolite. *Dye. Pigment.* 77. p.327–334.

INGLEZAKIS, V.J., STYLIANOU, M. & LOIZIDOU, M. (2010). Hydrodynamic Studies on Zeolite Fluidized Beds. *Int. J. Chem. React. Eng*. 8.

JAAFARI, J., MESDAGHINIA, A., NABIZADEH, R. & HOSEINI, M. (2014). Influence of upflow velocity on performance and biofilm characteristics of Anaerobic Fluidized Bed Reactor (AFBR) in treating high-strength wastewater. *Environ. Health.* 1–10.

JOVANOVIC, M., GRBAVCIC, Z., RAJIC, N. & OBRADOVIC, B. (2014). Removal of Cu(II) from aqueous solutions by using fluidized zeolite A beads: Hydrodynamic and sorption studies. *Chem. Eng. Sci.* 117. p.85–92.

KALAVATHI, D., UMA, L. & SUBRAMANIAN, G. (2001). Degradation and metabolization of the pigment—melanoidin in distillery effluent by the marine cyanobacterium *Oscillatoria boryana* BDU 92181. *Enzyme Microb. Technol*. 29. p.246–251.

LORANGER, E., DANEAULT, C., CHABOT, B. & VALLERAND, R. (2010). Hydrodynamic behaviour of a fluidized bed reactor for paper machine whitewater contaminant removal. *Can. J. Chem. Eng*. 88. p.12–17.

MANE, J.D., MODI, S., NAGAWADE, S., PHADNIS, S.P. & BHANDARI, V.M. (2006). Treatment of spentwash using chemically modified bagasse and colour removal studies. *Bioresour. Technol.* 97. p.1752–5.

MELAMANE, X.L., STRONG, P.J. & BURGESS, J.E. (2007). Treatment of wine distillery wastewater: A review with emphasis on anaerobic membrane reactors. *South African J. Enol. Vitic.* 28. p.25–36.

MELIDIS, P., GEORGIOU, D. & AIVASIDIS, A. (2003). Scale-up and design optimization of anaerobic immobilized cell reactors for wastewater treatment. *Chem. Eng. Process. Process Intensif.* 42. p.897–908.

MILÁN, Z., SÁNCHEZ, E., WEILAND, P., BORJA, R., MARTÍN, A. & ILANGOVAN, K. (2001). Influence of different natural zeolite concentrations on the anaerobic digestion of piggery waste. *Bioresour. Technol*. 80. p.37–43.

MOHANA, S., ACHARYA, B.K. & MADAMWAR, D. (2009). Distillery spent wash: Treatment technologies and potential applications. *J. Hazard. Mater*. 163. p.12–25.

MONTALVO, S., GUERRERO, L., BORJA, R., CORTÉS, I., SÁNCHEZ, E. & COLMENAREJO, M.F. (2008). Treatment of wastewater from red and tropical fruit wine production by zeolite anaerobic fluidized bed reactor. *J. Environ. Sci. Health. B.* 43. p.37–442.

MONTALVO, S., GUERRERO, L., BORJA, R., SÁNCHEZ, E., MILÁN, Z., CORTÉS, I. & ANGELES DE LA LA RUBIA, M. (2012). Application of natural zeolites in anaerobic digestion processes: *A review. Appl. Clay Sci.* 58. p.125–133.

MORAES, B.S., JUNQUEIRA, T.L., PAVANELLO, L.G., CAVALETT, O., MANTELATTO, P.E., BONOMI, A. & ZAIAT, M. (2014). Anaerobic digestion of vinasse from sugarcane biorefineries in Brazil from energy, environmental, and economic perspectives: Profit or expense? *Appl. Energy*. 113. p.825–835.

MORAES, B.S., ZAIAT, M. & BONOMI, A. (2015). Anaerobic digestion of vinasse from sugarcane ethanol production in Brazil: Challenges and perspectives. *Renew. Sustain. Energy Rev*. 44. p.888–903.

NAGPAL, S., CHUICHULCHERM, S., LIVINGSTON, A. & PEEVA, L. (2000). Ethanol utilization by sulfate-reducing bacteria: An experimental and modeling study. *Biotechnol. Bioeng*. 70. p.533–543.

O'FLAY, V., COLLINS, G. & MAHONY, T. (2006). The Microbiology and Biochemistry of Anaerobic Bioreactors with Relevance to Domestic Sewage Treatment. *Rev. Environ. Sci. Bio/Technology*. 5. p.39–55.

OCHIENG, A., ODIYO, J.O. & MUTSAGO, M. (2003). Biological treatment of mixed industrial wastewaters in a fluidised bed reactor. *J. Hazard. Mater*. 96. 79–90.

OLLER, I., MALATO, S. & SÁNCHEZ-PÉREZ, J.A. (2011). Combination of Advanced Oxidation Processes and biological treatments for wastewater decontamination--a review. *Sci. Total Environ*. 409. p.4141–66.

ONYANGO, M., KITTINYA, J., HADEBE, N., OJIJO, V. & OCHIENG, A. (2011). Sorption of melanoidin onto surfactant modified zeolite. *Chem. Ind. Chem. Eng. Q*. 17. p.385–395.

PAPIRIO, S., VILLA-GOMEZ, D.K., ESPOSITO, G., PIROZZI, F. & LENS, P.N.L. (2013). Acid Mine Drainage Treatment in Fluidized-Bed Bioreactors by Sulfate-Reducing Bacteria: A Critical Review. *Crit. Rev. Environ. Sci. Technol*. 43. p.2545–2580.

PRASAD, R.K. (2009). Color removal from distillery spent wash through coagulation using *Moringa oleifera* seeds: use of optimum response surface methodology. *J. Hazard. Mater.* 165. p.804–11.

RAMAKRITINAN, C.M., KUMARAGURU, A.K. & BALASUBRAMANIAN, M.P. (2005).

Impact of distillery effluent on carbohydrate metabolism of freshwater fish., *Cyprinus carpio. Ecotoxicology*. 14. p.693–707.

RIZZO, L. (2011). Bioassays as a tool for evaluating advanced oxidation processes in water and wastewater treatment. *Water Res*. 45. p.4311–40.

ROBLES-GONZÁLEZ, V., GALÍNDEZ-MAYER, J., RINDERKNECHT-SEIJAS, N. & POGGI-VARALDO, H.M. (2012). Treatment of mezcal vinasses: a review. *J. Biotechnol*. 157. p.524–546.

RYAN, D., GADD, A., KAVANAGH, J., ZHOU, M. & BARTON, G. (2008). A comparison of coagulant dosing options for the remediation of molasses process water. *Sep. Purif. Technol.* 58. p.347–352.

SANGAVE, P.C., GOGATE, P.R. & PANDIT, A.B. (2007). Combination of ozonation with conventional aerobic oxidation for distillery wastewater treatment. *Chemosphere*. 68. p.32–41.

SANKARAN, K., PREMALATHA, M., VIJAYASEKARAN, M. & SOMASUNDARAM, V.T. (2014). DEPHY project: Distillery wastewater treatment through anaerobic digestion and phycoremediation - A green industrial approach. *Renew. Sustain. Energy Rev*. 37. p.634–643.

SATYAWALI, Y. & BALAKRISHNAN, M. (2008). Wastewater treatment in molasses-based alcohol distilleries for COD and color removal: a review. *J. Environ. Manage*. 86. p.481–97.

SHU, Z., BOLTON, J.R., BELOSEVIC, M. & EL DIN, M.G. (2013). Photodegradation of emerging micropollutants using the medium-pressure UV/H2O2 Advanced Oxidation Process. *Water Res*. 47. p.2881–9.

SILES, J.A., GARCÍA-GARCÍA, I., MARTÍN, A. & MARTÍN, M.A. (2011). Integrated ozonation and biomethanization treatments of vinasse derived from ethanol manufacturing. *J. Hazard. Mater*. 188. p.247–253.

SINGH, S.P. & PRERNA, P. (2009). Review of recent advances in anaerobic packed-bed biogas reactors. Renew. Sustain. *Energy Rev.* 13. p.1569–1575.

SOWMEYAN, R. & SWAMINATHAN, G. (2008). Performance of inverse anaerobic fluidized bed reactor for treating high strength organic wastewater during start-up phase. *Bioresour. Technol*. 99. p.6280–4.

SPALDING-FECHER, R. (2011). What is the carbon emission factor for the South African electricity grid ? *J. Energy South Africa.* 22. p.8–12.

TADA, C., YANG, Y., HANAOKA, T., SONODA, A., OOI, K. & SAWAYAMA, S. (2005). Effect of natural zeolite on methane production for anaerobic digestion of ammonium rich organic sludge. *Bioresour. Technol*. 96. p.459–64.

TONDEE, T., SIRIANUNTAPIBOON, S. & OHMOMO, S. (2008). Decolorization of molasses wastewater by yeast strain, Issatchenkia orientalis No. SF9-246. *Bioresour. Technol.* 99. p.5511–5519.

VOICE, T., PAK, D., ZHAO, X., SHI, J. & HICKEY, R. (1992). Biological activated carbon in fluidized bed reactors for the treatment of groundwater contaminated with volatile aromatic hydrocarbons. *Water Res*. 26. p.1389–1401.

WANG, H.-Y., QIAN, H. & YAO, W.-R. (2011). Melanoidins produced by the Maillard reaction: Structure and biological activity. *Food Chem*. 128. p.573–584.

WEIß, S., ZANKEL, A., LEBUHN, M., PETRAK, S., SOMITSCH, W. & GUEBITZ, G.M. (2011). Investigation of mircroorganisms colonising activated zeolites during anaerobic biogas production from grass silage. *Bioresour. Technol*. 102. p.4353–4359.

YASAR, A., AHMAD, N., CHAUDHRY, M.N., REHMAN, M.S.U. & KHAN, a. a a. (2007). Ozone for color and COD removal of raw and anaerobically biotreated combined industrial wastewater. *Polish J. Environ. Stud*. 16. p.289–294.

YASAR, A., AHMAD, N. & KHAN, a. a a. (2006). Energy requirement of ultraviolet and AOPs for the post-treatment of treated combined industrial effluent. *Color. Technol*. 122. p.201–206.

YASAR, A., ALI, A., TABINDA, A.B. & TAHIR, A. (2015). Waste to energy analysis of shakarganj sugar mills; biogas production from the spent wash for electricity generation. *Renew. Sustain. Energy Rev*. 43. p.126–132.

YASAR, A. & TABINDA, A.B. (2010). Anaerobic Treatment of Industrial Wastewater by UASB Reactor Integrated with Chemical Oxidation Processes ; an Overview. *Polish J. Environ. Stud.* 19. p.1051–1061.

ZAYAS, T., RÓMERO, V., SALGADO, L., MERAZ, M. & MORALES, U. (2007). Applicability of coagulation/flocculation and electrochemical processes to the purification of biologically treated vinasse effluent. *Sep. Purif. Technol*. 57. p.270–276.

Chapter 3

3. Hydrodynamic studies of fluidised bed anaerobic reactor and photoreactor

Abstract: The efficiency of a fluidised bed reactor (FBR) depends on its hydrodynamic conditions. Therefore, for effective operation of an FBR it is necessary to determine the optimal hydrodynamic conditions. In this work the hydrodynamics of a liquid-solid and a gas-liquid-solid system in anaerobic reactor and photoreactor respectively, was studied. Optical attenuation technique (OAT) was used to determine particle and gas distribution in the respective reactors. Best particle distribution in the bioreactor was found to be at superficial liquid velocity of between 0.6 cm/s and 0.75 cm/s. The radial bubble distribution in the photoreactor was found to vary with superficial gas velocity (U_g) and aspect ratio. The bubble trajectory was found to be spiral or zig-zag in nature due to large bubble size, which ranged between 6 and 11 mm depending on the applied U_g. The optimal gas hold up and solid hold up for the photoreactor were found to be 0.077 and 0.003, respectively. The total organic carbon (TOC) and colour reductions of 68% and 97%, respectively were achieved by the photoreactor at the optimal conditions when treating distillery effluent.

3.1 Introduction

Fluidised bed reactors (FBRs) have been applied in either biological or physicochemical processes for industrial wastewater treatment (Papirio et al., 2013) The findings from lab-scale and pilot-scale application of fluidised bed reactors have consistently demonstrated their technical advantages over other reactor types such as fixed bed reactors or continuously stirred tank reactors. In biological application, Rabah & Dahab (2004) reported that the efficiency of fluidised bed bioreactor could be 10 times better than that of the activated sludge system and it occupies about 10% of the space required by stirred tank reactors of similar capacity. The high performance of the fluidised bed bioreactor is attributed to the high ability of biomass retention and efficient mixing (Andalib et al., 2012). For instance, a biomass concentration of 40 g/L has been reported for fluidised bed reactor compared to 3 g/L when activated sludge was applied (Rabah & Dahab, 2004). Apart from the application of fluidised bed reactors for biochemical processes, their application in physicochemical processes have grown exponentially (Jovanovic et al., 2014). These reactors have been applied in adsorption processes (Jovanovic et al., 2014) and chemical oxidation such as photocatalysis used in wastewater treatment (Shet & Vidya, 2016).

Depending on the nature of the process, fluidised bed can be operated as either two phase (gas-liquid, gas-solid or liquid-solid) or three phase (gas-liquid-solid). Normally, gas, liquid or both

is applied to achieve the desired fluidisation in the reactor. The flow of gas or liquid in a fluidised bed reactor allows the effective contact between the reactants by enhancing mass transfer. Experimental determination of intrinsic factors like local particle distribution, bubble properties such as rise velocity, size, shape and local distribution have been applied to identify optimal operation conditions of FBR. When the operating conditions are not appropriately determined, operating fluidised bed reactors can be costly due to the fact that operating conditions determine degree of homogeneity which affects the overall efficiency of the process.

Analysis of the degree of homogeneity in the reactor is significant as it assists in identifying the optimal operating conditions. Various analytical techniques have been applied such as visual observation for larger particle (Ochieng et al., 2003). More refined techniques such as digital image analysis has also gained popularity for its simplicity and accuracy compared to visual observation (Fayolle et al., 2010; Oliveira et al., 2013). In this method dynamic digital images captured using digital camera during fluidization are analysed to determine the particle distribution or bubble size, shape and distribution. Apart from that, more robust methods such as optical techniques have been applied (Ochieng & Lewis, 2006). Optical attenuation technique (OAT) offers a direct method of establishing particle/bubble distribution based on the light scattering effect of particles/bubbles. Therefore, in this method light is illuminated on one side of the reactor using a light emitting diode (LED) while a light detector to capture the intensity of the transmitted light is placed at the same level to the LED but on the opposite side of the reactor. Thus the amount of light scattered by the particles, which is proportional to the particles concentration, can be determined. In this work the hydrodynamic conditions of fluidised bed anaerobic reactor and photoreactor were studied to determine the optimal mixing conditions using OAT.

3.2 Methodology

3.2.1 Equipment and material

Fluidization was carried out in a bioreactor and photoreactor. The bioreactor had a diameter of 11.8 cm with a height of 76 cm and volume of about 8 L. The photoreactor used had annular space created between the reactor inner wall and the UV lamp sleeve. The UV sleeve was made of quartz, 2 mm thick with an inner diameter of 36 mm while the outer wall of the reactor was constructed using Perspex. The outside diameter of the Perspex was 60 mm and it was 3 mm thick; the total volume of the photoreactor was 0.52 L. At the bottom of both the reactors (the inlet section) there was a distribution compartment fitted with a distribution plate. The details of the photoreactor can be found in our previous work (Apollo et al., 2013). South African natural

zeolite (Clinoptilolite) was used in the bioreactor as microbial carrier material. The zeolite size ranged between 150 and 300 μm with a density of 2.3 g/cm^3 and total mass used was 50 g. Titanium dioxide/Silica composite photocatalyst with size range between 38 and 75 μm was used in the photoreactor.

3.2.2 Technique for local solid and gas hold up determination

Hydrodynamic conditions of a fluidised bed anaerobic reactor and fluidised bed photoreactor were separately determined. An optical attenuation technique (OAT) equipment was designed and constructed for quantification of the gas holdup in the photoreactor and solid distribution in the bioreactor. The general representation of the experimental set-up is shown in Figure 3-1. The light source for the OAT was provided by three red light emitting diodes (LEDs) irradiating one side of the reactor. The LEDs were equally distributed along the reactor radial axis. On the opposite side of the reactor, an array of three visible light photodiodes each with an active area of 3 x 3 mm, was used as light detectors and converted the light passing through the reactor to electric current. The light through the reactor was attenuated by the particles in the reactor and the extent of attenuation was dependent on the amount of solids on the light path. The current generated by the photodiode was proportional to the light intensity reaching the photodiode surface. The current from the photodiodes was converted into voltage signals using operational amps. The voltage signals from each of the photodiodes were fed into a microcontroller (Arduino) which converted the analogue signals into digital signals. The digital signals were then sent to a computer for data logging using Microsoft Excel software. Once the light intensity on the radial direction was measured and logged on a computer, the photodiode array was moved to a different axial location. The whole system including the electronics were fitted on a rigid metallic frame which supported the electronic components. The OAT device was moved along the reactor height to record the axial particle distribution as the four LEDs simultaneously capture the radial particle distribution. The output signal was normalized with respect to the signal obtained in the particle free liquid using modified Beer Lambart equation:

$$A_T = \frac{-(Log\frac{I}{I_O})}{L} \quad (1)$$

where A_t is the measure of light attenuation, I_o is the signal obtained in particle free liquid (blank), I is the signal in a liquid with bubbles or particles and L is the path length (cm).

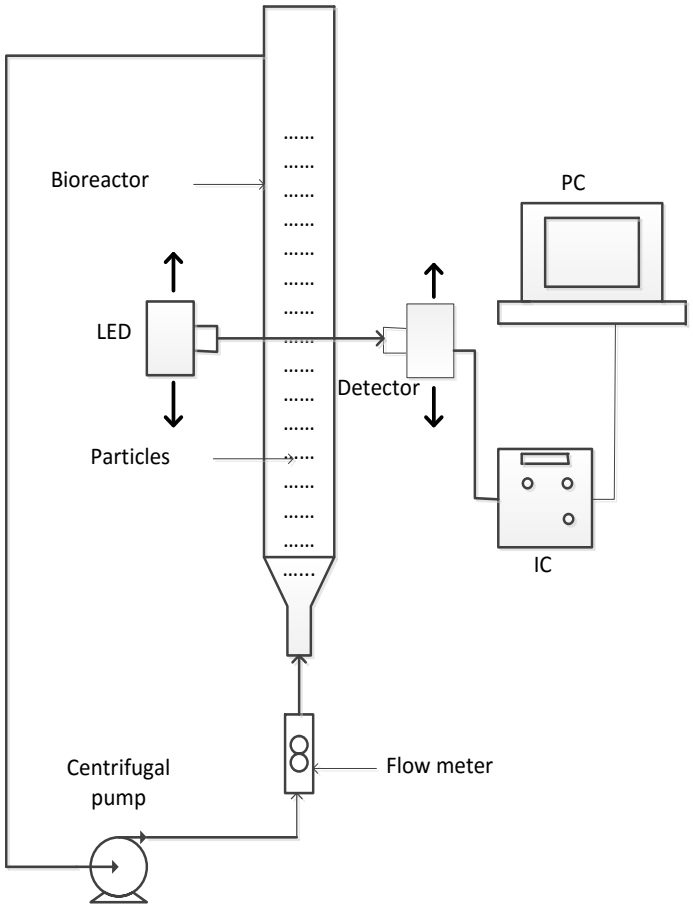

Figure 3-1: Set-up for the data acquisition using the OAT.

Global gas holdup and solid holdup which could not be determined using OAT were measured using the quick stop method as described in literature (Abraham et al., 1992; Ochieng et al., 2002). In this method, water and 1.0 g/L of the catalyst was added into the reactor. A mark was then made on the reactor wall corresponding to the gas-free static liquid height. Then air sparging was started and maintained at the appropriate flow rate for 10 minutes. Then, another mark was made on the reactor wall to indicate the expanded liquid height. The difference in the two marks was used to calculate the gas holdup according to equation (2).

$$\varepsilon_g = \frac{H_e - H_s}{H_e} \tag{2}$$

where H_e represents the expanded bed height and H_s represents the static bed height. Finally, the effect of different hydrodynamic conditions in photodegradation was studied in the photoreactor.

3.2.3 Experimental analysis

Gas hold up was obtained by measuring, with a ruler, the expansion in liquid level when air was introduced. Total organic carbon was analysed using a TOC analyser (TELEDYNE Tekmar),

while colour was analysed using UV-Vis spectrophotometer (T80 + UV/VIS Spectrophotometer, PG instruments Ltd).

3.3 Results and discussion

3.3.1 Data acquisition and calibration

The signals were automatically acquired at the rate of one data point per second. The data was recorded once steady values had been reached for a duration of 1 minute. In Figure 3-2a the data obtained when calibrating the system with clean water as blank is shown against that acquired during operation when the reactor was loaded with 50 g solid at superficial liquid velocity (U_L) of 0.6 cm/s. The standard deviation from the mean values for both conditions was found to be ~ 2% indicating that the OAT applied had good repeatability for solid-liquid system. However, there was relatively higher noise when measuring attenuation due to bubble, compared to that for the blank in liquid-gas system (Figure 3-2b) due to the fact that bubbles were less dispersed in liquid compared to solid dispersion in liquid. The slight difference in the recorded signal for the blank between the solid-liquid and liquid-gas system was due to the difference in the reactor dimensions for the two respective systems. In both cases, the signal acquired for blank was used for normalization in calculating the actual degree of attenuation due to particles or bubbles in solid liquid fluidisation or liquid-gas fluidisation in bioreactor or photoreactor, respectively using equations (1).

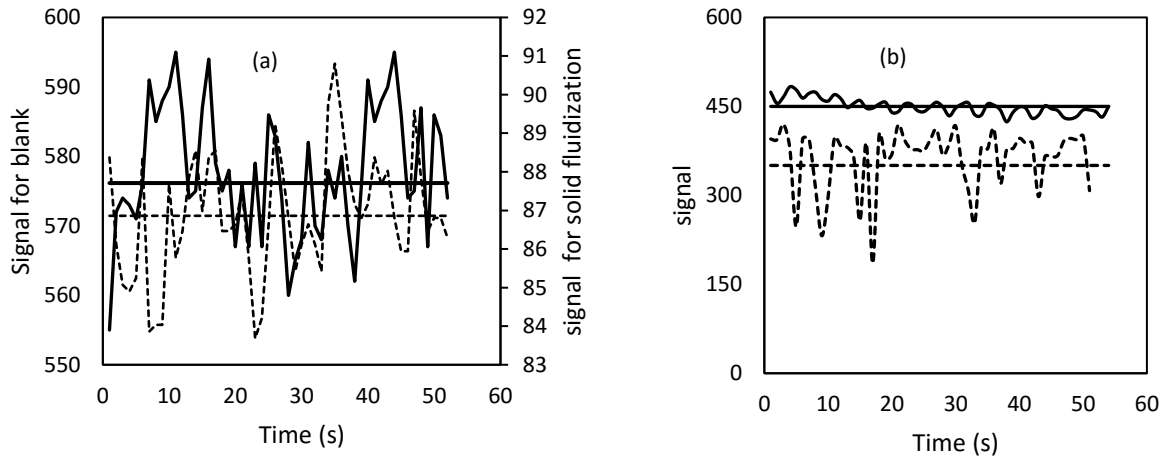

Figure 3-2: Signal-time relationship for (a) liquid-solid system in bioreactor, blank (—), with solids (---) and (b) gas-liquid system in photoreactor, blank (—), with bubbles (---).

3.3.2 Axial particle distribution in solid-liquid fluidised bed bioreactor

The OAT was applied to determine axial particle distribution in the reactor. The variation in axial particle distribution at various superficial liquid velocities (Figure 3-3a) showed that at low U_L of 0.3 and 0.45 cm/s the particles distribution was poor.

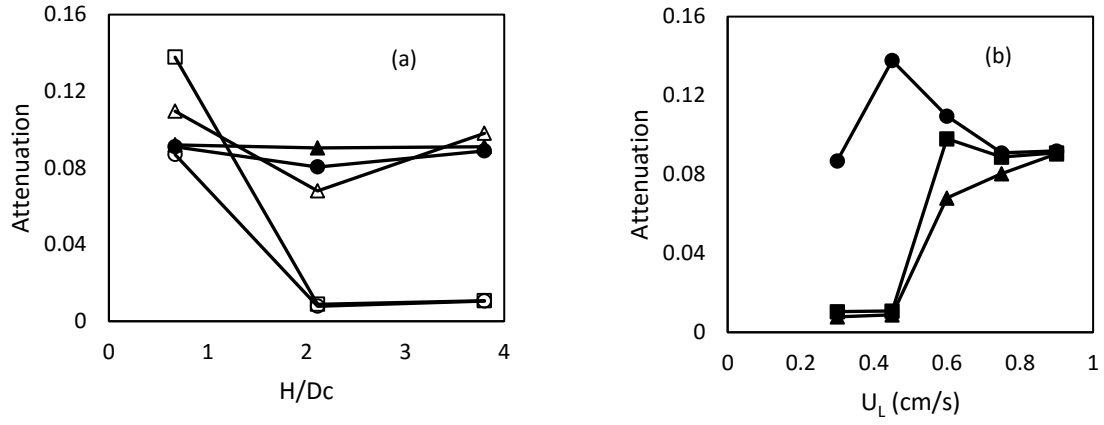

Figure 3-3: Axial particle distribution in bioreactor (a) particle distribution with aspect ratio at various U_L 0.3 cm/s (○), 0.45 cm/s (□), 0.6 cm/s (Δ), 0.75 cm/s (●) and 0.9 cm/s (▲). (b) Particle distribution at various aspect ratio (●) 0.67, (▲) 2.1 (■) 3.8.

At low U_L most of the particles were majorly at the bottom of the reactor due to the fact that the applied upward force supplied by the fluid was not sufficient to fluidise the particles. However, as the U_L increased to 0.6 cm/s the distribution improved and a nearly uniform distribution was obtained at 0.75 cm/s with an optimal distribution at U_L equal to 0.9 cm/s. At the bottom section of the reactor there was a more uniform particle distribution irrespective of the U_L as compared to the middle and the top sections (Fig 3b). However, there was an increase in attenuation at the bottom of the reactor when U_L was increased from 0.3 to 0.45 cm/s followed by a drop as U_L was further increased from 0.45 to 0.75 cm/s. The increase in the attenuation could be due to the fact that, initially at 0.3 cm/s most particles could not be fluidised up to the point H/D_c =0.67 whereas the decrease in attenuation when U_L was increased above 0.45 cm/s at H/Dc = 0.67 was due to an increase in bed expansion which resulted in increased particle dispersion.

3.3.3 Determination of particle terminal velocity

Generally, the characteristics of solid-liquid fluidised bed depends on the correspondence between the applied U_L and the resulting volume fraction of solids ($\emptyset_s$). These parameters can be related as (Galvin & Nguyentranlam, 2002; Jovanovic et al., 2014):

$$U_L = U_t(1-\emptyset_s)^n \quad (3)$$

where U_t is the terminal velocity of the particles (cm/s) and *n* is the bed expansion index. The volume fraction of solids ($\emptyset_s$) at any bed height is calculated as:

$$\emptyset_s = \frac{m}{\rho_p A_c H} \quad (4)$$

where m is the mass (g) of the particles in the reactor, ρ_p is the density of the particles (g/cm^3), A_c is the cross sectional area of the reactor (cm^2) and H is the fluidised bed height (cm) at any U_L.

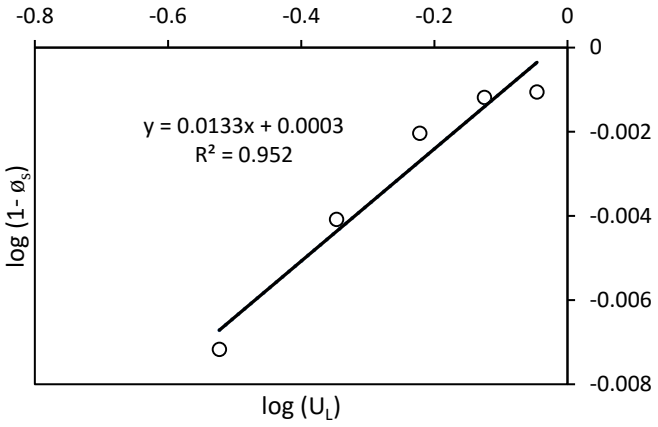

Figure 3-4: Determination of terminal velocity.

The bed expansion index and the terminal velocity were determined from linear regression of the plot of log (U_L) against log (1- $\emptyset_s$) from equation (2) as explain in various studies (Gallant et al., 2011; Jovanovic et al., 2014). From Figure 3-4 U_t was calculated as ~1 cm/s and expansion index was 0.0133. Therefore, generally operating the reactor at values below 1 cm/s should not lead to particle entrainment. Jovanovic et al. 2014 reported that U_L should be less than U_t to prevent particle entrainment.

3.3.4 Radial bubble distribution in the annular photoreactor

Radial distribution of bubbles at three different axial points corresponding to aspect ratios of 0.89, 2.67 and 4.46 in the annular photoreactor was determined using OAT. It was found that the nature of radial distribution was dependent on the aspect ratio (Figure 3-5). Close to the distributor the bubbles were closer to the centre of the reactor than towards the reactor outer walls (Figure 3-5a). As the bubbles rose up to the middle of the reactor, their distribution was higher towards the wall than at the centre (Figure 3-5b). The distribution then alternated towards the centre at the top of the reactor resuming the high distribution at the centre of the annulus reactor (Figure 3-5c). This phenomenon has been reported by various researchers in liquid-gas fluidization (Shew et al., 2006; Hassan et al., 2012). This observation was an indication that the bubbles movement was either zig zag or spiral in nature after aspect ratio of 0.89.

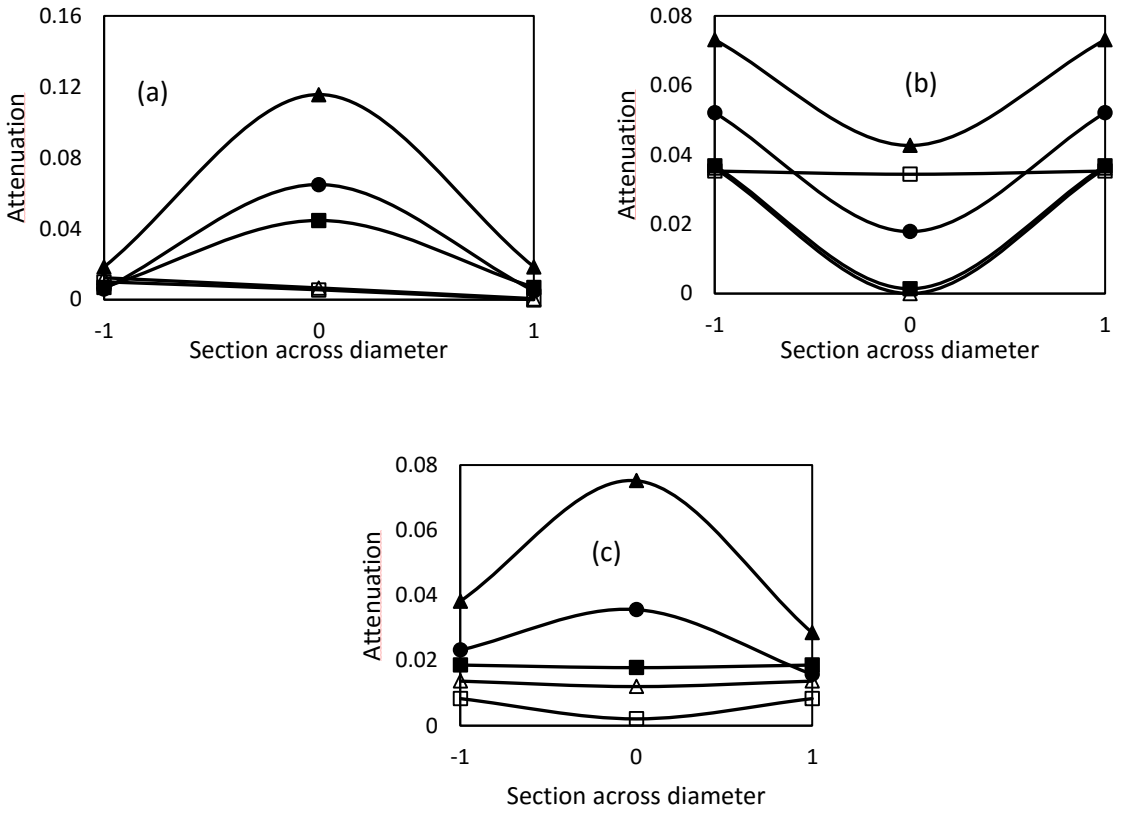

Figure 3-5: Radial distribution of bubbles in photoreactor at various aspect ratios (a) 0.89, (b) 2.67 and (c) 4.46 at different U_g (□) 0.23 cm/s, (Δ) 0.46 cm/s, (■) 0.92 cm/s, (●) 1.38 cm/s and (▲) 1.84 cm/s.

A bubble rising through a liquid experiences most resistance directly on its top, initially the bubble moves along a straight vertical trajectory then develops a zig zag motion which consequently changes into a spiralling motion depending on resistance and its size (Hassan et al., 2012). Most studies report that small bubbles with diameter of less than 1 mm rise through water in a straight vertical motion maintaining their shape due to high surface tension. However, bubbles with diameter of greater than 1 mm encounter significant deformation due to variation in hydrostatic and dynamic pressure over the surface of the bubble (Magnaudet & Eames, 2000). This leads to a change in the shape, size, velocity and trajectory of the bubble (Abbas & Mahdy, 2015). Shew et al. (2006) established that the spiralling frequency of raising bubbles increases with bubble size. Figure 3-5 further shows that at low U_g of 0.23 cm/s the bubble distribution was uniform along the radial profile of the reactor irrespective of the aspect ratio probably because the flow was laminar or because the bubbles were smaller as compared to those at high U_g.

3.3.5 Effect of gas velocity on bubble size

The size of bubbles was determined using images taken by a camera. In this method a ruler was placed against the reactor wall and the image of rising bubbles captured (Fayolle et al., 2010; Coward et al., 2014). In Figure 3-6, the bubble size increased with an increase in applied U_g due to an increased bubble coalescence (Ribeiro & Lage, 2004). The increase in bubble size was also captured by OAT which detected an increase in attenuation with an increase in U_g. As the U_g increased the rate of bubble coalescence increased leading to the formation of large bubbles.

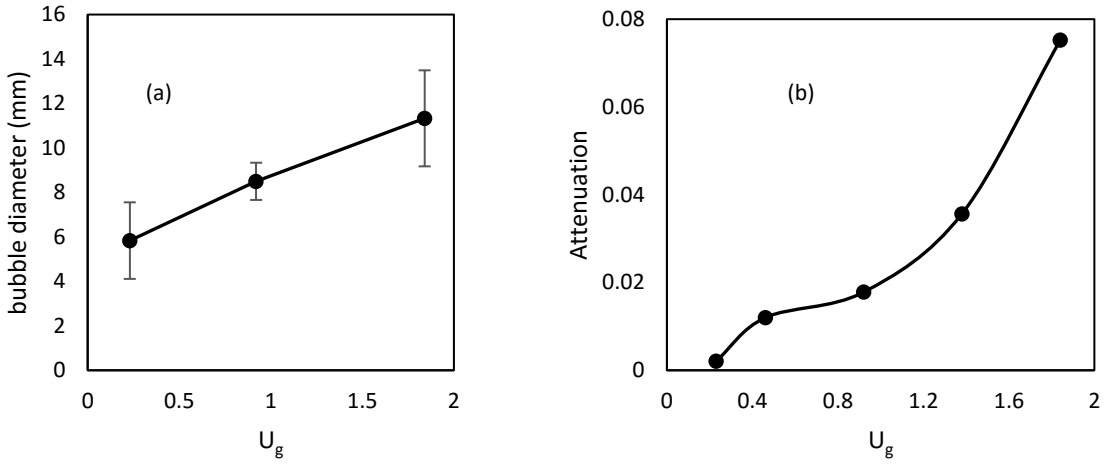

Figure 3-6: (a) Estimated bubble size at various superficial gas velocities (b) the relationship between attenuation and superficial gas velocity captured by OAT.

3.3.6 Effect of gas hold up

The influence of superficial gas velocity on gas hold up was investigated. The gas hold up at various velocities was obtained by measuring the expansion in volume of liquid when air was introduced. The dependence of gas hold up on gas velocity is generally described as (Moshtari et al., 2009):

$$\varepsilon_g = AU^a_g \quad (5)$$

where ε_g is gas hold up and U_g is superficial gas velocity (cm/s). The value of *a* depends on flow regime, for homogenous flow regime *a* ranges from 0.7 to 1.2 while for turbulent regime it varies from 0.4 to 0.7. The value of A depends on reactor design and physical properties of the system (Moshtari et al., 2009).

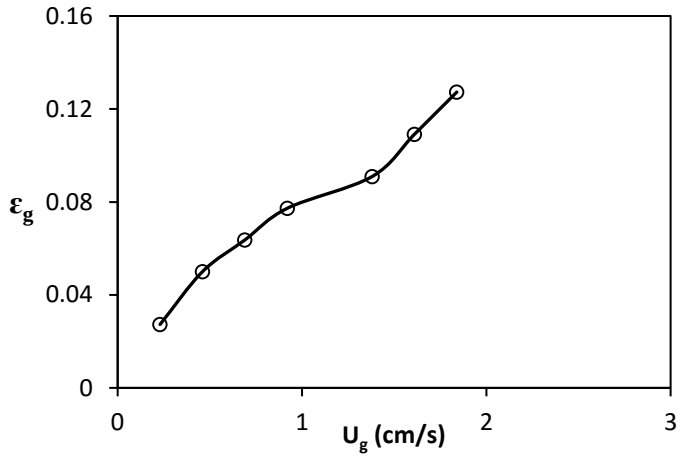

Figure 3-7: Gas hold up as a function of superficial gas velocity.

From Figure 3-7 and equation (5), the correlation between gas hold up and superficial gas velocity for the photoreactor could be expressed as:

$$\varepsilon_g = 0.07 U_g^{0.6937} \quad (6)$$

The *a* value for the photoreactor was an indication that the system operated around the boundary of homogenous and turbulent regime.

Investigating the effect of gas hold up on photodegradation is important as it may influence the process in two major ways. First, gas hold up is associated with air velocity which in turn affects mixing in the reactor. At low velocity there is low mixing and this does not enhance reaction while at extremely high velocities, a lot of bubbles are produced which may cause light attenuation thereby reducing reaction rate (Pareek et al., 2001).

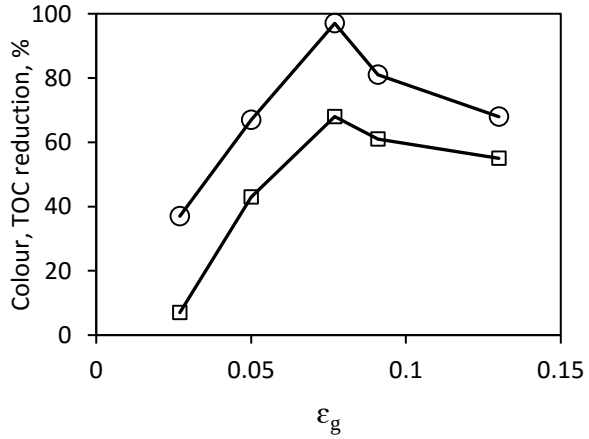

Figure 3-8: Effect of gas hold up on photodegradation UV reactor and TOC (□), colour (○).

Moreover, at high U_g coalescence leads to production of larger bubbles which lowers mixing efficiency. In Figure 3-8 the optimum gas hold up was found to be 0.077 corresponding to superficial gas velocity of 0.92 cm/s. At gas hold up lower than the optimum, the observed low photodegradation could also be attributed to inadequate oxygen supply since oxygen acts as electron acceptor during photocatalysis thereby improving degradation efficiency (Lim & Kim, 2005). As gas hold up increased above the optimum value, there was a resultant decrease in catalyst liquid contact and this could cause a decrease in the catalyst activity.

3.3.7 Effect of solid hold up on photodegradation

Application of an appropriate amount of catalyst in photoreactor can enhance photodegradation efficiency, however, at exceedingly high dosage, catalyst can alter the physical property of the solution which may result in reduced efficiency. In addition, at catalyst concentrations above the optimum, the solids hinder reaction as they cause light attenuation (Pareek et al., 2001). Moreover, at very high catalyst concentrations mass transfer is hindered due to increased solution viscosity leading to a reduction in reaction rate. An increase in viscosity also affects fluidisation and therefore adequate mixing. In Figure 3-9, the optimum solid hold up was 0.003 corresponding to catalyst loading of 2 g/l.

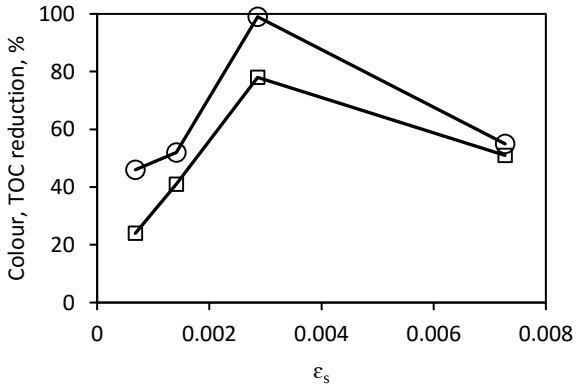

Figure 3-9: Effect of solid hold up on photodegradation, TOC reduction (□), colour reduction (○).

Conclusion

Hydrodynamics of anaerobic reactor and photoreactor were studied using OAT. The axial solid distribution was used to determine the best operating superficial liquid velocity for the anaerobic reactor. The reactor could effectively be operated between U_L of 0.6 cm/s and 0.75 cm/s due to the attainable effective solid distribution. The average terminal velocity of the zeolite particles was estimated as 1 cm/s, therefore, operating the reactor at or above this value was inappropriate

due to particle entrainment considering the wide particle size range used (150 – 300 μm). The radial bubble distribution in the photoreactor was found to depend on the reactor aspect ratio. It was therefore established that the bubble trajectory was either spiral or zig zag in nature. This was attributed to the recorded bubble size of greater than 1 mm. The performance of the photoreactor was strongly dependent on gas hold up and solid hold up with the optimum values found to be 0.077 and 0.03, respectively.

References

ABBAS, F.I. & MAHDY, A.H. (2015). Mathematical models for movement bubble in the water based on the capture images using 4. p.333–343.

ABRAHAM, M., KHARE, A.S., SAWANT, S.B. & JOSHI, J.B., (1992). Critical gas velocity for suspension of solid particles in three-phase bubble columns. *Ind. Eng. Chem. Res.* 31., p.1136-47.

ANDALIB, M., HAFEZ, H., ELBESHBISHY, E., NAKHLA, G. & ZHU, J. (2012). Treatment of thin stillage in a high-rate anaerobic fluidized bed bioreactor (AFBR). *Bioresour. Technol*. 121. p.411–8.

APOLLO, S., ONYANGO, M.S. & OCHIENG, A. (2013). An integrated anaerobic digestion and UV photocatalytic treatment of distillery wastewater. *J. Hazard. Mater*. 261. p.435–42.

COWARD, T., LEE, J.G.M. & CALDWELL, G.S. (2014). The effect of bubble size on the efficiency and economics of harvesting microalgae by foam flotation. *J. Appl. Phycol*. p.733–742.

FAYOLLE, Y., GILLOT, S., COCKX, A., BENSIMHON, L., ROUSTAN, M. & HEDUIT, A. (2010). In situ characterization of local hydrodynamic parameters in closed-loop aeration tanks. *Chem. Eng. J*. 158. p.207–212.

GALLANT, J., PRAKASH, A. & HOGG, L.E.W. (2011). Fluidization and hydraulic behaviour of natural zeolite particles used for removal of contaminants from wastewater. *Can. J. Chem. Eng*. 89. p.159–165.

GALVIN, K.P. & NGUYENTRANLAM, G. (2002). Influence of parallel inclined plates in a liquid fluidized bed system. *Chemical Engineering Science.*

HASSAN, N.M.S., KHAN, M.M.K. & RASUL, M.G. (2012). Bubble Rise Phenomena in Non-Newtonian Crystal Suspensions. In. p.15–80.

JOVANOVIC, M., GRBAVCIC, Z., RAJIC, N. & OBRADOVIC, B. (2014). Removal of Cu(II) from aqueous solutions by using fluidized zeolite A beads: Hydrodynamic and sorption studies. *Chem. Eng. Sci.* 117. p.85–92.

LIM, T.H. & KIM, S.D. (2005). Photocatalytic degradation of trichloroethylene (TCE) over TiO 2/silica gel in a circulating fluidized bed (CFB) photoreactor. *Chem. Eng. Process. Process Intensif.* 44. p.327–334.

MAGNAUDET, I. & EAMES, I. (2000). The Motion of High-Reynolds-Number Bubbles in Inhomogeneous Flows. *Annu. Rev. Fluid Mech*. 32. p.659–708.

MOSHTARI, B., BABAKHANI, E.G. & MOGHADDAS, J.S. (2009). Experimental Study of Gas Hold-Up and Bubble Behavior in Gas – Liquid Bubble Column. Pet. *Coal*. 51. p.27–

32.

OCHIENG, A. & LEWIS, A.E. (2006). Nickel solids concentration distribution in a stirred tank. *Miner. Eng*. 19. p.180–189.

OCHIENG, A., OGADA, T., SISENDA, W. & WAMBUA, P., (2002). Brewery wastewater treatment in a fluidised bed bioreactor. *J. Hazard. Mater.* 90., p.311-321.

OCHIENG, A., ODIYO, J.O. & MUTSAGO, M. (2003). Biological treatment of mixed industrial wastewaters in a fluidised bed reactor. *J. Hazard. Mater*. 96. p.79–90.

OLIVEIRA, T.J.P., CARDOSO, C.R. & ATAÍDE, C.H. (2013). Bubbling fluidization of biomass and sand binary mixtures: Minimum fluidization velocity and particle segregation. *Chem. Eng. Process. Process Intensif.* 72. p.113–121.

PAPIRIO, S., VILLA-GOMEZ, D.K., ESPOSITO, G., PIROZZI, F. & LENS, P.N.L. (2013). Acid Mine Drainage Treatment in Fluidized-Bed Bioreactors by Sulfate-Reducing Bacteria: A Critical Review. Crit. Rev. *Environ. Sci. Technol*. 43. p.2545–2580.

PAREEK, V.K., BRUNGS, M.P. & ADESINA, a. a. (2001). Continuous Process for Photodegradation of Industrial Bayer Liquor. *Ind. Eng. Chem. Res*. 40. p.5120–5125.

RABAH, F.K.J. & DAHAB, M.F. (2004). Biofilm and biomass characteristics in high-performance fluidized-bed biofilm reactors. *Water Res*. 38. p.4262–4270.

RIBEIRO, C.P. & LAGE, P.L.C. (2004). Experimental study on bubble size distributions in a direct-contact evaporator. *Brazilian J. Chem. Eng*. 21. p.69–81.

SHET, A. & VIDYA, S.K. (2016). Solar light mediated photocatalytic degradation of phenol using Ag core – TiO2 shell (Ag@TiO2) nanoparticles in batch and fluidized bed reactor. *Sol. Energy*. 127. p.67–78.

SHEW, W.L., PONCET, S. & PINTON, J.-F. (2006). Force measurements on rising bubbles. *J. Fluid Mech*. p.569, 51.

Chapter 4

4 Performance and kinetics of a fluidized bed anaerobic reactor treating distillery effluent

Abstract

The kinetic analysis of an anaerobic fluidized bed bioreactor treating distillery effluent was carried out. The hydraulic retention time was varied between 3 and 20 days while OLR was varied between about 0.33 and 9 kg COD/m^3.d, corresponding to a TOC loading rate between 0.25 to 8.1 kg TOC/m^3.d. The degradation followed first order kinetics and fitted Michaelis-Menten kinetic model for substrate utilization. The kinetic analysis showed that 9% of the TOC was non-biodegradable which corresponds to about 14% COD. The non-biodegradable component was responsible for the dark-brown colour of the distillery effluent and therefore there was a need for employing a post-treatment technology for their removal. Biomass yield was found to be 0.4658 g/g while endogenic micro-organisms decay coefficient was 0.0293, which suggested that there was a need to install a sludge handling unit prior to post-treatment. The maximum micro-organisms' growth rate was found to be 0.136 d^{-1}while the specific growth rate of the micro-organisms reduced with an increase in HRT at constant feed concentration. The specific substrate utilization rate was found to increase linearly with an increase in the ration of food to micro-organisms and the mean cell residence time was found to be at least 2.5 times the HRT due to application of zeolite as microbial support in the reactor.

4.1 Introduction

Anaerobic digestion is widely applied in the organic load removal and bioenergy recovery from distillery wastewater (Satyawali & Balakrishnan, 2008). Robust anaerobic digesters such as fluidised bed reactors achieve high organic removal efficiency and good energy recovery in terms of biomethane due to efficient mixing in the reactor (Andalib et al., 2012). Bioconversion of organic matter into biomethane is a complex process involving a consortia of micro-organisms. Due to the complex nature of the process, a poorly operated digester is often prone to inhibition due to accumulation of volatile fatty acids which may lead to total digester failure (Aiyuk et al., 2006). During the anaerobic digestion, the operating parameters such as organic loading rate (OLR), hydraulic retention time (HRT), pH and food to micro-organisms ratio need to be well regulated to avoid a possible digester failure. This is due to the fact that these parameters directly affect the micro-organisms' activity in the digester.

In this regard, a lot of research work has been done to improve the performance of fluidised bed reactors in the treatment of distillery effluent. One of the improvements which has been

made is the application of appropriate biomass support material with a large surface area such as zeolite or activated carbon (Fernández et al., 2008). These support materials have the advantage in that they have a high capacity to carry micro-organisms, thereby increasing the contact between the pollutants and the microbes leading to an increased reaction rate (Montalvo et al., 2012). Also, the effect of superficial liquid velocity has been studied as this affects both mixing and microbial growth (Jaafari et al., 2014). For instance, operating a fluidised bed reactor at an excessively high superficial liquid velocity results in dislodging of the microbes attached onto the carrier resulting in reduced efficiency, while operating at very low velocities hinders adequate mixing (Rabah & Dahab, 2004; Jaafari et al., 2014)

It is therefore important to obtain important information regarding the state of the reactor during anaerobic digestion to avoid impending reactor failure due to poor operation. Kinetic modelling is an acceptable approach in determining the condition in the bioreactor based on substrate utilization and microbial growth (Senturk et al., 2013). The result of kinetic modelling can be used to determine suitable system parameters which leads to stability and therefore high efficiency of the reactor. Moreover, the results obtained from the kinetic modelling can be used to design an industrial-scale reactor operating under similar conditions. In this study, anaerobic digestion was carried out in a fluidised bed reactor and its operation defined using various kinetic models in order to determine the suitable reactor operating conditions.

4.2 Methodology

4.2.1 Experimental set up

The fluidized bed used had an internal diameter of 118 mm and height of 760 mm with a total and working volume of 8.3 L and 6 L respectively. The reactor was packed with 50 g of zeolite (particle size 150 – 300 μm) and fluidisation was attained by the recycle stream using a centrifugal pump (Figure 4-1). The superficial velocity was maintained at about 0.6 cm/s and monitored by a flow meter. The reactor was fed using a peristaltic pump and the biogas produced was collected using the water displacement method.

4.2.2 Start-up and operation of the bioreactor

The start-up of the reactor was first carried out in batch, and then followed by continuous mode. In the batch start-up, the reactor was first inoculated with cow dung slurry filtered through 0.3 mm sieve to remove large particulate solids (Hampannavar & Shivayogimath, 2010). Diluted distillery effluent (COD =650 mg/l) and glucose (COD= 400 mg/l) in the ratio of 1:1 was then added to the cow dung slurry in the reactor and digestion allowed to proceed for 15 days while monitoring pH, COD, biogas and methane.

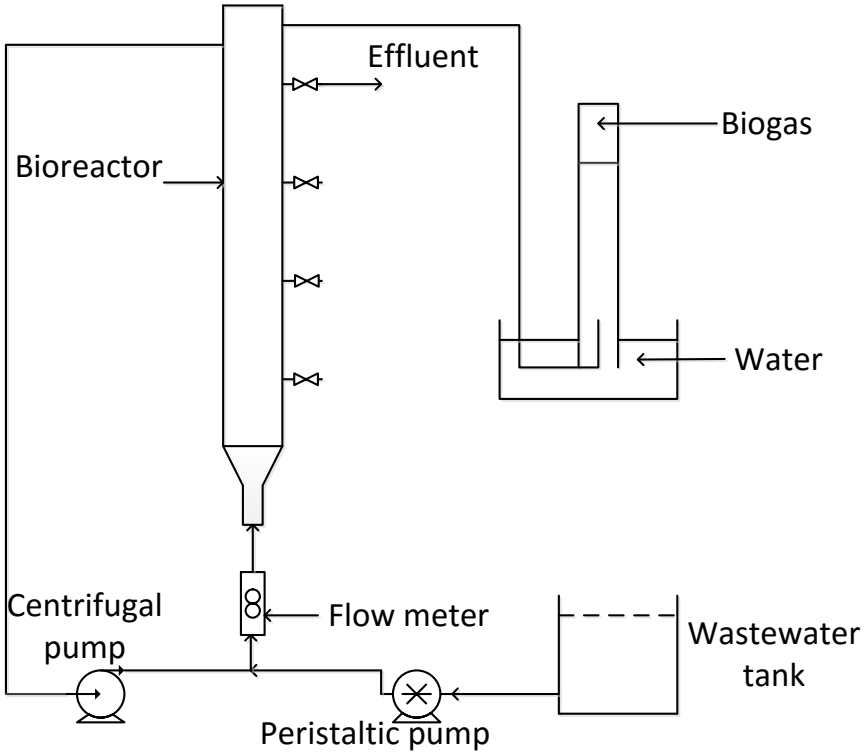

Figure 4-1: Set up of the fluidised bed anaerobic digester.

Once biogas production had stopped, fresh feed was added to the reactor with the concentration of distillery effluent gradually increased step-wise as the concentration of glucose was reduced such that the ratio of glucose to distillery wastewater was reduced progressively in the order 1:1, 1:1.5, 1:2, 1:4, and 0:1 for another 15 days. The ratio was changed every time stability had been achieved. By the 30th day the reactor could achieve 80% TOC reduction with methane production of about 65% and the pH and alkalinity were stable. The operation of the reactor was then changed from batch to continuous at mesophilic condition with low organic loading of 0.33 kg COD/m^3.d at HRT of 6 days for 3 retentions. At this point the reactor was very stable as was indicated by constant daily methane production, nearly constant effluent COD and nearly constant pH (Fernández et al., 2008). Once stable conditions were attained, the reactor was operated at organic loading rates (OLR) ranging between 0.33 and 9 kg COD/m^3.d corresponding to 0.25 to 8.1 kg TOC/m^3.d at constant hydraulic retention time (HRT) of 6 at a feed flow rate of 1 L/d.

4.2.3 Experimental analysis

Total organic carbon was analysed using a TOC analyser (TELEDYNE Tekmar). Dissolved organic carbon was analysed in the similar manner as TOC except that the samples were filtered

through a 0.45 μm filter syringe. Gas was analysed using a gas chromatograph (Trace 1310 gas chromatograph) fitted with a thermal conductivity detector, while colour was analysed using UV-Vis spectrophotometer (T80 + UV/VIS Spectrophotometer, PG instruments Ltd). Alkalinity was analysed according to the standard method for wastewater analysis involving titrating samples against 0.02N H_2SO_4 solution. Biomass concentration was determined as volatile suspended solids. The volatile suspended solids were determined by evaporating the residue obtained from centrifuged samples at 105 ^oC for 24 hours (until constant mass was obtained) then calcined at 450 ^oC for an hour.

4.3 Results and discussion

The TOC and colour reduction efficiencies were found to slightly increase with an increase in HRT (Table 4-1). This was due to the fact that at high HRT the substrate had a higher residence time in the reactor than at low HRT. The more time in the reactor means increased contact with micro-organisms leading to higher removal efficiency. The colour reduction efficiency was found to be much lower than that of the TOC due to the presence of biorecalcitrant components of distillery effluent which cause colour. The biorecalcitrant component is majorly melanoidin (Wang et al., 2011)

Table 4-1: Parameters and efficiencies of the fluidised bed reactor at constant feed concentration.

			Influent		Effluent		Efficiency	
HRT (d)	OLR kg TOC/m^3.d	Influent flow, Q (l/d)	tTOC (g/l)	sTOC (g/l)	tTOC (g/l)	sTOC (g/l)	TOC removal%	Colour removal%
3	1.77	2	5.82	5.315	1.56	1.151	78	34
6	0.88	1	5.82	5.315	1.3	0.803	85	40
10	0.53	0.6	5.82	5.315	1.18	0.635	88	50
15	0.35	0.4	5.82	5.315	1.04	0.552	90	52
20	0.26	0.3	5.82	5.315	0.89	0.472	91	54

4.3.1 Substrate balance model

Substrate balance around the reactor was formulated based on the following assumption (Borja et al., 2002; Rincón et al., 2006): The assumption was that the anaerobic reactor operated at steady-state conditions as depicted by nearly constant effluent substrate concentration, and biogas production rate. Further assumption was that, even though the feed carried suspended solids (SS) it was too little as it was only 2.3% of the feed total TOC; this SS was assumed to be biodegradable, thus it was considered that the volatile suspended solids (VSS) in the reactor and effluent corresponded to generated biomass.

Therefore, TOC balance for the reactor could be expressed as:

$$(tTOC)_o = (sTOC)_e + (tTOC)_{biogas} + (tTOCvss)_e + (tTOC)_m \quad (1)$$

where $(tTOC)_o$ is the influent total TOC, $(sTOC)_e$ is soluble TOC in the effluent, $(tTOC)_{biogas}$ is the fraction of $(tTOC)_o$ converted into biogas, $(tTOC_{vss})_e$ is the fraction of $(tTOC)_o$ converted into biomass and $(tTOC)_m$ is the fraction of $(tTOC)_o$ used for cell maintenance and growth.

Considering feed flow rate and methane flow rate, equation (1) can be expressed as:

$$QS_{to} = QS_e + qCH_4Y_{s/g} + q(S_{te}-S_{se}) + K_mXV \quad (2)$$

where Q is the feed flow rate (Ld^{-1}), S_{to} is the feed concentration (g $tTOCL^{-1}$), S_{te} is the total effluent concentration (g $tTOCL^{-1}$), S_{se} is the soluble effluent concentration (g $sTOCL^{-1}$), qCH_4 is methane production rate (LCH_4d^{-1}), $Y_{substrate/gas}$ is the coefficient of substrate conversion into methane (g $tTOCL^{-1}CH_4$), K_m is cell maintenance coefficient, X and V are biomass concentration and reactor volume (L), respectively.

On rearrangement, equation (2) can be written as:

$$q(S_{to}-S_{te}) = qCH_4Y_{s/g} + k_mXV \quad (3)$$

Since HRT=V/q, by dividing both sides by V, equation (3) becomes:

$$(S_{to}-S_{te})/HRT = qCH_4Y_{s/g}/V + XK_m \quad (4)$$

From equation (4), a plot of $(S_{to}-S_{te})/HRT$ versus qCH_4/V gives a straight line with slope equal to Ys/g and y-axis intercept equals to XK_m. In Figure 4-2 the plot supports the validity of this model in describing the anaerobic process in this particular study with a regression coefficient of 0.996. The y-axis intercept was very small indicating that a very small portion of the feed TOC was used for cell maintenance. The Ys/g value was found to be 3.58 g $tTOC/LCH_4$. The inverse of the Ys/g which is Yg/s is the methane yield coefficient which was found to be 0.28 LCH_4/g tTOC corresponding to 0.257 L CH_4/g COD. This is close to theoretical methane yield of 0.35 LCH_4/g tTOC when glucose is used as substrate (Fernández et al., 2008).

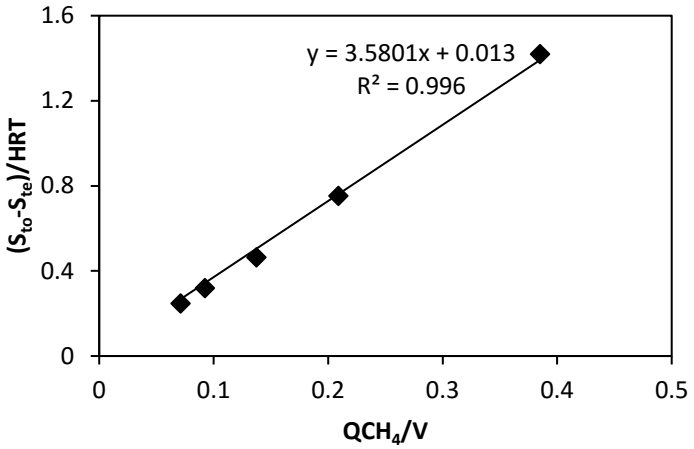

Figure 4-2: Determination of methane yield coefficient

The fraction of influent tTOC converted into biogas, biomass and that which is in the effluent can be calculated from equation (1) by expressing each term in the right hand side as a fraction of $(tTOC)_o$. Figure 4-3a shows the percentages of TOC converted into biogas, biomass and unremoved TOC, it was found that, generally, most of the feed TOC was converted into biogas. The percentage converted into biogas increased slightly with an increase in HRT. This suggests that at high HRT, the feed had higher residence time in the reactor thus achieving maximum conversion than at lower HRT where residence time is shorter. The proportion of feed converted into biomass was nearly constant at various HRTs while there was a slight decrease in proportion of feed in the effluent with an increase in HRT. However, the proportion of feed TOC converted into biogas, biomass and that which remained in the effluent does not give a very clear indication of the possible characteristics of the effluent in terms of residual pollution load as it only presents percentages. Figure 4-3b shows the actual amount of TOC converted and the residual TOC in the effluent. The information on the amount of residual TOC in the effluent is necessary as it determines whether a post-treatment technique is required or not. Moreover, determination of the amount of biomass in effluent is necessary, more so, if photodegradation is to be applied as a post-treatment. This is due to the fact that for photodegradation as a post-treatment technique, quantification of the biomass generated in AD step is necessary as suspended biomass may lead to light attenuation during UV photodegradation. Besides, determination of biomass yield is necessary in designing a system for sludge handling.

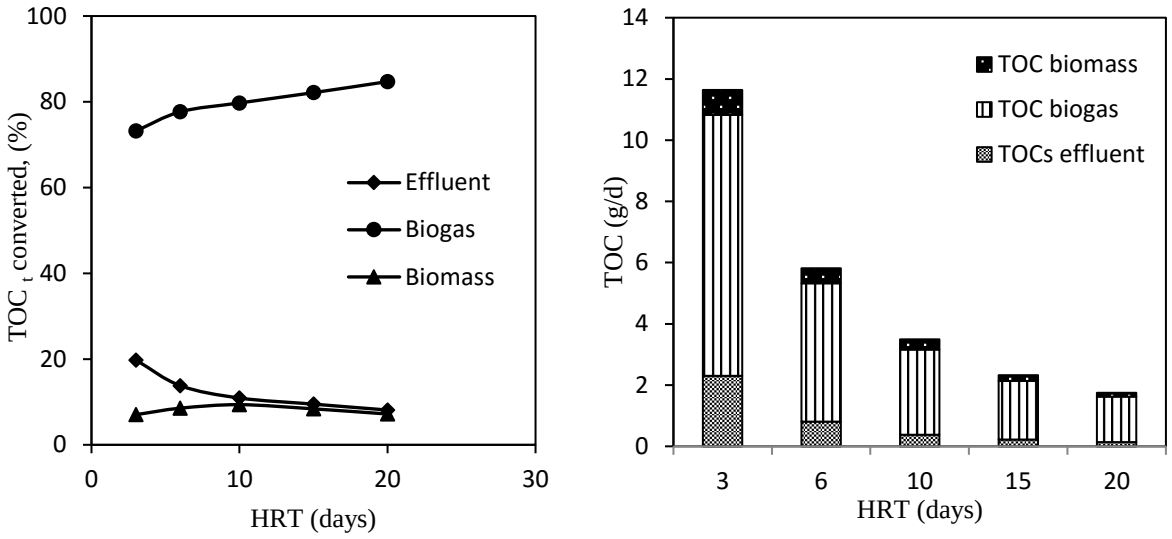

Figure 4-3: (a) Fraction and (b) actual amount of feed TOC converted into biogas biomass and that which remained in the effluent.

4.3.2 Biorecalcitrant component of distillery effluent.

Distillery effluent is considered as fairly biodegradable with traces of biorecalcitrant compounds such as melanoidins (Acharya et al., 2008). The biodegradability of the distillery effluent was measured by determining the BOD_5/COD ratio and it was found to be 0.41 indicating that the distillery effluent is fairly biodegradable. Good biodegradability is achieved when BOD_5/COD is greater than 0.4 (Rizzo, 2011). However, the recalcitrant parts of distillery effluent which are majorly melanoidins often pass through anaerobic treatment without being degraded and they impart a dark colour to biomethanated effluent (Satyawali & Balakrishnan, 2008; Kalavathi et al., 2001). The amount of non-biodegradable component can be determined by the relationship between the organics remaining after digestion and HRT. It is proposed that a plot of Ln($COD_{effluent}$ or $TOC_{effluent}$) against 1/HRT gives a straight line, and recalcitrant component can be calculated at infinite HRT. A similar model has been applied in the determination of biodegradable component of some food waste wastewater (Rincón et al., 2006; Borja et al., 2002). In Figure 4-4, the amount of non-biodegradable component is calculated as TOC or COD equivalent at y-axis intercept when HRT is infinite. It was found that the non-biodegradable TOC and COD were 477 mg/l and 756 mg/l, respectively, under prevailing digestion conditions. The amount of non-biodegradable COD was higher than that of TOC due to the fact that TOC only caters for carbons while COD caters for all oxidizable compounds in wastewater. Apart from organics, distillery effluent has high concentrations of cations and halogen ions (Satyawali & Balakrishnan, 2008). Considering that the influent TOC was 5318 mg/l, the non-biodegradable TOC only formed ~9% of the feed TOC indicating that

distillery effluent is biodegradable. However, the non-biodegradable portion is majorly melanoidins which impart a dark brown colour to distillery effluent (Kalavathi et al., 2001; Satyawali & Balakrishnan, 2008). Thus anaerobic treatment of distillery effluent is not effective for colour removal as shown in Table 4-1.

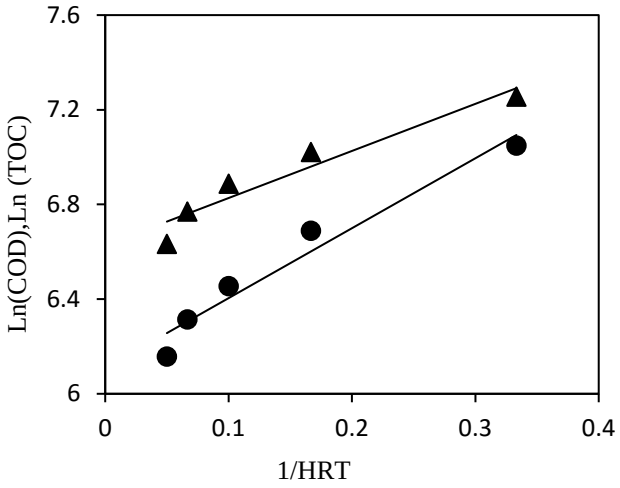

Figure 4-4: Determination of recalcitrant component of distillery effluent, TOC (●) and COD (▲).

4.3.3 Substrate utilization kinetics

The kinetics of degradation of total and biodegradable constituents of the effluent were compared applying first order rate model:

$$\ln\left(\frac{S_e}{S_o}\right) = kt \qquad (5)$$

where S_o and S_e are feed and effluent TOC respectively, *k* is rate constant (d^{-1}) and t is HRT (days). For the biodegradable component, the S_o and S_e were modified to S_{ob} and S_{eb} for biodegradable feed and effluent, respectively. Figure 4-5 shows that the rate of uptake of biodegradable constituent was four times faster than that of the total organic compounds in the wastewater sample. The uptake of the biodegradation component fitted first order kinetics better than that of total organic substrate with R^2 values of 0.9754 and 0.9096, respectively. The difference can be attributed to a larger proportion of undigested TOC when considering total feed TOC than in the case of biodegradable TOC, due to slow degradation of the recalcitrant components.

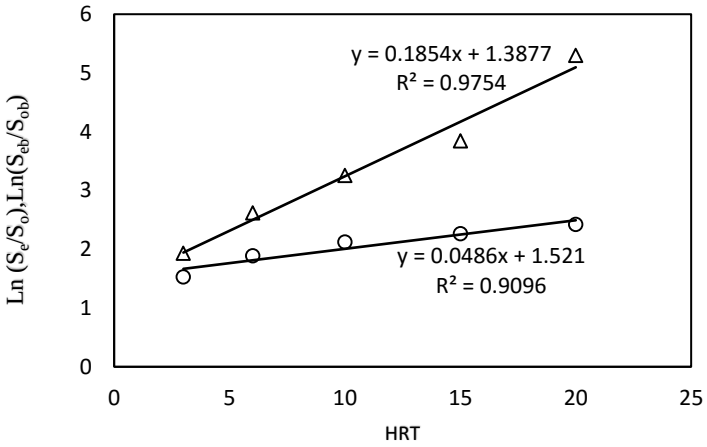

Figure 4-5: First-order reaction kinetic of biodegradable and total organic carbon, biodegradable TOC (∆) and total TOC (○).

4.3.4 Michaelis-Menten kinetic model

According to the Michaelis-Menten kinetic model, the specific substrate utilisation rate and biodegradable substrate concentration can be related by the following equation:

$$r = \frac{kS_b}{(K_s + S_b)} \quad (6)$$

where r is the specific substrate utilization rate, k is the maximum substrate utilisation rate (g $sTOCg^{-1}VSSd^{-1}$), S_b is the concentration of the biodegradable substrate in the reactor and K_s is the Michaelis constant. The non-biodegradable TOC obtained in Figure 4-4 was subtracted from the experimental total TOC to obtain the biodegradable TOC in this experiment (Rincón et al., 2006). The specific substrate utilization rate can be expressed as (Rincón et al., 2006):

$$r = \frac{(S_o - S_b)}{HRT.X} \quad (7)$$

where S_o is the biodegradable feed concentration and X is the biomass concentration in the reactor (g $VSSL^{-1}$). By combining equations 6 & 7, we obtain equation 8. The specific substrate utilization rate (r) is plotted against S_b (Figure 4-6).

$$r = \frac{(S_o - S_b)}{HRT.X} = \frac{kS_b}{(K_s + S_b)} \quad (8)$$

The plot was found to represent a hyperbolic function which is an indication that the substrate utilization followed the Michaelis-Menten model (Borja et al., 2002).

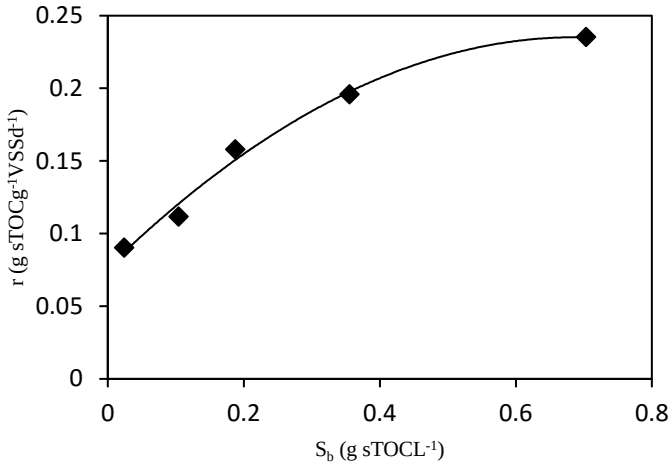

Figure 4-6: Specific substrate utilization rate against biodegradable TOC in the reactor.

To determine k and K_s, equation 8 was linearized as (Eqn 9) and 1/r was plotted against $1/S_b$ where K_s was determined from the slope and k from the y intercept. Accordingly, from Figure 4-7, the values of k and K_s were found to be 0.2916 g $sTOCg^{-1}VSSd^{-1}$ and 0.166 g sTOC L^{-1}. Senturk et al. (2013) reported a maximum substrate utilization rate (k) of 0.106 g sCOD $g^{-1}VSSd^{-1}$ and K_s value of 0.535 g $sCODL^{-1}$.

$$\frac{1}{r} = \frac{K_s}{k}\left(\frac{1}{S_b}\right) + \frac{1}{k} \tag{9}$$

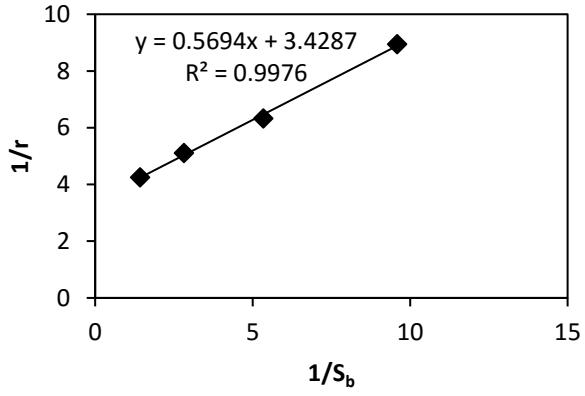

Figure 4-7: A plot of 1/r against $1/S_b$ for determination of K and Ks

If the values of k and K_s are substituted in equation 6, the theoretical rate of substrate uptake can be determined (Rincón et al., 2006). Figure 4-8 shows that the model predicts well the kinetic activity of the micro-organisms involved in the degradation. The model strongly depicts the behaviour of the reactor at experimental r values greater than 0.09 g sTOC g^{-1} $VSSd^{-1}$.

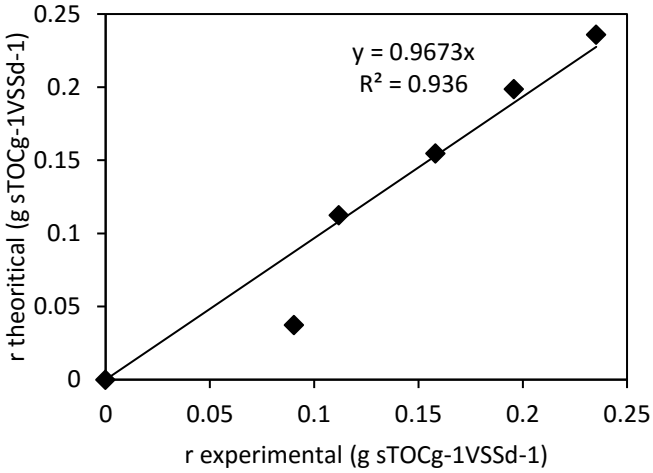

Figure 4-8: A comparison of the theoretical and experimental specific substrate utilization rate.

4.3.5 The mean cell residence time

The mean cell residence time (MCRT) or sludge retention time (SRT) also known as sludge age is the average amount of time the anaerobic micro-organisms are retained in the reactor. The MCRT directly affects the kinetics of substrate utilization, biogas production and sludge production. It also affects micro-organisms' growth kinetics since the time spent in the reactor determines feed-microbes contact time which affects growth. It is a function of biosolids in the system and rate of biosolids loss from the system. Mean cell residence time is calculated as (Ng et al., 2006):

$$\theta = \frac{B_r \,.\, V}{Q.B_{eff}} \qquad (10)$$

where θ is mean cell residence time (days), B_r is the concentration of biomass in the reactor (g VSS/L), V is the reactor volume (L), Q is effluent flow rate (L/d) and B_{eff} is the biomass concentration in the effluent (g VSS/L). The mean cell residence time can be related to the specific substrate utilization rate as (Nweke et al., 2014):

$$\frac{1}{\theta} = Yr - K_d \qquad (11)$$

where r is the specific rate of substrate utilization, Y is the microbial growth yield (biomass yield) and K_d is the endogenous decay coefficient (d^{-1}). This correlation helps to calculate Y and K_d and these two parameters are very significant as biomass yield can be applied to estimate the amount of sludge produced during anaerobic treatment, while K_d is used to calculate the net amount of sludge to be handled. This information can be useful in choosing and designing a post-treatment system. In case UV photodegradation is to be applied as an appropriate post-

treatment method, then sludge production should be minimised or an appropriate method should be applied to remove the sludge produced. If not regulated or removed, suspended sludge will lead to light attenuation thereby reducing the efficiency of the UV post treatment process. A plot of 1/θ against r gives a straight line with Y as gradient and y-axis intercept as the $K_{d.}$ In Figure 4-9 the Y value was found to be 0.4658 g/g while K_d was 0.0293d^{-1}. This compares well with the values in literature of 0.357 g/g and 0.083d^{-1} for Y and K_d, respectively (Enitan & Adeyemo, 2014). The specific rate of substrate utilization has an inverse relationship with the MCRT due to the fact that low MCRT is achieved at high feed flow rate which translates into higher OLR. Therefore, there is a lot more substrate available as feed at low MCRT than at high MCRT. However, this also depends and interlinks with micro-organisms' growth kinetics and food to micro-organism ratio at any time in the reactor.

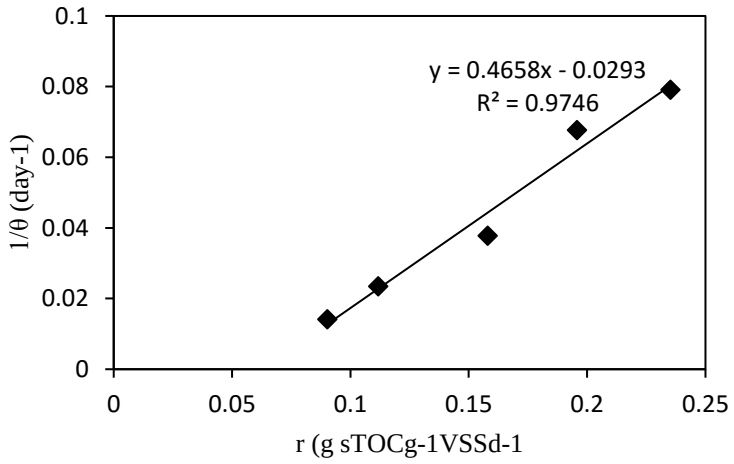

Figure 4-9: Correlation between sludge age and specific substrate utilization rate

4.3.6 Micro-organisms' growth kinetics

Substrate utilization rate and methane production rate are functions of the micro-organism population in the reactor. Micro-organisms present in sufficient amounts effectively convert substrate into methane, whereas the process can be inhibited if the amount of micro-organisms is below a given limit as compared to the available feed. It is therefore important to monitor the rate of micro-organism growth in the reactor. Micro-organisms' growth rate is a function of biomass yield. Maximum specific micro-organisms' growth rate (μ_{max}) (d^{-1}) can be determined using Y (g/g) and K (g $sTOCg^{-1}VSSd^{-1}$).

$$K = \frac{\mu_{max}}{Y} \quad (12)$$

The maximum micro-organisms' growth rate was found to be 0.1358 d^{-1}. Considering Monod equation which relates the specific micro-organisms' growth rate with substrate concentration as follows (Yu et al., 2013);

$$\mu = \mu_{max} \frac{S}{K_s + S} - K_d \quad (13)$$

where μ is the specific growth rate of the microorganisms, μ_{max} is the maximum specific growth rate of the microorganisms, S is the concentration of the limiting substrate for growth, K_d is the endogenous decay coefficient, K_s is the substrate utilization constant which is numerically equal to the substrate concentration when $\mu = ½\ \mu_{max}$.

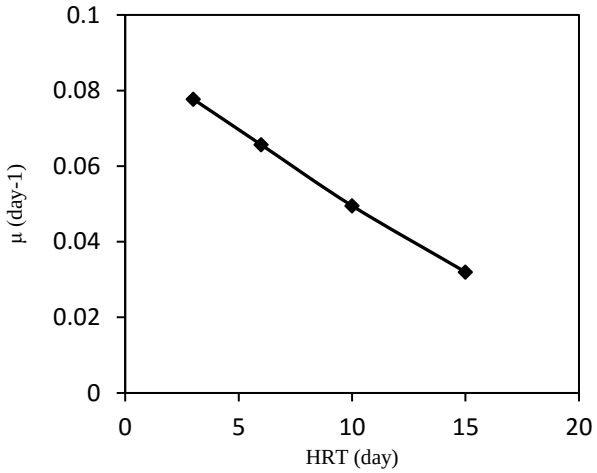

Figure 4-10: Specific micro-organisms growth rate as a function of HRT at constant feed concentration.

In Figure 4-10 the net specific growth rate of the micro-organisms reduced with an increase in HRT. This may be due to the fact that at low HRT more feed was available in the reactor due to the high flow rates applied than at high HRTs when less food is available. At low HRT, the high organic loading rate, which did not show any substantial organic loading shock, (as indicated by pH and alkalinity in Table 4-2) led to increased activity of the microorganisms resulting in higher specific growth rate. The slight increase in pH can be due to the consumption of VFAs which results in a corresponding slight increase in alkalinity.

Table 4-2: pH and alkalinity values during AD process.

HRT (d)	3	6	10	15	20
pH	7.21	7.34	7.5	7.4	7.4
Alkalinity (mg/l)	2320	2840	3020	3040	3018

4.3.7 Food to micro-organisms ratio

Food to micro-organisms ratio (F:M) is the amount of biodegradable substrate exposed to micro-organisms per day. The F:M can be used as a parameter to evaluate the performance of a digester as it can directly affect the TOC conversion efficiency (substrate utilization rate), methane production rate and sludge production (Perez et al., 2001). The F:M can be calculated as:

$$\frac{F}{M} = \frac{Q.S_0}{B_r.V} \quad (14)$$

where Q is the feed flow (L/d), S_o is the feed concentration (g TOC/L), B_r is the biomass concentration in the reactor (g VSS/L) and V is the volume of the reactor. Table 4-3 shows the effect of F:M on biogas production rate and methane yield. Biogas production increased with an increase in F:M while methane composition of the biogas reduced slightly after F:M values 0.16 g TOC/g VSS.d and above. The increase in gas production with an increase in F:M can be due to the fact that more feed was available for digestion at higher F:M ratios. The reduction in methane composition at higher F:M values cannot be attributed to organic overloading as the VFA to alkalinity ratio (Table 4-3) showed that it was at a value under which reactor is stable. The reactor is stable when this ratio is below 0.3 to 0.4 (Hampannavar & Shivayogimath, 2010). According to Cardinali-Rezende et al. (2013) variation in F:M ratio has an impact on the diversity of micro-organisms in the reactor and this directly affects methanogenic activity. The study reported that shifts in the composition of methanogenic community at different F:M values can lead to variation in pathway of methane formation. The study showed that at high F:M, acetotrophic methanogens are in abundance and methane is produced majorly via the acetate route while at low F:M there is a mixture of hydrogenotrophic, methylotrophic and acetotrophic methanogens and therefore methane production is through multiple pathways. This can explain the superior methane quality at lower F:M compared to higher F:M values.

Table 4-3: Performance of the reactor at different F:M values.

F/M	VFA/alk	biogas (l/d)	CH_4%	$TOC_{effluent}/TOC_{feed}$
0.27	0.34	3.3	70	0.22
0.21	0.26	1.75	71.6	0.15
0.16	0.24	1.1	75	0.12
0.11	0.23	0.74	75	0.10
0.09	0.22	0.58	74.5	0.09

There was a slight decrease in TOC reduction with an increase in F:M. This observation may be due to high organic load at high F:M, which means there was excess feed for microbes to degrade while at low F:M the micro-organisms population was sufficient to consume most of the feed. Similar observations have been reported by Perez et al. (2001). Alternatively, the reduction in efficiency at high F:M could be attributed to the low MCRT attained (Figure 4-11) due to high flow rate. Moreover, even though there is an increase in feeding rate at high F:M, there is also a corresponding increase in biomass as compared to that at low F:M due to the increase in the available food which results in a rapid cell growth. Therefore, the relative increase in biomass at a fixed reactor volume can increase the viscosity of the wastewater in the reactor due to the increase in VSS leading to mass transfer hindrance. Cardinali-Rezende et al. (2013) reported a decrease in bacterial cell density at lower F:M than at higher F:M, however, a higher bacterial diversity was recorded at low F:M than at higher F:M. Therefore, the high bacterial diversity at low F:M could degrade more diversified substrate leading to high substrate conversion. Generally, at high F:M the amount of biomass available was not sufficient to remove a substantial amount of TOC; similar observations have been reported (Hafez et al., 2012; Perez et al., 2001).

4.3.8 MCRT and HRT

The total duration the biomass resides in the reactor as compared to liquid retention time is an important factor in anaerobic wastewater treatment. In Figure 4-11 the mean cell residence time (MCRT) was compared to hydraulic retention time (HRT) at various F:M. Generally, the MCRT was always at least 2.5 times higher than the HRT. The higher MCRT as compared to HRT can be attributed to the fact that biomass was attached onto zeolite thus being retained in the reactor instead of being washed out by the effluent. The advantage of attached biomass is that the biomass is able to reside in the reactor for a longer time fostering adaptation to the environment than if old cells are frequently replaced by new ones in a case where the biomass

is not attached in the reactor. Attachment also ensures that a sufficient amount of biomass is usually in the reactor thereby ensuring high efficiency.

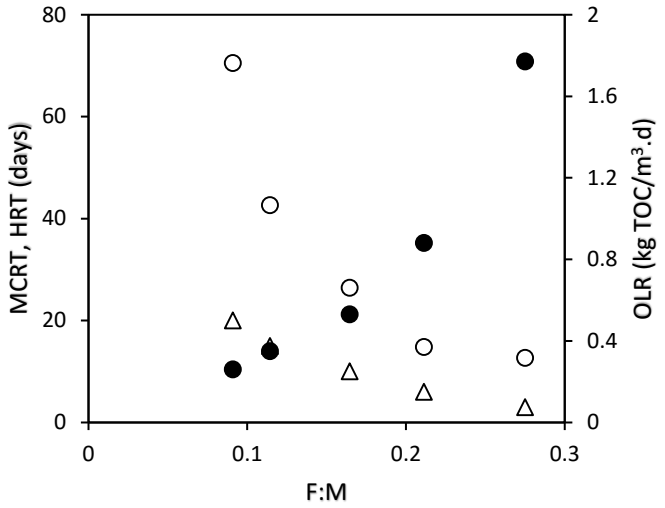

Figure 4-11: A comparison of HRT and MCRT at different F:M values, HRT (∆), MCRT (○) and corresponding OLR (●).

The specific rate of substrate utilization, r, (g TOC/gVSS.d) at various F:M values were evaluated. In Figure 4-12 it was found that r increased linearly with an increase in F:M. This is an indication that at low F:M the micro-organisms were near starvation as the feed was little. As the feed increased, thus increasing F:M, the TOC uptake per unit biomass mass increased as there was sufficient feed.

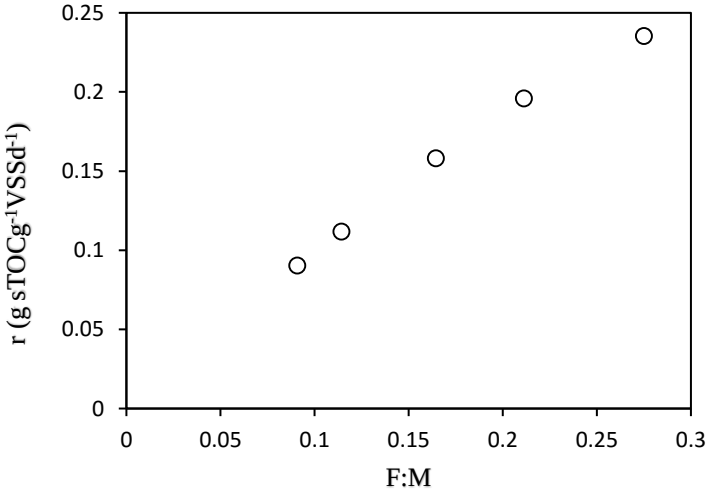

Figure 4-12: Effect of F:M on specific substrate utilization rate.

4.3.9 Effect of organic loading rate on anaerobic digestion

The effect of OLR at fixed HRT was studied and the kinetics of biogas production and organic removal were analysed. The influent COD was varied as: 2, 5.8, 19.7, 37.1 and 54.2 g/L at constant feed flow rate of 1 L/d corresponding to HRT of 6 days. This corresponded to OLR of 0.33, 0.97, 3.3, 6.1 and 9 kg COD/m^3.d, respectively as shown in Table 4-4.

Table 4-4: Feed and effluent characteristics at various OLR and fixed HRT.

OLR (kg COD/m^3.d)	Feed		Effluent	
	COD (mg/L)	TOC (mg/L)	COD (mg/L	TOC (mg/L)
0.33	2108	1384	306	252
0.97	5807	4230	740	520
3.3	19700	12680	4620	2300
6.2	37100	30900	10400	6030
9	54200	41700	19800	13500

4.3.10 Effect of OLR on biogas production rate

During the study, steady state in each OLR was indicated by constant biogas production, constant methane production, constant pH and constant effluent COD concentration for at least three consecutive days after running the experiments for 2-3 HRTs for each OLR (Fernández et al., 2008). Figure 4-13 shows that biogas production rate increased with an increase in OLR. This was due to the increase in the available organic substrate which could be consumed by the micro-organisms. This may be an indication that the activity of the consortia of biogas-producing bacteria was not hampered with in the OLR range studied (Fernández et al., 2008). Figure 4-13 further shows that, for low OLR (0.33-3.28 kg COD/m^3.d), the stability of the reactor was achieved faster than for higher OLR (6.2-9 kg COD/m^3.d) as indicated by the effluent load implying that at higher concentrations microorganisms need a longer time to adapt. An increase in effluent COD with the increase in OLR was observed; this has been reported in continuous anaerobic digestion of distillery effluent and other various effluents (Acharya et al., 2008; Borja, 2001; Wang & Wu, 2004).

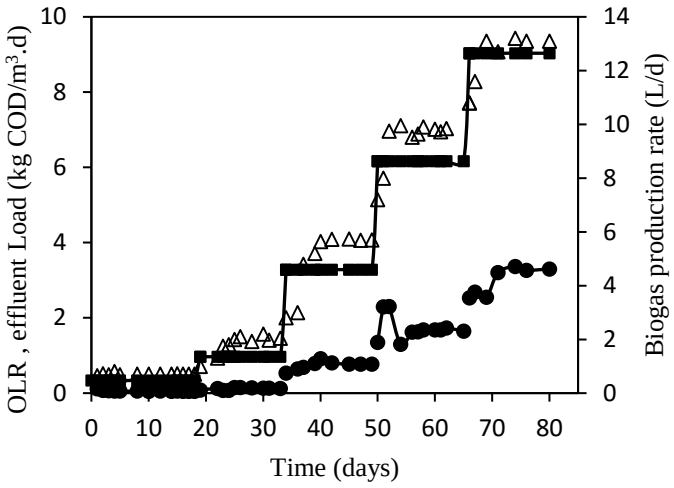

Figure 4-13: Effect of OLR on biogas production and effluent load, OLR (■), biogas production rate (Δ) and effluent load (●)

4.3.11 Effect of OLR on Methane production

Analysis of the methane proportion of the biogas produced at different OLR showed that biogas with methane content of above 63% was produced up to OLR of 6 kg COD/m^3 while at 9 kg COD/m^3it dropped to 33% (Figure 4-14). This indicated that high OLR led to inhibition of methanogenesis due to organic overloading. Organic overloading may lead to production of high amounts of volatile fatty acids that cause acidity as shown in Figure 4-19. Consequently, high acidity in the reactor compromises the ability of the digester to buffer itself as methanogensis is hindered while acidogenesis is favoured.

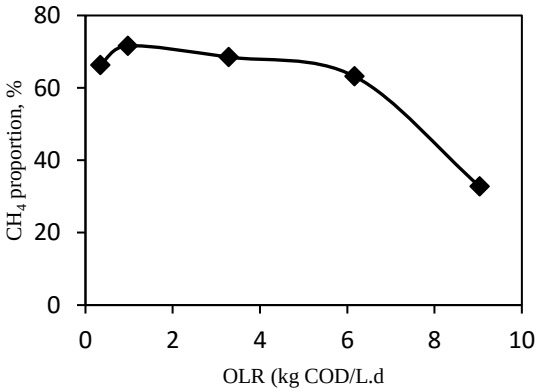

Figure 4-14: The effect of OLR on methane composition.

4.3.12 Methane production rate and methane yield coefficient

In Figure 4-15, methane production rate was found to increase with an increase in OLR up to organic loading rate of 9 kg COD/m^3. Below this OLR, the reactor was stable and the organic load feed could efficiently be converted into biogas indicating that the methanogesis was not

inhibited. Methane yield of between 0.29 and 0.23 L/g COD was recorded during steady operation, however at 6 kg COD/m^3 the methane coefficient dropped to 0.124 L/g COD. Generally, theoretical methane coefficient is considered to be 0.35 L/g COD , assuming that all of the COD fed into the reactor is transformed into methane and there are no biorecalcitrant components of the feed, also assuming further, that there is no COD used for cell growth and cell maintenance (Borja et al., 2004). Moreover, the presence of other substances like sulphates which leads to the consumption of COD without producing methane via the sulphate reducing bacteria pathway is not accounted for in this case (Fernández et al., 2008). Values close to theoretical yield can be obtained if a biodegradable substrate like glucose is used (Borja, 2001).

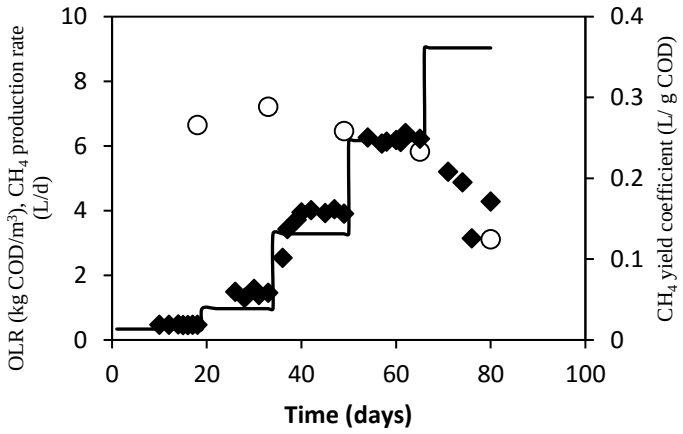

Figure 4-15: Effect of OLR (—) on volumetric methane production rate (■) and methane yield coefficient (○).

4.3.13 Effect of OLR on COD and colour reduction

The performance of wastewater treatment system is evaluated on the basis of the pollution reduction efficiency. The efficiency of the system in COD and colour reduction was evaluated at different OLR (Figure 4-16). A COD reduction of 85% was achieved at lower OLR while at high OLR the efficiency reduced to 64%. At OLR of 6 kg COD/m^3.d, COD reduction of 73% could still be achieved. However, colour reduction was always low ranging between 56% and 21%, from low to high OLR. The low colour reduction is attributed to the presence of biorecalcitrant melanoidins in distillery effluent.

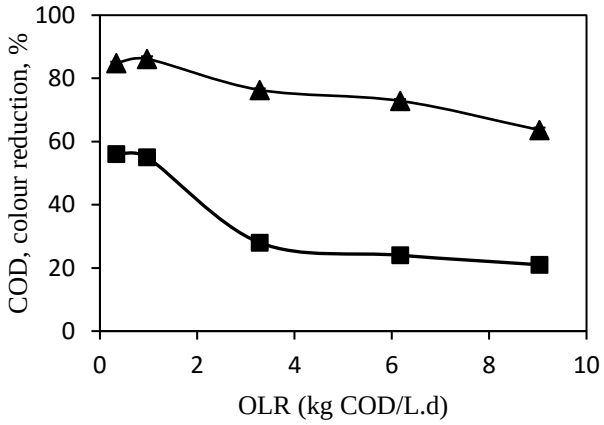

Figure 4-16. Effect of OLR on COD (▲) and colour (■) reduction efficiency.

4.3.14 COD reduction model

The investigation on the variation in COD removal rates with OLR showed that the removal rate increased linearly with OLR (Figure 4-16). The effect of feed concentration on the COD removal rate can be described by the following equation (Fernández et al., 2008; Borja et al., 2004);

$$R_s = K(S)^n \quad (15)$$

where R_s is the COD removal rate (kg COD/m^3.d), K is the reaction constant (d^{-1}), S is the feed substrate concentration (kg COD/m^3) and *n* is the reaction order. Considering first order reaction kinetics, *n* is equal to unity. Therefore, a plot of R_s against S gives a straight line with slope equal to K and y intercept equal to zero. This describes the influence of feed concentration on COD reduction rate. In Figure 4-17, the experimental data fitted the theoretical model with reaction constant equal to 0.67 d^{-1} and R^2 equal to 0.9806. A similar model has been used to describe anaerobic digestion in fluidised bed reactors (Borja et al., 2004; Fernández et al., 2008). The observed increase in COD removal rate with an increase in OLR can be attributed to a corresponding increase in the concentration gradient between the fluid and biofilm (Fernández et al., 2008). The increase in COD removal rate with an increase in feed concentration can also be attributed to the stability of the anaerobic fluidised bed reactor attributed to the immobilization of micro-organisms to small fluidised zeolite particles (Borja et al., 2004).

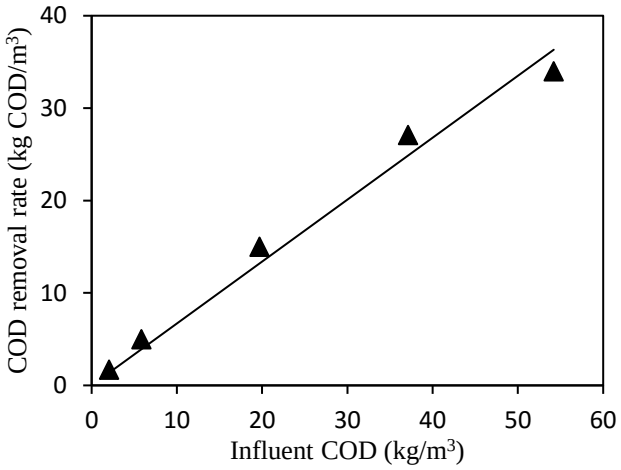

Figure 4-17: The effect of feed concentration on COD removal rate.

A model has been proposed to determine methane yield coefficient using experimental data of volumetric methane production rate and COD removed. Based on the assumption that the volume of methane produced per day is proportional to the amount of COD consumed, the following equation can be used to relate the parameters (Fernández et al., 2008);

$$\eta = Y_p Q(S_o - S_e) \quad (16)$$

where η is methane production rate (L/d), Y_p is the methane yield coefficient, Q is feed flow rate (L/d) S_o and S_e are feed and effluent concentrations (g COD/l), respectively.

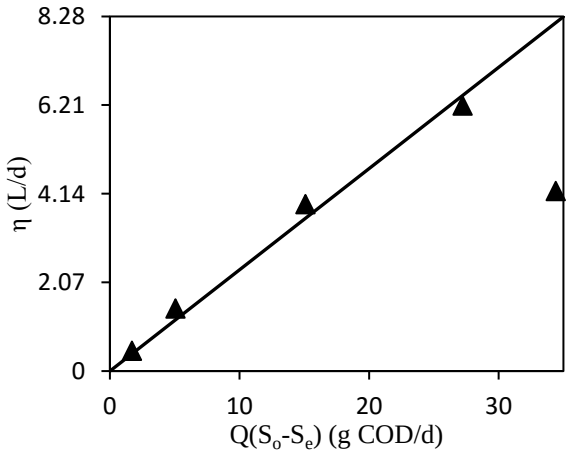

Figure 4-18: Variation of methane production rate with substrate removal.

A plot of V_{CH4} against $Q(S_o-S_e)$ in Figure 4-18 gives a straight line with a slope of 0.236 g COD/L corresponding to Y_p, for the first 4 OLR studied. However, the point corresponding to OLR of 9 kg COD/m^3 was out of the model limit. This is due to reactor instability caused by organic overloading which results in accumulation of VFAs (Fig. 18). A Y_p value of 0.29 g

COD/L was reported for anaerobic treatment of distillery effluent in a fluidised bed reactor (Fernández et al., 2008).

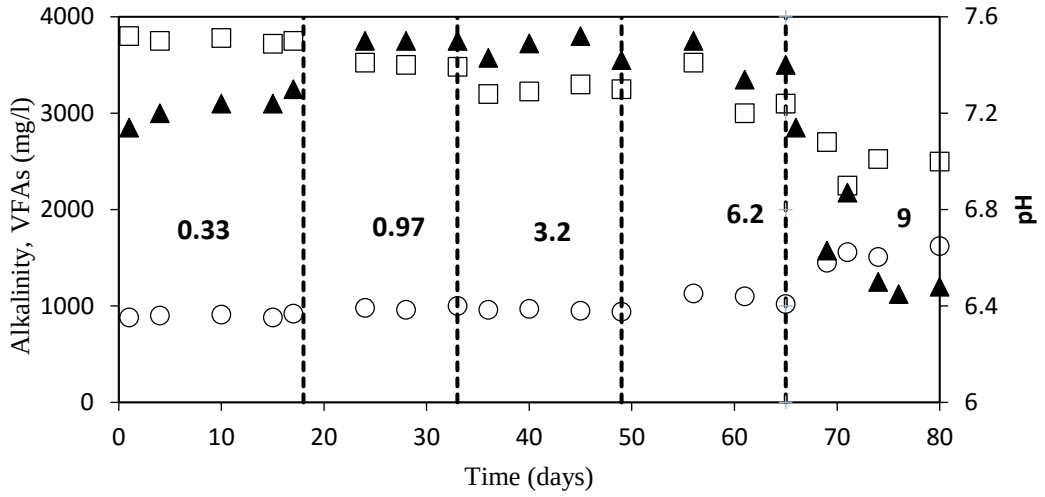

Figure 4-19: Alkalinity (□), VFAs (○) and pH (▲) profile during anaerobic digestion.

4.3.15 Alkalinity, Volatile fatty acids and pH

The balance between VFAs, alkalinity and pH can be used as a measure for biodigester stability. A stable reactor will operate at a pH range of 6.7-8 with total alkalinity higher than VFAs concentration. Figure 18 shows that the anaerobic process was stable until day 65 which marked the onset of operation at OLR of 9 kg COD/m^3. The reduction in methane composition (Figure 4-14) and the reduction in total alkalinity and pH with a corresponding increase in VFAs at high organic loading rate (Figure 4-19) is an indication that the process was unstable at 9 kg COD/m^3. In Fig 18, the pH dropped from stable value of about 7.3 to 6.4 at high OLR while alkalinity reduced from 3100 mg/l to 2500 mg/l as a result of VFA increase from 1020 mg/l to 1620 mg/l. The decrease in pH was as a result of high VFAs production rate. The increase in VFAs production led to an increase in the consumption of alkalinity causing a significant drop in alkalinity. Normally, the VFA/Alkalinity ratio is used to evaluate reactor stability, with a ratio below 0.3 to 0.4 indicating a stable operating reactor (Hampannavar & Shivayogimath, 2010; Borja et al. 2004). The VFA/Alkalinity ratio was always below 0.3 but it increased to above 0.5 at OLR of 9 kg COD/m^3 indicating instability.

4.3.16 Effect of OLR on biomass density

Determination of the amount of biomass in the reactor and in the effluent is important for two major reasons. Firstly, the microbial mass in the reactor is responsible for substrate conversion and maintaining their density is very important. Secondly, the amount of biomass in the effluent

can be used as an indication of microbial wash-out capacity. Moreover, information about biomass in effluent can be used when designing a post-treatment facility.

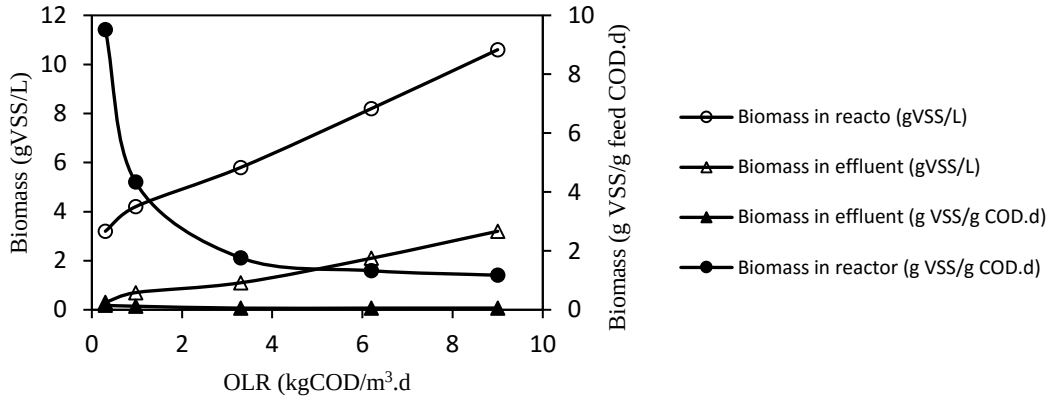

Figure 4-20: Effect of OLR on microbial density in the reactor and in the effluent.

Figure 4-20 shows the amount of biomass in the reactor and in the effluent where it was observed that the amount of biomass (g VSS/L) in reactor and in effluent increased with an increase in organic loading rate. However, the amount of biomass expressed as g VSS/g feed COD.d decreased with an increase in OLR in the reactor while it was always almost negligible for the effluent. The wide difference in the amount of biomass in the reactor from that in the effluent is an indication of biomass retention in the reactor and this can be attributed to zeolite which is a good biomass support.

Conclusion

The kinetics of a fluidised bed anaerobic digester treating distillery effluent was evaluated. Degradation in the reactor followed first order rate kinetics and the recalcitrant component of the effluent was determined to be ~ 10% TOC of the feed. The amount of the biorecalcitrant organic compounds suggested that a post-treatment method is required. The biorecalcitrant compounds were found to be the major colour causing compounds in distillery effluent. This was due to the fact that AD was ineffective in colour reduction despite a superior TOC reduction. The bioreactor was found to be stable when operating at an OLR of below 6 kg COD/m^3d, above this, there was accumulation of VFAs in the reactor. The zeolite applied in the reactor was very effective in biomass retention as the sludge retention time was 2.5 higher than the HRT. The maximum micro-organisms' growth rate was 0.136 d^{-1} and biomass yield was 0.4658 g/g. A micro-organisms' decay coefficient of 0.03 was an indication that the bioreactor effluent needed a settling tank for the removal of suspended biomass if photocatalysis is to be applied as a preferred post- treatment method.

References.

ACHARYA, B.K., MOHANA, S. & MADAMWAR, D. (2008). Anaerobic treatment of distillery spent wash - a study on upflow anaerobic fixed film bioreactor. *Bioresour. Technol*. 99. p.4621–6.

AIYUK, S., FORREZ, I., LIEVEN, D.K., VAN HAANDEL, A. & VERSTRAETE, W. (2006). Anaerobic and complementary treatment of domestic sewage in regions with hot climates--a review. *Bioresour. Technol*. 97. p.2225–41.

ANDALIB, M., HAFEZ, H., ELBESHBISHY, E., NAKHLA, G. & ZHU, J. (2012). Treatment of thin stillage in a high-rate anaerobic fluidized bed bioreactor (AFBR). *Bioresour. Technol*. 121. p.411–8.

BORJA, R. (2001). Performance evaluation of a mesophilic anaerobic fluidized-bed reactor treating wastewater derived from the production of proteins from extracted sunflower flour. *Bioresour. Technol.* 76. p.45–52.

BORJA, R., GONZALEZ, E., RAPOSO, F., MILLAN, F. & MARTIN, a. (2002). Kinetic analysis of the psychrophilic anaerobic digestion of wastewater derived from the production of proteins from extracted sunflower flour. *J Agric Food Chem*. 50. p.4628–4633.

BORJA, R., RINCÓN, B., RAPOSO, F., DOMÍNGUEZ, J.R., MILLÁN, F. & MARTÍN, A. (2004). Mesophilic anaerobic digestion in a fluidised-bed reactor of wastewater from the production of protein isolates from chickpea flour. *Process Biochem*. 39. p.1913–1921.

CARDINALI-REZENDE, J., ARAÚJO, J.C., ALMEIDA, P.G.S., CHERNICHARO, C. A L., SANZ, J.L., CHARTONE-SOUZA, E. & NASCIMENTO, A.M. a. (2013). Organic loading rate and food-to-microorganism ratio shape prokaryotic diversity in a demo-scale up-flow anaerobic sludge blanket reactor treating domestic wastewater. Antonie van Leeuwenhoek. *Int. J. Gen. Mol. Microbiol*. 104. p.993–1003.

ENITAN, A.M. & ADEYEMO, J. (2014). Estimation of Bio-Kinetic Coefficients for Treatment of Brewery Wastewater. 8. p.400–404.

FERNÁNDEZ, N., MONTALVO, S., BORJA, R., GUERRERO, L., SÁNCHEZ, E., CORTÉS, I., COLMENAREJO, M.F., TRAVIESO, L. & RAPOSO, F. (2008). Performance evaluation of an anaerobic fluidized bed reactor with natural zeolite as support material when treating high-strength distillery wastewater. *Renew. Energy.* 33. p.2458–2466.

HAFEZ, A.I., KHEDR, M.A. & OSMAN, R.M. (2012). Flax Retting Wastewater Part 1 : Anaerobic Treatment by Using UASB Reactor. p.191–200.

HAMPANNAVAR, U. & SHIVAYOGIMATH, C. (2010). Anaerobic treatment of sugar industry wastewater by Upflow anaerobic. *Int. J. Environ. Sci*. 1. p.631–639.

JAAFARI, J., MESDAGHINIA, A., NABIZADEH, R. & HOSEINI, M. (2014). Influence of upflow velocity on performance and biofilm characteristics of Anaerobic Fluidized Bed Reactor (AFBR) in treating high-strength wastewater. *Environ. Health*. p.1–10.

KALAVATHI, D., UMA, L. & SUBRAMANIAN, G. (2001). Degradation and metabolization

of the pigment—melanoidin in distillery effluent by the marine cyanobacterium *Oscillatoria boryana* BDU 92181. *Enzyme Microb. Technol*. 29. p.246–251.

MONTALVO, S., GUERRERO, L., BORJA, R., SÁNCHEZ, E., MILÁN, Z., CORTÉS, I. & ANGELES DE LA LA RUBIA, M. (2012). Application of natural zeolites in anaerobic digestion processes: A review. *Appl. Clay Sci*. 58. p.125–133.

NG, H.Y., TAN, T.W. & ONG, S.L. (2006). Membrane fouling of submerged membrane bioreactors: Impact of mean cell residence time and the contributing factors. *Environ. Sci. Technol.* 40. p.2706–2713.

NWEKE, C., IGBOKWE, P. & NWABANNE, J. (2014). Kinetics of Batch Anaerobic Digestion of Vegetable Oil Wastewater. *Open J. Water Pollut. Treat*. p.1–10.

PEREZ, M., ROMERO, L.I. & SALES, D. (2001). Organic Matter Degradation Kinetics in an Anaerobic Thermophilic Fluidised Bed Bioreactor. *Anaerobe*. 7. p.25–35.

RABAH, F.K.J. & DAHAB, M.F. (2004). Biofilm and biomass characteristics in high-performance fluidized-bed biofilm reactors. *Water Res*. 38. p.4262–4270.

RINCÓN, B., RAPOSO, F., DOMÍNGUEZ, J.R., MILLÁN, F., JIMÉNEZ, A. M., MARTÍN, A. & BORJA, R. (2006). Kinetic models of an anaerobic bioreactor for restoring wastewater generated by industrial chickpea protein production. *Int. Biodeterior. Biodegrad*. 57. p.114–120.

RIZZO, L. (2011). Bioassays as a tool for evaluating advanced oxidation processes in water and wastewater treatment. *Water Res*. 45. p.4311–40.

SANKARAN, K., PREMALATHA, M., VIJAYASEKARAN, M. & SOMASUNDARAM, V.T. (2014). DEPHY project: Distillery wastewater treatment through anaerobic digestion and phycoremediation - A green industrial approach. Renew. Sustain. *Energy Rev.* 37. p.634–643.

SATYAWALI, Y. & BALAKRISHNAN, M. (2008). Wastewater treatment in molasses-based alcohol distilleries for COD and color removal: a review. *J. Environ. Manage*. 86. p.481–97.

SENTURK, E., ÝNCE, M. & ONKAL ENGIN, G. (2013). Assesment of kinetic parameters for thermophilic anaerobic contact reactor treating food-processing wastewater. *Int. J. Environ. Res.* 7. p.293–302.

WANG, H.-Y., QIAN, H. & YAO, W.-R. (2011). Melanoidins produced by the Maillard reaction: Structure and biological activity. *Food Chem*. 128. p.573–584.

WANG, J.-L. & WU, L.-B. (2004). Wastewater treatment in a hybrid biological reactor (HBR): nitrification characteristics. *Biomed. Environ. Sci*. 17. p.373–379.

YU, L., WENSEL, P., MA, J. & CHEN, S. (2013). Mathematical Modeling in Anaerobic Digestion (AD). *J. Bioremediatoin Biodegrad*. S4. p.12.

Chapter 5

5 Combined anaerobic digestion and photocatalytic treatment of distillery effluent in batch fluidised bed reactors

Abstract

Anaerobic digestion (AD) can remove a substantial amount of organic load when applied in treating distillery effluent but it is ineffective in colour reduction due to the presence of traces of biorecalcitrant melanoidins. Ultra-violet (UV) photocatalysis applied as a post-treatment method can be used to remove colour from anaerobically digested effluent. A study on a combined AD and photodegradation treatment of distillery effluent was carried out in fluidised bed batch reactors to evaluate total organic carbon (TOC) and colour reduction. Anaerobic digestion as a stand-alone process removed 78% TOC and 41% colour. The combined process improved colour removal from 41% to 85% compared to that of AD employed as a stand-alone process. Photodegradation post-treatment mineralized the biorecalcitrant melanoidins via a reductive path way as was indicated by the formation of NH_4^+ in large quantity compared to NO_3^-. The bioenergy production by the AD step was 14.2 kJ/g TOC biodegraded while UV lamp energy consumption was 900 kJ/g TOC degraded. Electrical energy per order analysis for the photodegradation process showed that the bioenergy produced was 20% of that required by the UV lamp to photodegrade 1 m^3 of undiluted pre-AD treated effluent up to 75% colour reduction. It was concluded that a combined AD-UV system for treatment of distillery effluent is effective in organic load removal and can be operated at a reduced cost.

5.1 Introduction

Anaerobic digestion is effective in converting huge amounts of organic load of distillery effluent into biomethane. However, it is ineffective in colour reduction (Satyawali & Balakrishnan, 2008). This is due to the presence of colour-causing biorecalcitrant melanoidins (Wang et al., 2011). Therefore, different post-treatment methods for biomethanated distillery effluent have been proposed for colour removal. Physicochemical methods such as coagulation (Arimi et al., 2015; Chaudhari et al., 2007), adsorption (Onyango et al., 2011), catalytic thermolysis and wet oxidation (Chaudhari et al., 2005) have been applied with varying degrees of success. Recently, studies have been carried out on advanced oxidation processes (AOPs) such as the application of photodegradation in the treatment of distillery effluent and good colour removal has been reported (Apollo et al., 2014b; Vineetha et al., 2013). Photodegradation has an advantage in that it can rapidly degrade organic contaminants to

mineralization without producing sludge. Even though photodegradation can be used as a pre-treatment before the AD process to enhance the biodegradability of recalcitrant compounds (Apollo et al., 2014a), this step is not recommended for wastewater with a high proportion of biodegradable components with traces of biorecalcitrant components such as distillery effluent. This is due to the fact that the biodegradable components will compete with the recalcitrant compounds during photodegradation leading to unnecessary consumption of chemicals and longer irradiation time (Oller et al., 2011). In such a case, an initial step involving biological treatment for the removal of biodegradable components followed by an AOP post-treatment as a polishing step is more economical due to reduced energy and chemicals consumption (Hörsch et al., 2003; Vidal et al., 2004). Moreover, photodegradation was found not to significantly improve biodegradability of distillery effluent towards anaerobes (Apollo et al., 2013). It is therefore more effective to apply photodegradation as a post-treatment to AD pre-treated distillery effluent.

The application of fluidised bed reactors in a combined AD and photodegradation process can result in better pollution removal due to the good mixing attained by fluidised bed reactors, which promotes mass transfer thereby increasing reaction rate. Due to the achievable fast reaction rates, chemical dose and the energy requirement of the UV photodegradation could be reduced while the bioenergy from the AD process could be enhanced. This may result in improvement on the overall efficiency of the integrated process. In this study, the efficiency of fluidised bed reactors in a combined anaerobic digestion and photodegradation process was investigated for TOC and colour reduction when treating distillery effluent. The effect of operating parameters on the efficiency of photodegradation of biodigested effluent was evaluated and the degradation of melanoidins monitored through the formation of NO_3^- and NH_4^+.

5.2 Methodology

5.2.1 Materials

Distillery effluent with the characteristics listed in Table 5-1 was outsourced from a local treatment plant and stored in a fridge at 4 ^oC before use. Titanium dioxide catalyst, degusa P 25, was purchased from Acros Organics.

Table 5-1: Characteristics of distillery effluent.

Parameter	Value
Chemical oxygen demand (mg/l)	2600 ± 250
Total organic carbon (mg/l)	1807 ± 120
Total suspended solids (mg/l)	43 ± 5
Total sulphates (mg/l)	249 ± 21
Total phosphates (mg/l)	35 ± 4
pH	5.5

5.2.2 Experimental set up

Anaerobic fluidized bed reactor (AFBR) and fluidized bed annular photoreactor (FBAP) assembled as shown in Figure 5-1 was used. The detailed description of each reactor is in Chapter 3.

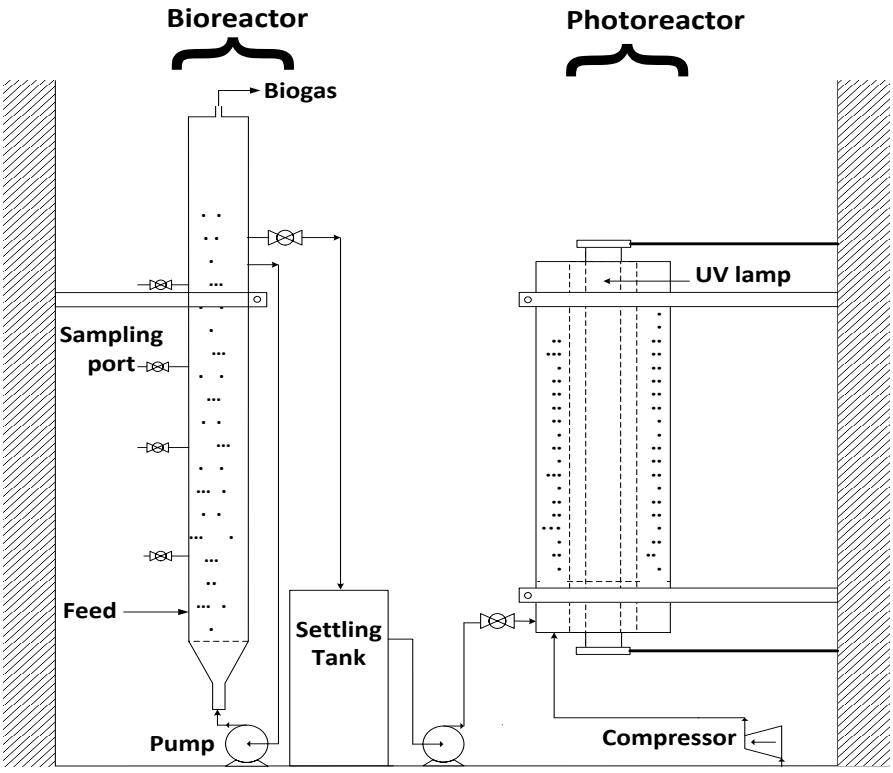

Figure 5-1: Experimental set-up for the integrated anaerobic digestion and photodegradation.

Fluidization in the AD reactor was achieved by a centrifugal pump (Foras veronilla-Italy) which was used to circulate the effluent in the reactor while fluidization in the photoreactor was achieved by air from a compressor (Jun Air OF302). The effluent from AFBR was fed into

a settling tank to remove suspended solids, which resulted from flocs formed by biomass in the bioreactor. Prior to photodegradation, the pH of the biodegraded effluent was lowered to 4 using 0.1 M H_2SO_4 solution which was the best pH for photodegradation of distillery effluent (Apollo et al., 2014b). For the photoreactor, the catalyst and wastewater was thoroughly mixed using a magnetic stirrer to ensure uniform catalyst distribution. The mixture was then fed into the reactor using a peristaltic pump and air from the compressor was passed upward through a column of distillery wastewater containing suspended TiO_2 catalyst via a flow distributor compartment at the bottom of the reactor.

5.2.3 Experimental procedure

The optimum superficial gas velocity or liquid velocity for the photoreactor and bioreactor, respectively, were determined from the hydrodynamic studies in Chapter 3. However, preliminary experiments were carried out to find the best operating conditions such as the amount of TiO_2 in the composite catalyst, catalyst loading and hydrogen peroxide dose as indicated in Table 5-2.

Table 5-2: Operating parameters for the photoreactor and AD reactor.

Photoreactor		Biodigester	
Parameter	Value	Parameter	Value
Average catalyst size	57 µm	Zeolite particle size	150-300 µm
TiO_2/silica ratio of catalyst	10 – 95%	Zeolite amount	50 g
Catalyst amount	0.5 – 5 g/l	Superficial liquid velocity (U_L)	0.6 cm/s
Superficial air velocity (U_g)	0.92 cm/s	Bed height at U_L	500 mm
H_2O_2 dosage	1.2 – 19.6 mM		

After establishing these conditions, firstly, the anaerobic process was conducted in a batch mode at 37 ^oC and biogas was collected by a water displacement method. The biogas was analysed for methane content using a gas chromatograph. The anaerobically treated effluent was centrifuged and then fed into the photoreactor for further colour and TOC reduction. The electrical energy consumption of UV lamp in the photodegradation process was analysed using electrical energy per order (E_{UV}) as reported by Shu et al.(2013):

$$E_{UV} = \frac{P\,t}{V \log(\frac{C_i}{C_f})} \quad (1)$$

where P is the lamp power (kW), t is the irradiation time (hours), V is the volume (m^3) of water treated, and C_i and C_f are the initial and final concentrations of the target contaminant. The energy consumption of the photodegradation process was compared to the energy produced by the AD process.

5.2.4 Experimental analysis

Monitoring of the performance of each treatment process was carried out by analysing aliquot samples after a specific period of treatment. The total organic carbon was analysed using a TOC analyser (TELEDYNE Tekmar), sulphates, nitrates and ammonium were analysed using Ion chromatography (882 compact IC plus fitted with an 863 compact auto sampler), gas was analysed using a gas chromatograph (Trace 1310 gas chromatograph) fitted with thermal conductivity detector, while colour was analysed using UV-Vis spectrophotometer (T80 + UV/VIS Spectrophotometer, PG instruments Ltd). Alkalinity, VFAs, COD and BOD_5 were analysed according to the standard method. According to the standard method for wastewater analysis VFAs and alkalinity were analysed by titration (Lahav & Morgan, 2004) while COD was analysed by nanocolour calorimeter after digestion using potassium permanganate.

5.3 Results and discussion

5.3.1 TOC, Sulphates and colour reduction

After the reactor had acclimatised/stabilised, its efficiency in TOC, colour and sulphate reduction was evaluated. High TOC reduction of 78% was achieved after 7 days with a corresponding colour reduction of 41% (Figure 5-2). Anaerobic digestion in fluidised bed reactors has been reported as an efficient treatment technology for TOC reduction when treating distillery effluent due to the fact that the major component of distillery effluent is biodegradable (Satyawali & Balakrishnan, 2008). Despite containing large amount of biodegradable organic substances, distillery effluent also contains melanodins, which are biorecalcitrant. Melanoidins form about 2% of distillery effluent and is responsible for the intense dark brown colour (Kalavathi et al., 2001). Due to the biorecalcitrant nature of melanoidin, AD treatment of distillery effluent has been reported to result in low colour reduction (Satyawali & Balakrishnan, 2008).

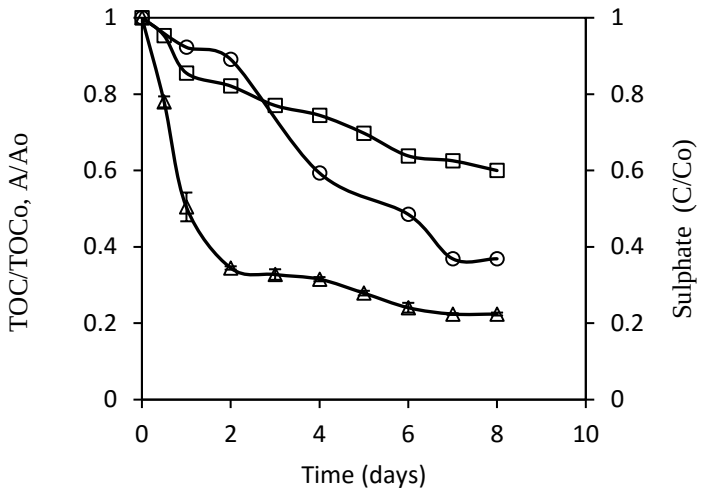

Figure 5-2: Colour, TOC and sulphate reduction during anaerobic digestion, TOC (Δ), Colour (□), Sulphates (○).

Sulphate reduction was also observed during the AD process. In anaerobic conditions, sulphate reducing bacteria (SRB) use sulphate as a terminal electron acceptor for the degradation of organic compounds and hydrogen. Therefore, in the presence of sulphates, methanogens compete with SRB for available organic substrates. This competition may result in low methane production in cases where sulphate rich wastewater is treated as there will be production of hydrogen sulphide (Acharya et al., 2008). In this study, the methane content of biogas produced (Figure 5-3) was within the expected range suggesting that substrate utilization by methanogens predominated that of SRB. Under stable conditions and when sulphate concentration is much lower than TOC, sulphate reduction can majorly be due to utilization as nutrients by the micro-organisms (Vijayaraghavan & Ramanujam, 2000).

5.3.2 Biogas production and methane yield.

Figure 5-3 shows that the anaerobic digestion produced about 4.82 L of biogas after 7 days. This corresponded to a biogas production rate of 0.57 L of biogas/g TOC. The methane content of the biogas produced within the first day was 41%, its production increased with time reaching maximum of 66% on day 5. The mean methane production was therefore calculated as ~ 0.35 L CH_4/g TOC while the value in literature varies between 0.29 and 0.4 (Fernández et al., 2008; Zupancic et al., 2007).

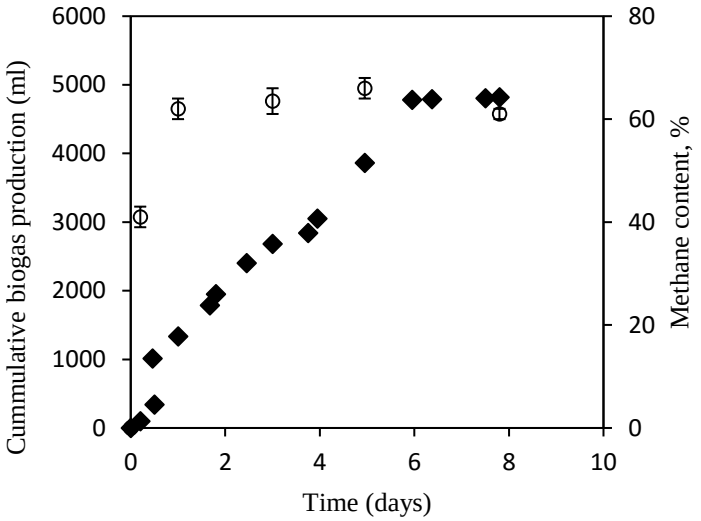

Figure 5-3: Biogas and methane production during the anaerobic process, biogas production (■), Methane yield (○).

The low methane content of the biogas during the onset of the anaerobic process could have been due to the acclimatisation of the micro-organisms to fresh organic load. Also, it could be due to the fact that acidogenesis proceeded faster than methanogenesis at this stage, leading to production of carbon dioxide. However, by day 2 stability was achieved between acidogenesis and metanagenosis thus acidogenesis products were consumed in the methanogenesis process, producing CH_4. From day 6, biogas production reduced remarkably and nearly came to a stop. The reduction in biogas production during this period could have been due to the fact that most organic carbon had been removed, therefore little substrate was available for the micro-organisms.

5.3.3 Alkalinity and pH

Alkalinity and pH analysis showed that there was adequate buffering in the reactor (Table 5-3). The anaerobic digestion process is pH sensitive with optimum operational pH of about 7 (Acharya et al., 2008). Stable operating bioreactors often have the ability for self- buffering since the acid produced by the acidogenesis process is neutralized by the methanogenesis, which is an alkalizing step, due to the fact that it consumes hydrogen and H_3O^+ ions (Patel & Madamwar, 2000).

Table 5-3: Alkalinity and pH during the anaerobic digestion.

Time (days)	0	1	2	4	6	7	8
pH	7.11	7.18	7.29	7.44	7.58	7.62	7.62
Alkalinity (mg/l)	4760	4114	4100	4160	4060	4100	4100

5.3.4 *Photodegradation of distillery effluent*

The efficiency of photodegradation on the decolourization of the distillery effluent was studied. This was necessary due to the fact that anaerobic digestion was not effective in colour removal. In the first place, various factors which affect photodegradation were investigated to establish the best operating conditions. Secondly the possible mechanism of melanoidin photodegradation was investigated.

5.3.4.1 *Catalyst loading and catalyst composition*

The experiments were conducted with catalyst loading ranging from 0.5 g/l to 5 g/l while keeping other parameters constant (air velocity of 0.9 cm/s and initial effluent concentration of 120 mg/l TOC). Initially, adsorption studies were conducted in the dark before photodegradation. Generally, adsorption concentrates the pollutants on the catalyst surface thus facilitating the photodegradation process. In Figure 5-4, the adsorption equilibrium was achieved after 20 minutes for all catalyst loadings. However, catalyst loading above optimum value led to reduction in adsorption due to hindered mass transfer. Similarly, the photodegradation efficiency increased when catalyst loading was increased from 0.5 g/l to 2 g/l, then there was a decrease in the photodegradation efficiency when the catalyst loading was increased to 5 g/l. This may be attributed to the light scattering effect caused by the catalyst at high loading, leading to a reduction in reaction rate (Huang et al., 2008).

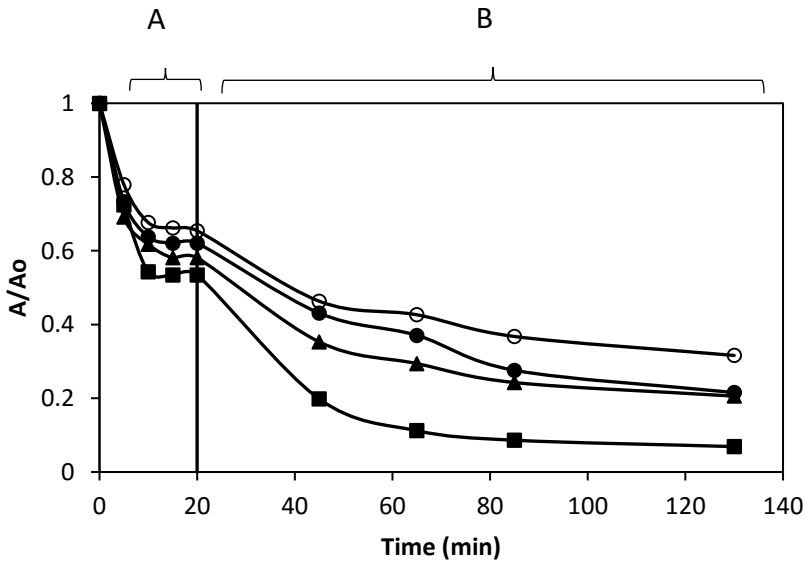

Figure 5-4: Effect of catalyst loading on adsorption (A) and photodegradation (B) using 50% wt/wt TiO_2/SiO_2 composite catalyst 5 g/l (●), 2 g/l (■), 1 g/l (▲), 0.5 g/l (○).

Silica materials such as silica gels have been commonly applied as photocatalyst supports to facilitate the separation of the photocatalyst after the photocatalytic reaction in aqueous

systems due to the high sedimentation ability of silica gel (Shan et al., 2010). Moreover, silica gel has become famous for supporting TiO_2 due to the fact that it is an adsorbent therefore concentrates the pollutants on the catalyst surface and it also allows penetration of photons to the catalyst due to its transparent nature (Lim & Kim, 2005). In Figure 5-5, colour removal by the photodegradation process increased with an increase in the amount of TiO_2 in the TiO_2/silica composite catalyst. However, removal by adsorption decreased with an increase in TiO_2 composition suggesting that the SiO_2 had higher adsorption ability than the TiO_2. It has been reported that an increase in the amount of TiO_2 in the composite leads to a reduction in the surface area and pore size of the silica gel therefore resulting in a reduction in adsorption (Lim & Kim, 2005; Shan et al., 2010). Generally, silica gel is mainly used to bind TiO_2 to facilitate post-treatment separation which can be very expensive if TiO_2 is used as slurry since it has poor settling ability.

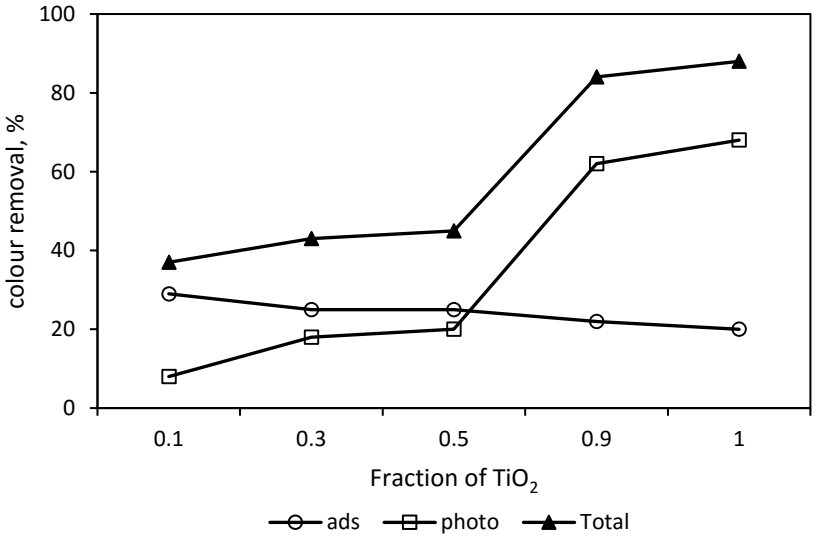

Figure 5-5: Effect of catalyst composition on adsorption (○), photodegradation (□) combined adsorption-photodegradation (▲) using catalyst loading of 2 g/l.

5.3.4.2 *Colour removal mechanism via NO_3^- and NH_4^+evolution during photocatalysis.*

More insight into the degradation of organic compounds such as melanoidins, which have heteroatoms, can be obtained by monitoring the formation of inorganic ions formed in solution due to the degradation of the associated heteroatoms (Alberici et al., 2001). Melanoidins in distillery effluent are formed as a result of a reaction between amino acids and glucose, therefore melanoidins contain nitrogen atom as heteroatom (Wang et al., 2011). In Figure 5-6a the colour removal efficiency by the photodegradation was higher than that of TOC reduction. This suggests that photocatalysis degraded the colour causing bonds (chromophores) of the

melanoidin faster than organic carbon mineralization. Since the colour in melanoidin is caused by C-N and C=C bonds (Chandra et al., 2008), it is therefore, inferred that the photogenerated radicals attacked the chromophores faster than the C-C bond due to the highly reactive centres in the chromophore compared to that in C-C bonds.

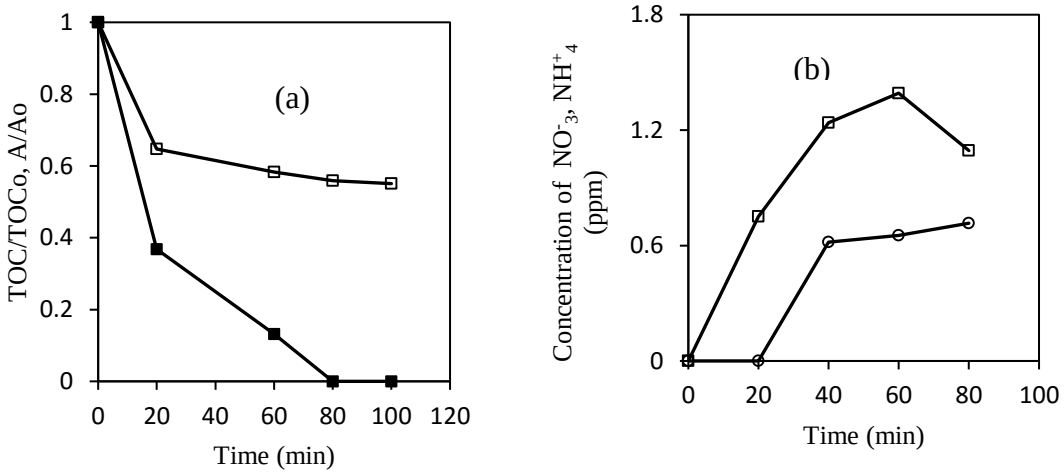

Figure 5-6: (a) Colour (■) and TOC (□) reduction. (b) NO_3^- (○) and NH_4^+ (□) formation during photodegradation.

Figure 5-6b shows the production of nitrate and ammonium during photodegradation indicating the mineralization of nitrogen in the melanoidin structure that led to colour reduction. Photocatalytic degradation of nitrogen-containing organic compounds like melanoidins depends largely on the position and oxidation state of the nitrogen atom within the organic structure (Jing et al., 2011). In the degradation of such compounds, NH_4^+ and NO_3^- are produced in different proportions depending on the degradation pathway. If the nitrogen atom exists in high oxidation state, the nitrogen constituent degrades through a reductive pathway and NH_4^+ is formed from unstable intermediates. However, if the initial oxidation state of nitrogen in organic compound is low, the nitrogen constituent is degraded through an initial oxidation step to produce NO_3^- (Jing et al., 2011). In this study, more NH_4^+ evolved than NO_3^- , indicating that more nitrogen atoms in melanoidin structure had a high oxidation state, and therefore they were degraded through the reductive pathway.

5.3.4.3 *FTIR analysis of the photodegradation process*

To further analyse the effect of photodegradation in breaking down the organic molecules in the distillery effluent, the photodegraded samples were analysed using FTIR after 20 minutes interval of UV irradiation. The appearance and disappearance of some peaks as well as shift in peaks are indications of degradation. In Figure 5-7, the FTIR spectrum of melanoidin shows

peaks majorly at 3400 cm^{-1} due to stretching vibration of OH and NH_2 bonds, at 2850 cm^{-1} due to CH stretching vibration, 1620 cm^{-1} due to amide (Dolphen & Thiravetyan, 2011; Kim et al., 1985; Olennikov & Tankhaeva, 2012).

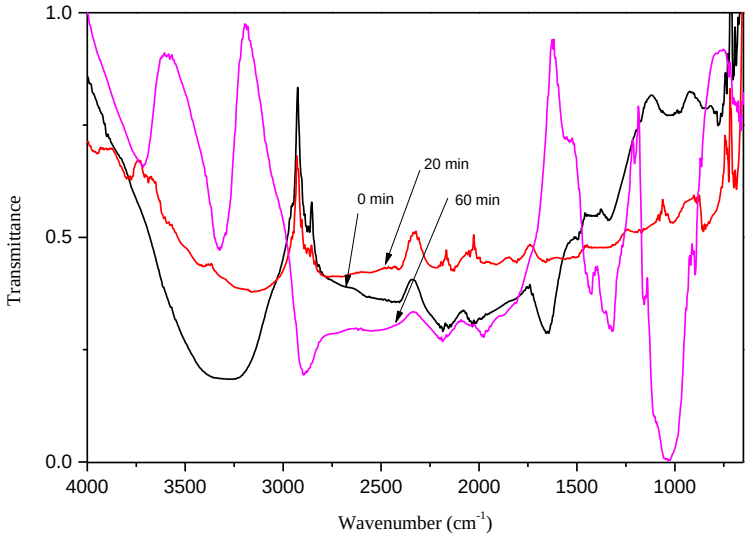

Figure 5-7: FTIR spectra of distillery effluent at different times of photodegradation.

Generally, the peak at 3400 reduced after 60 minutes of irradiation while the peak at 2850 increased suggesting a likely reduction in OH and or NH_2 groups and an increase in CH group, respectively. The absorption due to amide at 1620 cm^{-1} (Kim et al., 1985) also decreased during photodegradation. The increase in C-H peak intensity with a decrease in NH_2 or amide peaks' intensity may explain the high colour reduction with a corresponding low TOC reduction recorded during photodegradation, since colour in melanoidin is caused by C-N and C=C bonds (Chandra et al., 2008) The emergence of absorbance peaks at 1250 and 1050 cm^{-1} may indicate C-H deformation and C-O stretching, respectively (Dolphen & Thiravetyan, 2011; Olennikov & Tankhaeva, 2012). It was observed that photodegradation was effective in colour reduction but was inefficient in TOC reduction while anaerobic digestion was effective in TOC reduction but performed poorly in colour reduction. Therefore, integration of the two processes is necessary for both colour and TOC reduction. From these observations, AD treatment can be applied in the initial step to remove the TOC with bioenergy recovery while photodegradation can be employed as a final step to remove the colour resulting from a low concentration of biorecalcitrant compounds (melanoidins).

5.3.4.4 *Effect of hydrogen peroxide addition*

Hydrogen peroxide improves the photodegradation process as it acts as an additional source of hydroxyl radical which degrades organic contaminants. However, it is important to determine the most suitable amount of hydrogen peroxide required to achieve optimum degradation. This is due to the fact that very low hydrogen peroxide concentration does not improve photodegradation as it generates an insignificantly low amount of peroxide radicals. In contrast, at very high hydrogen peroxide concentrations, the reaction is retarded due to the scavenging effects of the excess peroxide radicals produced (Huang et al., 2008). In this study, colour removal efficiency was used to determine optimal hydrogen peroxide dosage for the reactor used under the prevailing conditions of 2 g/l, 95% TiO_2/silica composite catalyst and 120 mg/l TOC of the wastewater.

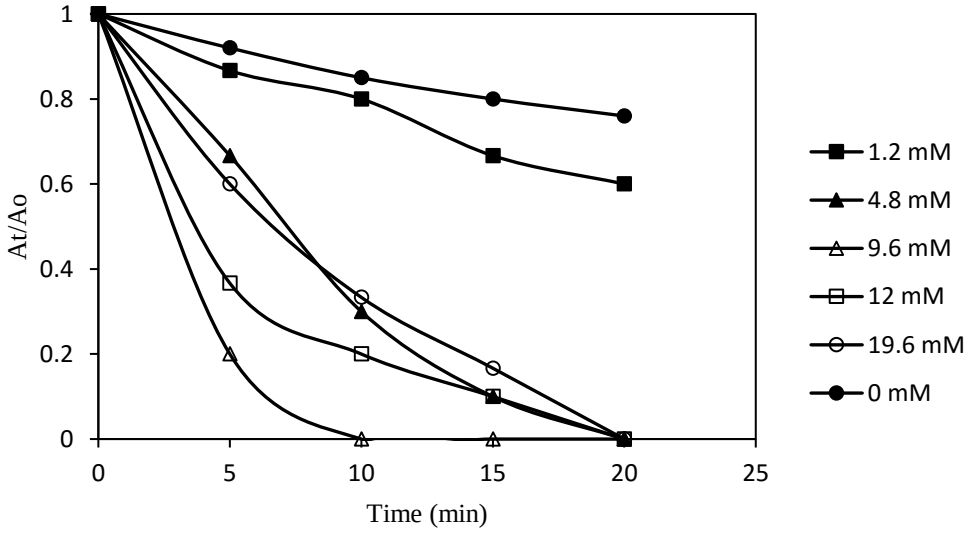

Figure 5-8: Effect of hydrogen peroxide dose on colour reduction of distillery effluent.

In Figure 5-8, it was found that the optimal hydrogen peroxide dose was 9.6 mM and this could remove total colour within 10 minutes of irradiation. The optimal hydrogen peroxide dose was used to study TOC reduction under similar reactor conditions. In Figure 5-9, it was observed that a TOC reduction of 81% was achieved using hydrogen peroxide while without adding hydrogen peroxide only 31% of TOC was removed. Hydrogen peroxide and UV irradiation alone achieved TOC reduction of about 20%. The increase in TOC reduction efficiency by the TiO_2/Silica catalyst/UV/H_2O_2 system compared to that of TiO_2/Silica catalyst/UV and UV/H_2O_2 is an indication that hydrogen peroxide increased the amount of peroxide radicals produced by the TiO_2/Silica catalyst/system resulting in improved degradation efficiency.

However, TOC reduction was much slower than colour reduction indicating that photodegradation is most suitable for colour reduction.

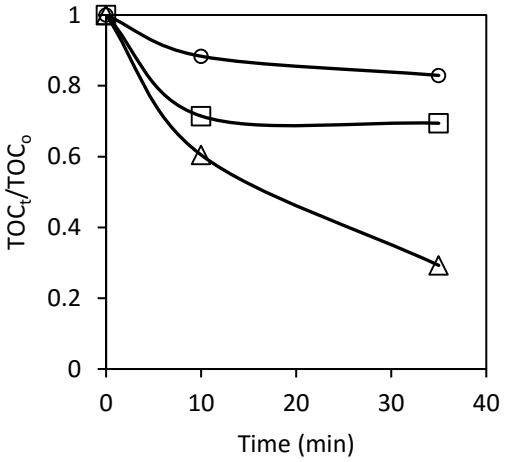

Figure 5-9: Effect of hydrogen peroxide on TOC reduction (○) UV/H_2O_2 (□) TiO_2/Silica catalyst/UV (∆) TiO_2/Silica catalyst/UV/H_2O_2.

5.3.5 Photodegradation post-treatment of AD pre-treated effluent.

The AD treated effluent, though had low TOC, was still very dark as the AD process achieved only 41% colour reduction. Therefore, even though the AD process is efficient in TOC reduction, it cannot be applied as a stand-alone process for distillery effluent treatment and therefore post-treatment method is necessary (Travieso et al., 2008). The anaerobically treated effluent from the AD reactor was centrifuged then treated by UV photodegradation since photodegradation is very effective in colour reduction. Due to the intense dark colour of the anaerobically digested effluent, dilution may be required for effective colour reduction during UV post-treatment depending on the photoreactor design. To study the effect of dilution of the AD effluent on the ensueing photodegradation process, the dilution factor was calculated as;

$$DF = \frac{V_e + V_w}{V_e} \quad (2)$$

where DF is the dilution factor, V_e is the effluent volume (L), V_w is the volume of dilution water (L). From the equation a DF value of 1 indicates no dilution since $V_w = 0$. Colour and TOC reduction rates increased with an increase in dilution (Figure 5-10a and b). This is due to the fact that dilution reduced the colour intensity leading to a reduction in light attenuation effect caused by the dark colour. Dilution is generally not an encouraged approach, however in this case, part of the treated effluent can be used for dilution to reduce the water requirement of the process.

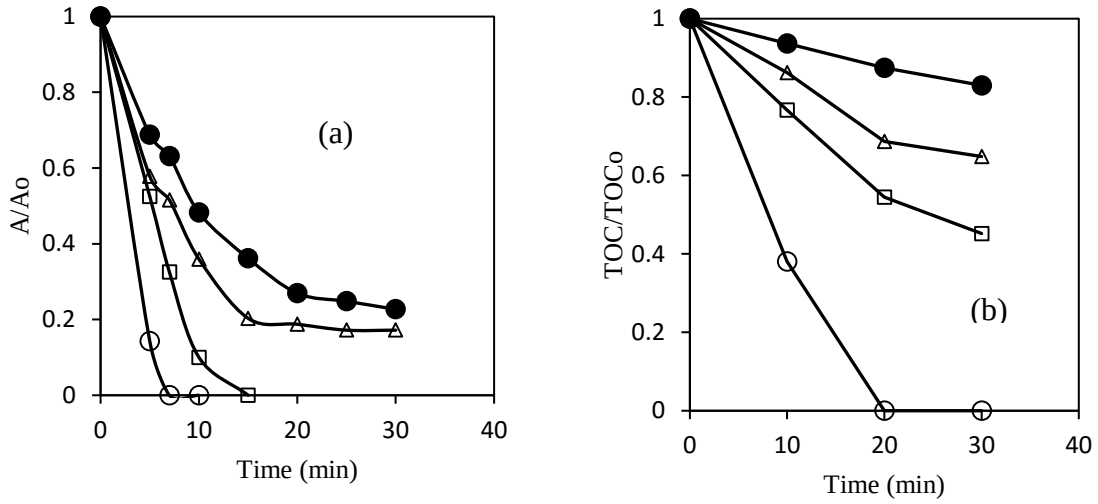

Figure 5-10: Effect of dilution on colour and TOC reduction during photodegradation, (a) colour (b) TOC; x10 v/v (○), x3.3 v/v (□), x2 v/v (Δ), x1v/v (●).

Irrespective of the dilution, colour removal was always higher than the TOC reduction. This could be an indication that the UV radiation process is more rapid in cleavaging the chromophore bonds of melanoidin but it is slower in mineralization of the melanoidins. Photodegradation has been reported to result in better colour reduction but low TOC reduction when treating distillery effluent (Vineetha et al., 2013). It was also observed that photodegradation could remove 77% and 11% colour and TOC, respectively, when treating undiluted (x1 v/v) effluent.

5.3.6 Combined anaerobic digestion and UV photodegradation.

As mentioned earlier anaerobic digestion was found to perform better in TOC reduction while it had a low performance on colour reduction due to the biorecalcitrant melanoidins in distillery effluent. However, photodegradation was found to be effective in colour reduction but performed low in TOC reduction. A combined treatment in which photodegradation was used as post-treatment for the AD treated effluent was found to be very effective in both colour and TOC reduction as shown in Figure 5-11. It was found that AD as first treatment step removed 78% of TOC and 41% of colour, photodegradation post-treatment resulted in additional 5% TOC reduction and additional 46% colour reduction of the original effluent. Therefore, the combined process resulted in overall efficiency of 83% and 87% TOC and colour reduction, respectively.

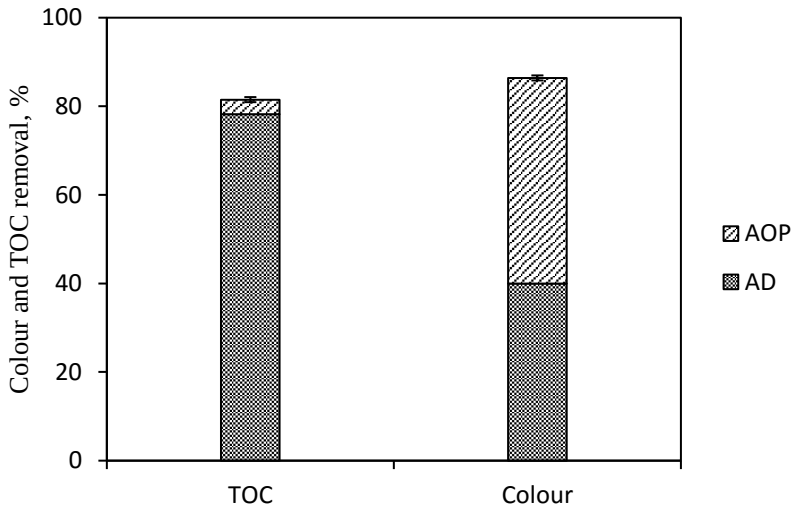

Figure 5-11: Overall performance of the combined AD and UV photodegradation process, after 7 days of AD and 30 minutes of photodegradation.

Table 5-4 summarises the pollution removal by each step and the final effluent concentration. Anaerobic digestion produces energy by breaking down organic molecules while UV photodegradation consumes energy to degrade organic molecules. Therefore, conducting energy analysis of the integrated process is necessary in order to determine the specific energy demand of the process.

Table 5-4: Characteristics of wastewater after two stage treatment.

Parameter	Before treatment	After initial AD treatment	After UV post-treatment
COD (mg/l)	2600	728	650
TOC (mg/l)	1807	405	325
BOD_5 (mg/l)	1079	162	122
Total suspended solids (mg/l)	43	-	-
Total sulphates (mg/l)	249	92	92
Total phosphates (mg/l)	35	7.5	7.5
pH	5.5	7.62	4.4
Colour (Abs at 475 nm)	0.235	0.141	0.032

5.3.7 Energy analysis

The specific energy (kJ/g TOC) production rate of AD and the specific energy consumption rate of UV photodegradation was determined. In the UV case, the energy required by the lamp to degrade unit mass of pollutant was considered. In this study, the average methane production

of the AD process was 0.35 l/ g TOC removed and this had an energy content of 14.2 kJ/g TOC removed, taking the reported energy value of methane as 38 mJ/m^3 (Duerr et al., 2007). Methane production from brewery slurry or molasses effluent has been reported to be in the range of 0.23 l CH_4/g COD to 0.42 l CH_4/g COD (Jiménez et al., 2004; Zupancic et al., 2007) resulting in energy of 8.74 kJ/ g COD to 15.96 kJ/g COD. The specific energy consumption for photodegradation was found to be about 900 kJ/g TOC leading to colour reduction of 52% - 100%, depending on dilution (Table 5-5).

Table 5-5: Energy analysis and performance of the combined process.

Dilution factor	x10	x3.3	x2	x1
Colour reduction, %	100	90	64	52
TOC reduction, %	62	24	14	6
Energy UV lamp (kJ/g TOC)	970	900	900	1000
AD (kJ/g TOC)	14.2	14.2	14.2	14.2

In the Table it was further observed that, unlike colour reduction, the energy requirement of the UV lamp to degrade a unit mass of pollutant was constant and did not depend on dilutions. Dilution only led to faster reaction rate due to lower concentrations but did not lead to reduction in energy consumption per unit mass of pollutants removed. Considering the observed faster colour removal rate compared to that of TOC reduction rate during photodegradation, colour reduction can consume less energy than TOC reduction. Considering the fact that UV photodegradation post-treatment is majorly for colour reduction since most of the TOC had been removed by the initial AD step, energy analysis for colour reduction is necessary.

5.3.8 Electrical Energy per order analysis of the combined process for colour reduction

The electrical energy per order (EE/O) is a key scale-up parameter for photodegradation systems. This is due to the fact that it combines into a single function the key design variables which are: UV radiation time, effluent volume, concentration and the targeted number of orders of magnitude of contaminant concentration to be removed. Application of EE/O in this work can give an insight into the performance of the integrated AD-UV system in a scaled up process for colour reduction. The EE/O was calculated as shown in equation (1). Since the initial anaerobic treatment step had removed 78% and 41% of TOC and colour, respectively, the UV post treatment was evaluated on the basis of removing further 75% of colour. In this case, the EE/O was calculated for 75% colour reduction. The study was conducted for raw effluent from the biodigester and for diluted effluent. The electrical energy required to power the UV lamp

to treat 1 m^3 effluent to 75% colour reduction was compared with the energy content of the biogas produced in the AD unit (Figure 5-12). It was found that the energy required to treat 1 m^3 of the effluent almost increased linearly with a reduction in dilution factor.

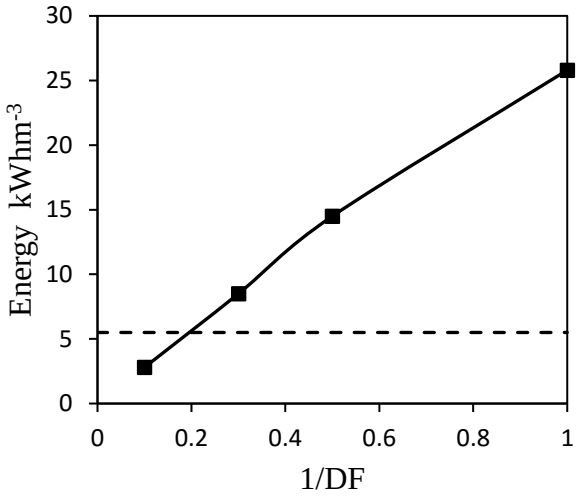

Figure 5-12: Electrical energy consumption of the UV lamp at various dilutions (■) and Energy content of the biogas produced by the AD process (- - -).

Based on biogas production of 4.82 L with an average methane production of 65% recorded, the energy content of the biogas produced was calculated as 5.5 $kWhm^{-3}$ of wastewater treated. It was found that at dilutions of 20% v/v and less, the energy produced by the AD system was equivalent or lower than the energy required by the UV lamp to treat the diluted wastewater to further 75% colour reduction. However, as the dilution factor reduced, more energy was required majorly due to the fact that more concentrated effluent has a darker colour thus leading to light attenuation in the reactor. Energy analysis further showed that the bioenergy produced could subsidise up to 20% of energy required by the UV lamp to photodegrade undiluted pre-AD treated effluent up to 75% colour reduction. Therefore, integration of the two processes has a potential of lowering photodegradation operation cost while ensuring effective pollution reduction.

Conclusion

A study on combined anaerobic digestion and photodegradation treatment of distillery effluent in batch fluidised bed reactors was carried out. It was found that anaerobic digestion as a single unit was efficient in TOC reduction but not in colour reduction while photodegradation was efficient in colour reduction but not in TOC reduction. However, a combined process resulted

in about 85% colour and TOC reduction. During photodegradation, nitrate (NO_3^-) and ammonium (NH_4^+) were formed indicating the degradation of the biorecalcitrant melanoidins. Energy analysis showed that AD produced 14.2 kJ/g TOC of energy while the UV lamp consumed 900 kJ/g TOC to further treat biodigested effluent. The energy analysis showed that the bioenergy produced by AD was equivalent to that required to photodegrade 1 m^3 of pre-digested distillery effluent diluted by 20% to achieve 75% colour reduction. Energy analysis further showed that the bioenergy produced could subsidise up to 20% of energy required by UV lamp to further photodegrade 1 m^3 undiluted biodigested effluent up to 75% colour reduction. Therefore, anaerobic digestions can subsidise the cost of UV photodegradation when applied combined in the treatment of distillery effluent. However, process optimization needs to be done in order to determine the best combination of factors such as organic load and retention time on overall performance of the integrated process. Furthermore, the performance of a continuously operated integrated process needs to be investigated to better assess the potential of its applicability in a large scale wastewater treatment unit.

References

ACHARYA, B.K., MOHANA, S. & MADAMWAR, D. (2008). Anaerobic treatment of distillery spent wash - a study on upflow anaerobic fixed film bioreactor. *Bioresour. Technol*. 99. p.4621–6.

ALBERICI, R.M., CANELA, M.C., EBERLIN, M.N. & JARDIM, W.F. (2001). Catalyst deactivation in the gas phase destruction of nitrogen-containing organic compounds using TiO2/UV–VIS. *Appl. Catal. B Environ*. 30. p.389–397.

APOLLO, S., ONYANGO, M.S. & OCHIENG, A. (2014a). Integrated UV photodegradation and anaerobic digestion of textile dye for efficient biogas production using zeolite. *Chem. Eng. J.* 245. p.241–247.

APOLLO, S., ONYANGO, M.S. & OCHIENG, A. (2013). An integrated anaerobic digestion and UV photocatalytic treatment of distillery wastewater. *J. Hazard. Mater*. 261. p.435–42.

APOLLO, S., ONYANGO, S. & OCHIENG, A. (2014b). UV / H 2 O 2 / TiO 2 / Zeolite Hybrid System for Treatment of Molasses Wastewater. *Iran. J. Chem. Chem. Enginering*. 33. p.107–117.

ARIMI, M.M., ZHANG, Y., GÖTZ, G. & GEIßEN, S.-U. (2015). Treatment of melanoidin wastewater by anaerobic digestion and coagulation. *Environ. Technol*. 36. p.2410–2418.

CHANDRA, R., NARESH, R. & RAI, V. (2008). Melanoidins as major colourant in sugarcane molasses based distillery effluent and its degradation. 99. p.4648–4660.

CHAUDHARI, P.K., MISHRA, I.M. & CHAND, S. (2007). Decolourization and removal of chemical oxygen demand (COD) with energy recovery: Treatment of biodigester effluent of a molasses-based alcohol distillery using inorganic coagulants. *Colloids Surfaces A Physicochem. Eng. Asp.* 296. p.238–247.

CHAUDHARI, P.K., MISHRA, I.M. & CHAND, S. (2005). Catalytic thermal treatment (catalytic thermolysis) of a biodigester effluent of an alcohol distillery plant. Ind. Eng. Chem. Res. 44. p.5518–5525.

DOLPHEN, R. & THIRAVETYAN, P. (2011). Adsorption of melanoidins by chitin nanofibers. *Chem. Eng. J.* 166. p.890–895.

DUERR, M., GAIR, S., CRUDEN, A. & MCDONALD, J. (2007). Hydrogen and electrical energy from organic waste treatment. *Int. J. Hydrogen Energy*. 32. p.705–709.

FERNÁNDEZ, N., MONTALVO, S., BORJA, R., GUERRERO, L., SÁNCHEZ, E., CORTÉS, I., COLMENAREJO, M.F., TRAVIESO, L. & RAPOSO, F. (2008). Performance evaluation of an anaerobic fluidized bed reactor with natural zeolite as support material when treating high-strength distillery wastewater. *Renew. Energy*. 33. p.2458–2466.

HUANG, M., WU, Z., HUANG, Y & LIN, J., (2008). Photocatalytic discolorization of methyl orange solution by Pt modified TiO_2 loaded on natural zeolite. *Dye and Pigments*. 77., p.327 - 34

HÖRSCH, P., SPECK, A. & FRIMMEL, F.H. (2003). Combined advanced oxidation and biodegradation of industrial effluents from the production of stilbene-based fluorescent whitening agents. *Water Res*. 37. p.2748–56.

JIMÉNEZ, A.M., BORJA, R. & MARTÍN, A. (2004). A comparative kinetic evaluation of the anaerobic digestion of untreated molasses and molasses previously fermented with *Penicillium decumbens* in batch reactors. *Biochem. Eng. J.* 18. p.121–132.

JING, J., LIU, M., COLVIN, V.L., LI, W. & YU, W.W. (2011). Photocatalytic degradation of nitrogen-containing organic compounds over TiO_2. *J. Mol. Catal. A Chem*. 351. p.17–28.

KALAVATHI, D., UMA, L. & SUBRAMANIAN, G. (2001). Degradation and metabolization of the pigment—melanoidin in distillery effluent by the marine cyanobacterium *Oscillatoria boryana* BDU 92181. *Enzyme Microb. Technol.* 29. p.246–251.

KIM, S.B., HAYASE, F. & KATO, H. (1985). Decolorization and Degradation Products of Melanoidins on Ozonolysis. *Agric. Biol. Chem*. 49. p.785–792.

LAHAV, O. & MORGAN, B.E. (2004). Titration methodologies for monitoring of anaerobic digestion in developing countries - A review. *J. Chem. Technol. Biotechnol*. 79. p.1331–1341.

LIM, T.H. & KIM, S.D. (2005). Photocatalytic degradation of trichloroethylene (TCE) over TiO 2/silica gel in a circulating fluidized bed (CFB) photoreactor. *Chem. Eng. Process. Process Intensif*. 44. p.327–334.

OLENNIKOV, D.N. & TANKHAEVA, L.M. (2012). Physicochemical characteristics and antioxidant activity of melanoidin pigment from the fermented leaves of *Orthosiphon stamineus. Brazilian J. Pharmacogn*. 22. p.284–290.

OLLER, I., MALATO, S. & SÁNCHEZ-PÉREZ, J.A. (2011). Combination of Advanced Oxidation Processes and biological treatments for wastewater decontamination--a review. *Sci. Total Environ*. 409. p.4141–66.

ONYANGO, M., KITTINYA, J., HADEBE, N., OJIJO, V. & OCHIENG, A. (2011). Sorption of melanoidin onto surfactant modified zeolite. *Chem. Ind. Chem. Eng. Q*. 17. p.385–395.

PATEL, H. & MADAMWAR, D. (2000). Biomethanation of low pH petrochemical wastewater using up-flow fixed-film anaerobic bioreactors. *World J. Microbiol. Biotechnol*. 16. p.69–75.

SATYAWALI, Y. & BALAKRISHNAN, M. (2008). Wastewater treatment in molasses-based alcohol distilleries for COD and color removal: a review. *J. Environ. Manage*. 86. p.481–97.

SHAN, A.Y., GHAZI, T.I.M. & RASHID, S.A. (2010). Immobilisation of titanium dioxide onto supporting materials in heterogeneous photocatalysis: A review. *Appl. Catal. A Gen*. 389. p.1–8.

SHU, Z., BOLTON, J.R., BELOSEVIC, M. & EL DIN, M.G. (2013). Photodegradation of emerging micropollutants using the medium-pressure UV/H2O2 Advanced Oxidation Process. *Water Res*. 47. p.2881–9.

TRAVIESO, L., BENÍTEZ, F., SÁNCHEZ, E., BORJA, R., LEÓN, M., RAPOSO, F. & RINCÓN, B. (2008). Assessment of a microalgae pond for post-treatment of the effluent from an anaerobic fixed bed reactor treating distillery wastewater. *Environ. Technol.* 29. p.985–992.

VIDAL, G., NIETO, J., MANSILLA, H.D. & BORNHARDT, C. (2004). Combined oxidative and biological treatment of separated streams of tannery wastewater. *Water Sci. Technol.* 49. p.287–292.

VIJAYARAGHAVAN, K. & RAMANUJAM, T.K. (2000). Performance of anaerobic contact

filter in series for treating distillery spentwash. *Bioprocess Eng*. 22. p.109–114.

VINEETHA, M.N., MATHESWARAN, M. & SHEEBA, K.N. (2013). Photocatalytic colour and COD removal in the distillery effluent by solar radiation. *Sol. Energy*. 91. p.368–373.

WANG, H.-Y., QIAN, H. & YAO, W.-R. (2011). Melanoidins produced by the Maillard reaction: Structure and biological activity. *Food Chem*. 128. p.573–584.

ZUPANCIC, G.D., STRAZISCAR, M. & ROS, M. (2007). Treatment of brewery slurry in thermophilic anaerobic sequencing batch reactor. *Bioresour. Technol*. 98. p.2714–22.

Chapter 6

6 Modelling the energy efficiency of the integrated system using surface response methodology

Abstract

The effects of operating parameters on the performance and energy efficiency of an integrated anaerobic digestion and UV photodegaradtion was studied. Response surface methodology (RSM) was applied to model the effects of operating parameters on bioenergy production and energy demand of photodegradation with a view to developing a sustainable process in which the biological step could supply energy to the energy intensive photodegradation step. The organic loading rate (OLR_{AD}) and hydraulic retention time (HRT_{AD}) of the initial biological step were the variables investigated. It was found that the initial biological step removed about 90% of COD and only about 50% of the colour while photodegradation post-treatment removed 98% of the remaining colour. Energy demand of the UV lamp was lowest at low OLR_{AD} irrespective of HRT_{AD}, with values ranging between 87 and 496 kWh/m^3. Energy analysis further showed that the electricity requirement of the UV lamp in photodegradation was 80% of the total energy requirement of a fluidised bed photoreactor while mixing consumed 20% of electricity. The AD process produced 59 kWh/m^3 of electricity which could supplement the electricity demand of the UV lamp by 30% leading to operation cost reduction of about USD 4.8/m^3. The presumed carbon dioxide emission reduction (CER) when electricity from bioenergy was used to power the UV lamp, was 28.8 kg CO_2e/m^3. Thus, the combined process was effective in pollution removal at a reduced energy cost.

6.1 Introduction

Anaerobic digestion (AD) has been preferred for treating distillery effluent due to its good performance in organic load reduction and bioenergy recovery potential in the form of biomethane (Satyawali & Balakrishnan, 2008). The AD treatment of distillery effluent has electricity generation potential of up to 74 kWh/m^3 and 50 kg/m^3 of steam in a co-generation process (Yasar et al., 2015). However, AD is not effective in removing colour from distillery effluent since melanoidins, which impart a dark brown colour to distillery effluent, are biorecalcitrant. Ultra-violet (UV) photocatalysis has been proposed for the post-treatment of anaerobically treated distillery effluent for colour removal.

Photocatalysis has an advantage in that it can rapidly degrade the pollutant without generating sludge, unlike in the case of other treatment methods such as adsorption, coagulation and

flocculation. However, photocatalysis is costly as the UV lamp used for irradiation is energy intensive. Oller et al. (2011) reported that electricity forms about 60% of the cost of operating a UV photoreactor with the UV lamp being one of the most energy demanding components. This was evidenced in a comparative study by Yasar et al. (2006) on energy requirement of various AOPs in wastewater treatment where it was reported that UV photolysis and UV/H_2O_2 required 160 and 86 kWh/m^3, respectively, in the treatment of mixed industrial wastewater with COD of 108 mg/l and colour absorbance of 0.085. The UV energy requirement compares well with the electricity production potential of AD treatment of distillery wastewater, which is about 74 kWh/m^3 (Yasar et al., 2015). This suggests that the AD process has the potential to produce energy to offset the energy requirement cost of UV photocatalysis in an integrated AD-photodegradation treatment system.

The challenge facing studies on the integrated wastewater process is that most of the studies have been conducted without considering the impact of the operating parameters of the initial step on the performance of the ensuing post-treatment step (Chaudhari et al., 2007; Yasar et al., 2007). This trend has led to modelling of the individual processes forming the integrated system instead of modelling the whole integrated system as a single unit as asserted by Oller et al. (2011). Therefore, Oller et al. (2011) recommended that modelling of the effects of operating parameters of an integrated biological and chemical process as a unit, besides considering the individual process, for wastewater treatment is necessary for process optimization and scale up. In the case of an integrated AD – UV system, the OLR and HRT employed in the initial AD step are very significant in evaluating the overall process performance. This is due to the fact that these factors not only determine the AD stability and biogas production rate but they also affect the characteristics of the AD treated effluent, which in turn, affects the efficiency of the post-treatment process.

To obtain best operating conditions for the integrated process, response surface methodology (RSM) using factorial experimental design is an appropriate technique. The RSM enables determination of the optimum operating conditions in an effective manner and evaluates the effect of interaction of multivariable systems using statistical methods, compared to a one variable at a time experimental design which is time consuming and does not cater for the interactive effects of variables (Chen et al., 2011). In this work, the performance of an integrated AD-UV system was evaluated in COD and colour reduction. Further, the bioenergy production of the initial AD step and the energy utilization of the UV lamp in the

photodegradation process were modelled using RSM. The interactive effects of HRT and OLR applied in the initial AD step on the overall process efficiency and best operating conditions, were established.

6.2 Methodology

6.2.1 Experimental procedure

The experimental set-up for the combined anaerobic digestion and photodegradation shown in Figure 5-1 of chapter 5 was applied in this study. The fluidised bed bioreactor was operated in continuous mode where the organic loading rate (OLR) was varied between 0.33 kg COD/m^3d and 9 kg COD/m^3d and the hydraulic retention time (HRT) was varied between 3 days and 20 days. The effects of OLR and HRT in the anaerobic digester (OLR_{AD} and HRT_{AD}, respectively) on the ensuing batch photodegradation process was studied. Subsequently, energy analysis of the integrated process per unit wastewater treated was carried out based on the effect of the OLR_{AD} and HRT_{AD} on the energy production by the initial AD step and energy utilization by the final UV step. Finally, the energy efficiency of the integrated process was modelled using response surface methodology (RSM).

6.2.2 Energy analysis

The energy production of the anaerobic unit was compared to the energy demand of the photodegradation process, with a view to develop a system in which the AD step could provide energy for UV photodegradation. The energy production by the AD process was calculated as (Moraes et al., 2014):

$$E_{bio} = LHV_{CH_4} \times E_{COD} \times C_{COD} \times \alpha_{CH_4} \quad (1)$$

where E_{bio} is the AD energy production kWh/m^3, LHV_{CH_4} is the low heating value of methane which is 38 MJ/m^3 (10.55 kWh/m^3) (Duerr et al., 2007), E_{COD} is the COD removal efficiency, C_{COD} is the feed concentration (kg COD/m^3) and α_{CH_4} is the methane production coefficient (m^3/kg COD removed). Electrical energy per order (EE/O) was used to calculate the energy consumption of the UV photodegradation process (E_{AOP}). The EE/O (kWh$m^{-3}$$order^{-1}$) is defined as the electrical energy (kWh) required to degrade a contaminant by one order of magnitude in 1.0 m^3 water and it was adopted from Shu et al. (2013):

$$E_{AOP} = \frac{Pt}{V \log(\frac{C_i}{C_f})} \quad (2)$$

where P is the UV lamp or compressor power consumption(kW), t is the irradiation time (hours), V is the volume (m^3) of water treated, C_i and C_f are the initial and final concentrations of the target contaminant. The calculation was based on additional colour reduction after the initial AD step by UV treatment after 30 minutes irradiation. Wastewater samples were diluted as appropriate and the dilution factors were incorporated in equation (2). Energy ratio (β), which is the efficiency indicator of the integrated system, was calculated as:

$$\beta = \left[\frac{E_{bio}}{E_{UV}}\right] \times 100 \quad (3)$$

where E_{uv} is the UV lamp energy consumption (kWh/m^3) and E_{bio} is the bioenergy production (kWh/m^3). To evaluate the energy efficiency and the environmental impact of the integrated process, the electricity from the national grid that was saved as a result of the application of electricity from bioenergy was determined. The conversion of biomethane to electricity was estimated assuming application of a generator with an overall output efficiency of 78% of which 33% was electricity and 45% was heat, in a co-generation process (Moraes et al., 2015). Therefore, electricity generated from biomethane was given as;

$$El_{bio} = 0.33[E_{bio}] \quad (4)$$

where El_{bio} is the electricity generated from biomethane per unit effluent volume (kWh/m^3) and E_{bio} is the total bioenergy from the anaerobic digestion (kWh/m^3_{feed}). The energy consumption of the centrifugal pump in the AD system was approximated as (Bagheri & Mohseni, 2015).

$$E_p = \frac{Q_c \rho h g}{\omega} \quad (5)$$

where Ep is pump power (W), Q_c is the flow rate of the recycle stream (m^3/s), ρ is fluid density (kg/m^3), g is the gravitational acceleration (m/s^2), h is the head (m) and ω is the pump efficiency which was assumed to be 0.6 (Bagheri & Mohseni, 2015). The carbon dioxide emission (CE) when electricity from national grid was applied to power the UV lamp of the photoreactor was calculated as a product of electricity requirement of the UV lamp (kWh/m^3) and the base line grid emission factor of 0.957 kg CO_2equivalent/kWh of electricity used (Spalding-Fecher, 2011). The carbon dioxide emission reduction (CER) when electricity from biomethane was presumably used to power the UV lamp as an alternative energy source, replacing that from national grid, was calculated as;

$$CER = GEF \times El_{bio} \quad (6)$$

where CER is the carbon dioxide emission reduction (kg CO_2e/m^3_{feed}), GEF is the grid emission factor (0.957 kg CO_2e/kWh) and El_{bio} is the electricity generated from biomethane (kWh/m^3_{feed}) and presumably applied to power the UV lamp.

6.2.3 Experimental design and modelling

In order to analyse the interaction between HRT_{AD} and OLR_{AD} regarding energy production of AD process and energy utilization by the UV lamp in the photodegradation post-treatment process, Design expert software (version 6.0.6) was used. In the software, response surface methodology (RSM) using 3-level factorial experimental design with four centre points was applied. Different OLR_{AD} values were obtained by varying feed concentrations by diluting the raw distillery effluent as appropriate at fixed feed flow rates over the ranges of OLR_{AD} and HRT_{AD} studied, ensuring that OLR_{AD} and HRT_{AD} were independent variables (Zinatizadeh et al., 2010). For instance, at HRT of 6 days the feed concentrations were varied as 2 g/L, 10 g/L and 19 g/L to obtain OLR of about 0.3, 1.7 and 3 kg COD/m^3d respectively, at a fixed feed flow rate of 1 L/d; this procedure was repeated for other HRTs studied according to equation (7) and the ranges of the variables studied are shown in Table 6-1.

$$OLR = \frac{S.Q}{V} \quad (7)$$

where S is the feed concentration kg/m^3, Q is the feed flow rate m^3/d and V is the reactor volume (m^3).

Table 6-1: Experimental range and level of variables.

		Range and variables		
Parameters	code	-1	0	1
OLR (kg COD/m^3d)	A	0.3	1.7	3
HRT (days)	B	6	13	20

In the RSM study, the responses were bioenergy production by the AD process, UV lamp energy consumption of the photodegradation process, and energy ratio of the two processes. In each case the data obtained was used to develop a mathematical model that best correlates HRT_{AD} and OLR_{AD} to the various responses in the form of quadratic polynomial equation:

$$Y = b_o + \sum_{i=1}^{k} b_i x_i + \sum_{i=1}^{k} b_{ii} x_i^2 + \sum_{i=1}^{k} \sum_{j>1}^{k} b_{ij} x_i x_j \quad (8)$$

where Y is the response, b_o is the offset term, b_i is the linear effect, b_{ii} is the quadratic effect and b_{ij} is the interaction effect.

6.2.4 Data analysis

The response data was analysed using the Design expert software and the fitting of the models was determined based on analysis of variance (ANOVA). Parameters such as F-value, probability > F and adequate precision, which is a measure of error or the signal to noise ratio, were used as the indicators of how the quadratic models fit the experimental values. A probability >F value less than 0.05 indicates that the model term is significant while an adequate precision value of ≥ 4 is desired.

6.2.5 Experimental analysis

The total organic carbon was analysed using a TOC analyser (TELEDYNE Tekmar) while biogas was analysed using a gas chromatograph (Trace 1310 gas chromatograph) fitted with a thermal conductivity detector using helium as carrier gas. Colour was analysed using UV-Vis spectrophotometer (T80 + UV/VIS Spectrophotometer, PG instruments Ltd) at 475 nm. The BOD and COD were analysed according to standard procedure (APHA 1998), in which COD was analysed using closed reflux method where potassium dichromate solution was used as oxidant and Nanocolor colorimeter was used for the colour analysis. Alkalinity was analysed according to the standard method for wastewater analysis involving titrating samples against 0.02N H_2SO_4 solution using methyl orange indicator (Wilson, 2013).

6.3 Results and discussion

6.3.1 Characteristics of distillery effluent.

Distillery effluent is considered as fairly biodegradable with traces of recalcitrant compounds such as melanoidins (Acharya et al., 2008). The biodegradability of the distillery effluent was measured by determining the BOD_5/COD ratio (Table 6-2) and it was found to be 0.41 indicating that the distillery effluent is biodegradable. Good biodegradability is achieved when BOD_5/COD is greater than 0.25-0.4 (Sankaran et al., 2014; Al-Momani et al., 2002). However, the biorecalcitrant part of distillery effluent which is majorly melanoidins (which form a small proportion) often pass through anaerobic treatment without being degraded and they impart a dark colour to biomethanated effluent (Satyawali & Balakrishnan, 2008; Kalavathi et al., 2001).

Table 6-2: Characteristics of distillery wastewater.

Parameter	Mean value
Chemical oxygen demand (mg/l)	68062 ±320
Total organic carbon (mg/l)	45175 ±147
Biochemical oxygen demand (mg/l)	28066±237
BOD_5/COD	0.412±0.002
Total sulphates (mg/l)	7525±78
Total phosphates (mg/l)	1009±59
pH	5.45±0.35

6.3.2 Determination of the recalcitrant component of distillery effluent

The amount of non-biodegradable component can be determined by the relationship between the organics remaining after digestion and HRT. Anaerobic digestion was carried out at various HRTs in the AFBR at constant feed concentration and the recalcitrant component was determined from data in Table 6-3.

Table 6-3: Anaerobic digestion at different HRT and constant feed concentration.

HRT	COD_{feed}	$COD_{effluent}$	Ln ($COD_{effluent}$)
3	5810	1415	7.25
6	5810	1120	7.02
10	5810	980	6.88
15	5810	871	6.76
20	5810	760	6.63

It is proposed that a plot of Ln ($COD_{effluent}$) against 1/HRT gives a straight line, and the recalcitrant component is calculated at infinite HRT. A similar model has been applied in the determination of biodegradable component of some food waste wastewater (Rincón et al., 2006; Borja et al., 2002). In Figure 6-1 the amount of non-biodegradable component was calculated as COD equivalent at y-axis intercept when HRT is infinite. It was found that the non-biodegradable COD was about 756 mg/l constituting ~ 13% of the feed and corresponding to a TOC of 477 mg/l under the prevailing digestion conditions. The low value suggests that distillery effluent was fairly biodegradable.

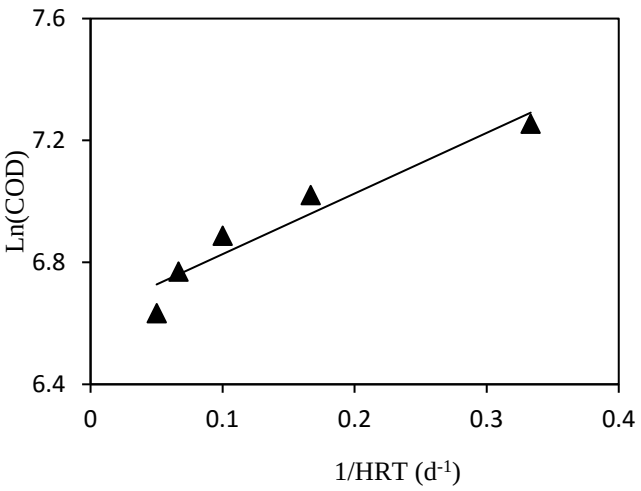

Figure 6-1: Determination of recalcitrant component of distillery effluent.

Kalavathi et al. (2001) reported that melanoidins constitute about 2% of distillery effluent with the rest being majorly biodegradable organic compounds. Removal of melanoidins from distillery effluent can be achieved by applying photodegradation.

6.3.3 Performance of the continuously operated fluidised bed anaerobic bioreactor

The stability of the bioreactor at various OLRs was studied at a fixed HRT of 6 days. In Figure 6-2 the reactor was stable up to an OLR of 6 kg COD/m^3d as shown by the VFA/alkalinity ratio of below 0.3 (Hampannavar & Shivayogimath, 2010). Under stable conditions, the COD and colour reductions were 86-73% and 56-40%, respectively. This was an indication that the anaerobic process has good efficiency in COD reduction but is not efficient in colour reduction due to the presence of melanoidins. However, at high OLR acidogenesis takes place faster than methanogenesis leading to the accumulation of VFAs which results in reduction in performance as indicated by low COD and colour reduction as well as low methane production.

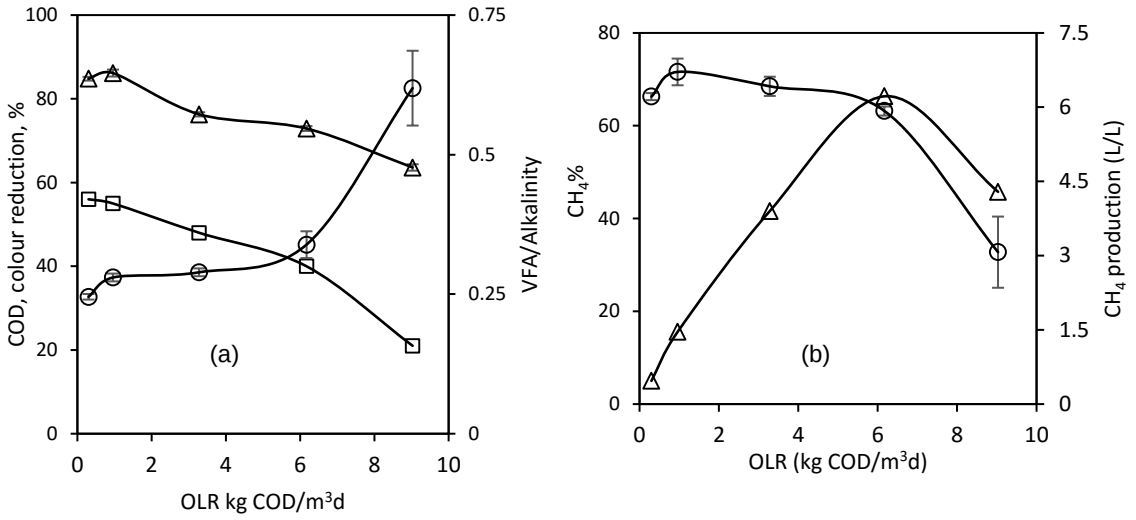

Figure 6-2: Effect of OLR on anaerobic digestion, (a) colour (□), COD (Δ), VFA/alkalinity (○); (b) methane production (Δ), methane proportion of the biogas (○).

The effect of HRT on the performance of the reactor at a fixed OLR of 3 kg COD/m^3d showed that an increase in HRT led to a corresponding increase in COD and colour reduction as well as an increase in methane production (Figure 6-3). This is due to sufficient contact time between the microbes and the substrate at high HRT compared to that at low HRT.

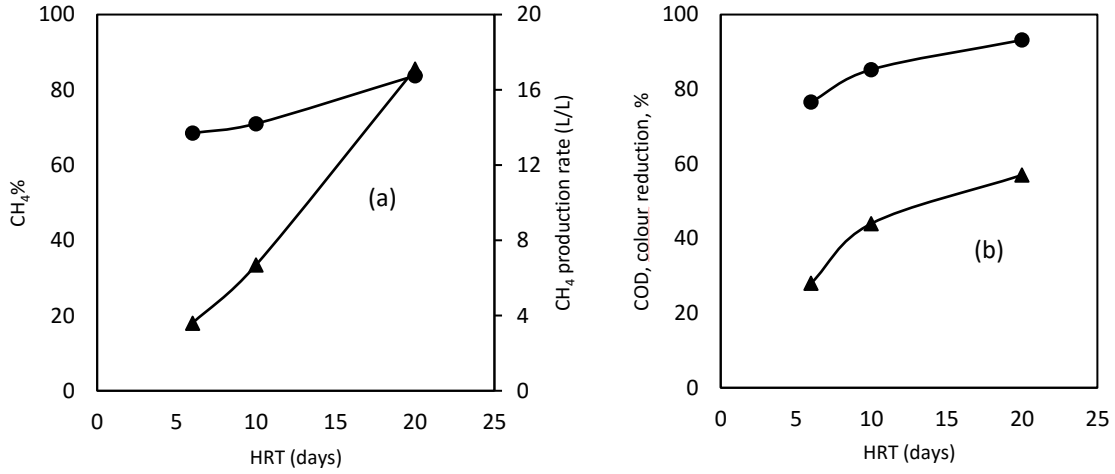

Figure 6-3: Effect of HRT on the AD process (a) CH_4 proportion of the biogas (●), CH_4 production (▲); (b) COD reduction (●) and colour reduction (▲).

The substantial increase in colour reduction with an increase in HRT could be an indication that melanoidins need a long degradation time. The increase in methane production per unit feed volume with an increase in HRT at fixed OLR is due to an increase in feed concentration at low flow rates.

6.3.4 Effects of biodigester parameters on the UV post-treatment

The AD effluent characteristic is very important when considering the design of a post-treatment process. This is due to the fact that it affects the performance of the post-treatment facility as it determines the reaction kinetics, energy requirement and the overall size of the post-treatment facility required to handle the discharge. Figure 4a shows the effects of applied AD OLR (OLR_{AD}) on the subsequent UV photodegradation process at a constant HRT_{AD} of 6 days. Generally, the photodegradation process was more efficient in colour reduction than TOC reduction for all the OLR_{AD} studied. This is contrary to AD treatment which had higher organic load reduction but low colour reduction, therefore integration of these two processes is necessary as they complement each other.

It was further established that (Figure 6-4a) the efficiency of the photodegradation process reduced with an increase in OLR_{AD} applied in the preceding AD process. This was due to the fact that at high OLR_{AD} the AD effluent had a higher concentration and more intense colour than at low OLR. This led to light attenuation in the preceding photodegradation process.

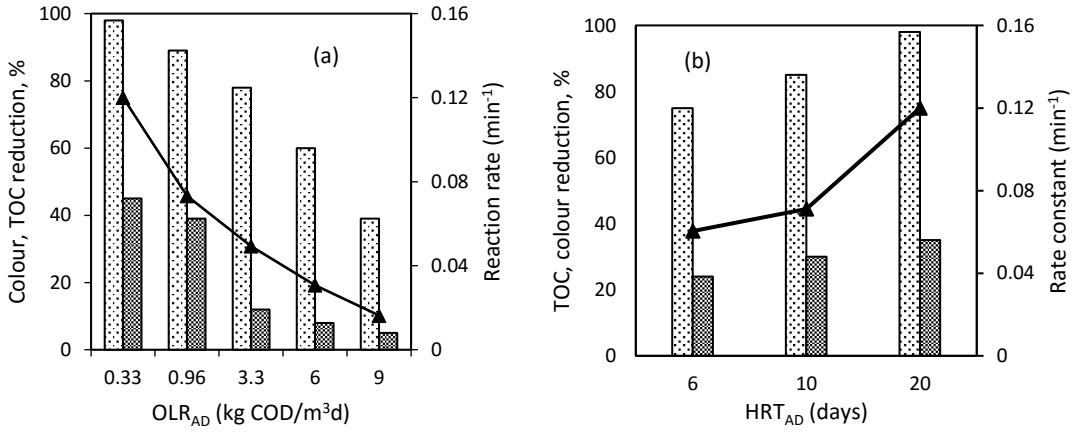

Figure 6-4: Effect of biodigester operating parameters on photodegradation post-treatment (a) OLR_{AD} and (b) HRT_{AD}, Colour (▒), TOC (▓), reaction constant (▲).

When the OLR_{AD} was fixed at 3 kg COD/m^3d while the HRT_{AD} was varied from 6 to 20 days (Figure 6-4b), it was found that the photodegradation efficiency increased with an increase in applied HRT_{AD} from 75% to 98% colour removal. This was due to the fact that the longer time the wastewater spent in the AD reactor, the more the biodegradable organic pollutants were removed due to sufficient contact time between pollutants and micro-organisms. Moreover, AD effluent had a more intense colour at low HRT_{AD} than at high HRT_{AD}. Overall performance of

the integrated process is shown in Table 6-4 where photodegradation post-treatment complemented the AD process in colour removal.

Table 6-4: Overall efficiency of the integrated process at various HRT_{AD} at fixed OLR_{AD} of 3 kg COD/m^3d.

	Initial removal by AD, %		Additional removal by UV, %		combined process, %	
HRT(d)	Colour	TOC	Colour	TOC	Colour	TOC
6	28	81	54	4.5	74	84.5
10	44	90.4	48	3	92	93.4
20	57	95.7	42	1.4	99	99

6.3.5 Kinetics of the integrated process

Both the AD and photodegradation were found to follow the first order rate model. Therefore, the first order rate model was used to study the effect of AD rate on the rate of the ensueing photodegradation process at various OLR_{AD}. In Figure 6-5 the rate of substrate utilization in the AD process increased with an increase in OLR. However, the rate of the succeeding photodegradation process decreased with an increase in OLR_{AD}.

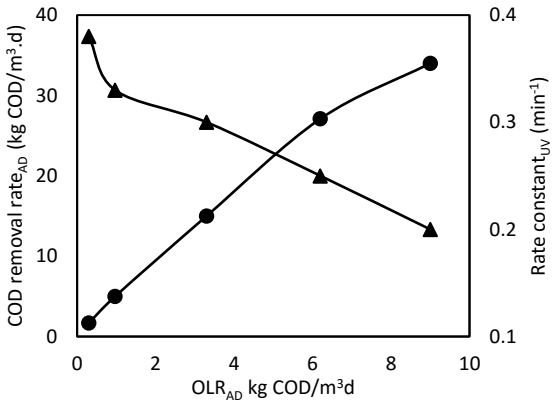

Figure 6-5: Organic removal rate by the AD process (●) and reaction rate constant of photodegradation post-treatment (▲) at various OLR_{AD}.

The observed increase in organic removal rate (AD rate) with increasing OLR_{AD} in AD could be attributed to a corresponding increase in the concentration gradient between the fluid and biofilm due to an increase in available feed (Fernández et al., 2008). It could also be attributed to the stability of the anaerobic fluidised bed reactor owed to immobilization of micro-organisms to small fluidised zeolite particles (Borja et al., 2004). In contrast, the reduction in photodegradation rate with an increase in OLR_{AD} could be attributed to light attenuation caused by high colour intensity when the system was operated at high OLR_{AD}. The performance of the

photodegradation post-treatment process increased with an increase in the colour and COD removal efficiency in the initial AD step but reduced with an increase in substrate utilization rate (Figure 6-2 and Figure 6-5). At high OLR_{AD} the substrate utilization is high due to the available feed and the effluent has a higher colour intensity than that at low HRT_{AD}.

6.3.6 Energy production of AD and energy demand of UV lamp

The photodegradation process is energy intensive majorly due to the energy demand of the UV lamp while the AD process produces energy in the form of methane. The effect of OLR_{AD} at a fixed HRT_{AD} of 6 days showed that the energy demand of the UV lamp always increased with an increase in OLR_{AD} due to increasing AD effluent concentration. In the case of AD, the energy production was maximum at OLR_{AD} of 6 kg COD/m^3d, after which it dropped due to inhibition caused by accumulation of VFAs as a result of organic overloading (Figure 6-6a). The energy ratio of the integrated process (β) was highest between OLR of 3 and 6 kg COD/m^3d. The low efficiency at OLR_{AD} of 9 kg COD/m^3d was due to both low bioenergy production due to organic overloading and high effluent load with intense colour which hindered photodegradation.

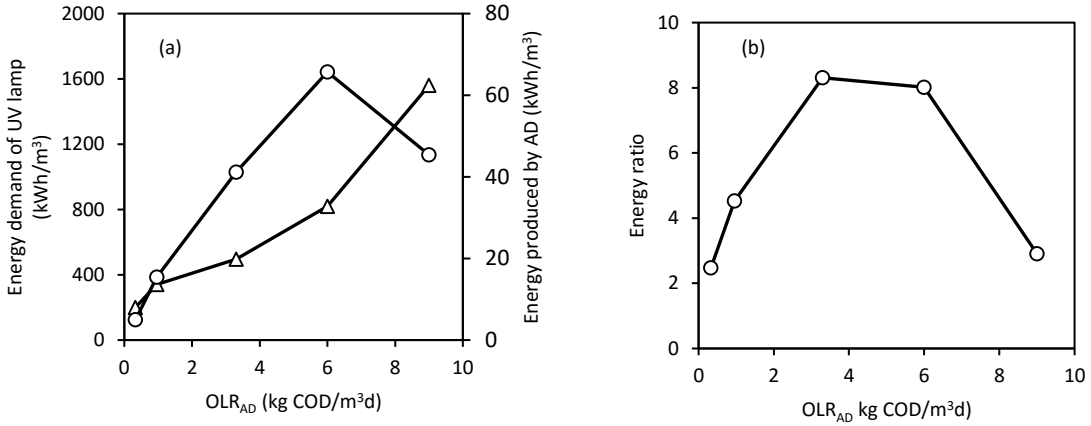

Figure 6-6: Effect of OLR_{AD} on the energy efficiency of the integrated process, (a), (○) Bioenergy production, (Δ) UV lamp energy consumption and (b) Energy ratio.

To increase the efficiency of the integrated process, the HRT_{AD} was increased stepwise from 6 to 20 days at constant OLR_{AD} of 3 kg COD/m^3d. The OLR_{AD} of 3 kg COD/m^3d was chosen due to the fact that it had good organic removal efficiency for both the processes and best energy ratio was attained at this OLR. In Figure 6-7 it was found that increasing the HRT_{AD} from 6 to 20 days at constant OLR_{AD} of 3 kg COD/m^3d increased the energy efficiency from ~ 9% to 93%. There were two combined factors which led to the high increase in efficiency with an increase in HRT_{AD}. In the first place, high HRT in the AD unit led to high degradation of

biodegradable constituents as well as better colour reduction resulting in a relatively easy to photodegrade effluent due to low concentration or colour intensity thus leading to lower E_{UV} than at low HRT_{AD}. Secondly, to achieve high HRT_{AD} at constant OLR_{AD} a feed with high concentration was fed into the digester at very low flow rate. This led to high methane production per unit feed volume than at low HRT_{AD} where relatively low concentrated feed was applied at high flow rate. However, increasing the HRT_{AD} may lead to an increase in the cost of operating the AD unit which may compromise the overall efficiency of the integrated process (this is discussed in section 6.3.11 and 6.3.12 which deals with cost analysis)

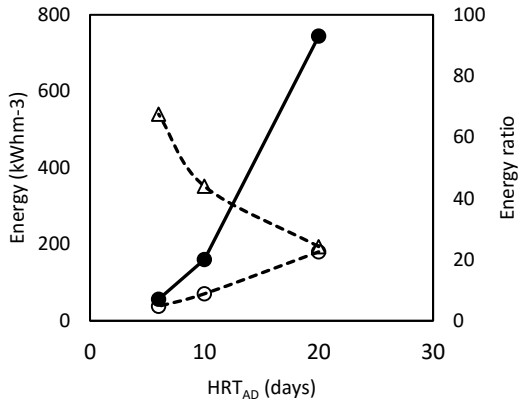

Figure 6-7 Effect of HRT_{AD} on energy efficiency of the integrated process, (○) Bioenergy production, (Δ) UV lamp energy consumption and (●) Energy ratio.

Generally, operating a bioreactor at an appropriately high OLR_{AD} (which the bioreactor can handle without shock) and high HRT_{AD} means high biogas production per unit feed volume and low effluent volume with less concentration compared to operating at the same OLR_{AD} but at low HRT_{AD} (Zinatizadeh et al., 2010). This can easily or effectively be handled by the UV post-treatment. However, this study could not investigate HRT_{AD} of beyond 20 days at OLR_{AD} of 3 kg COD/m^3d due to limitations in available feed concentration and reactor size.

6.3.7 Response surface methodology and ANOVA

According to the experimental design a total of 13 experimental runs were conducted including 4 centre points (Run 10-13) as indicated in Table 6-5. The responses of the centre points showed little variation indicating the consistency of the experimental runs. In all experimental conditions studied, biogas production ranged from 0.714 to 20.6 L/L_{feed} corresponding to bioenergy production in the range of 4.96 to 180.5 kWh/m^3 while the energy consumption of the UV lamp ranged from 93 to 496 kWh/m^3 corresponding to overall efficiencies of between 2.5 to 93% as shown in Table 6-5.

Table 6-5: Experiments conducted according to design and the corresponding responses.

Experiment	OLR (xi)	HRT (xii)	Biogas (L/L_{feed})	CH_4%	E_{bio}	E_{UV}	β%
1	0.3	6	0.714	66	4.96	200	2.5
2	1.65	6	3.1	74	24.3	135	18
3	3	6	5.7	68.5	38	496	7.6
4	0.3	13	1.85	75	14.5	105	13.8
5	1.65	13	5.08	74	40.1	115	34.8
6	3	13	9.4	71	70.6	352	20
7	0.3	20	1.93	73.5	14.7	87	16.9
8	1.65	20	10.1	71	76	100	76
9	3	20	20.6	83.7	180.5	194	93
10	1.65	13	5.08	74	40.1	119	33.7
11	1.65	13	5.1	73.8	40	115	34.8
12	1.65	13	5.12	73.5	40	115	34.8
13	1.65	13	5.08	74	40.1	110	36.4

Based on the probability > F values, the summary of ANOVA for various polynomial models relating the variables to the responses (Table 6-6) indicates that a two factor interaction model (2FI) described the interaction of OLR_{AD} (A) and HRT_{AD} (B) in bioenergy production while a quadratic model described UV lamp energy requirement and the energy efficiency.

Table 6-6: ANOVA for response surface models.

Response	Polynomial model	Source	Sum of squares	DF	Mean square	F value	Prob > F	Adeq. precision
Bioenergy	2 FI	Model	23510.75	3	7836.92	177.4	< 0.0001	44.25
		A	13088.46	1	13088.46	296.28	< 0.0001	
		B	7715.97	1	7715.97	174.67	< 0.0001	
		AB	4962.38	1	4962.38	112.33	< 0.0001	
		Residual	397.58	9	44.18			
UV lamp energy	Quadratic	Model	1.65E+05	5	32962.17	22.67	0.0003	16.23
		A	60122.16	1	60122.16	41.36	0.0004	
		B	33750	1	33750	23.22	0.0019	
		A^2	40681.72	1	40681.72	27.98	0.0011	
		B^2	4601.6	1	4601.6	3.17	0.1184	
		AB	9612.48	1	9612.48	6.61	0.0369	
		Residual	10176.25	7	1453.75			
E_{bio}/E_{UV} (β, %)	Quadratic	Model	7948.3	5	1589.66	69.41	< 0.0001	27.89
		A	1746.88	1	1746.88	76.28	< 0.0001	
		B	4144.88	1	4144.88	180.99	< 0.0001	
		A^2	895.37	1	895.37	39.1	0.0004	
		B^2	1.76	1	1.76	0.077	0.7898	
		AB	1543.44	1	1543.44	67.4	< 0.0001	
		Residual	160.31	7	22.9			

All the variables and their linear interactions were significant in the proposed models except the quadratic term of the HRT_{AD} (B) as indicated by probability > F value greater than 0.05. A significant interaction between OLR_{AD} and HRT_{AD} means that the effect of each of the variables depends on the value of the other variable. Adequate precision for all the models was greater than 4 suggesting high signal, hence the models can be used to navigate the design space.

6.3.8 Energy production by the anaerobic process

By applying multiple regression analysis, the bioenergy production was correlated to the operating parameters as described by equation (8). The predictive two factor interaction (2FI) model correlating bioenergy production to the applied OLR_{AD} and HRT_{AD} in the reactor in terms of coded values, is presented as:

$$E_{bio} = 55.90 + 47.37A + 34.21B + 34.19AB \quad (9)$$

The coefficients of all the model factors positively contributed to the model equation and the most influential parameter was OLR_{AD} (A) as it had the highest coefficient and F-value (Salam et al., 2015). Validation of the model was done by plotting the predicted values against the experimental values (Figure 6-8a) and R^2 value of 0.9778 was obtained, implying that the model accurately describes the effect of OLR_{AD} and HRT_{AD} in the digestion process.

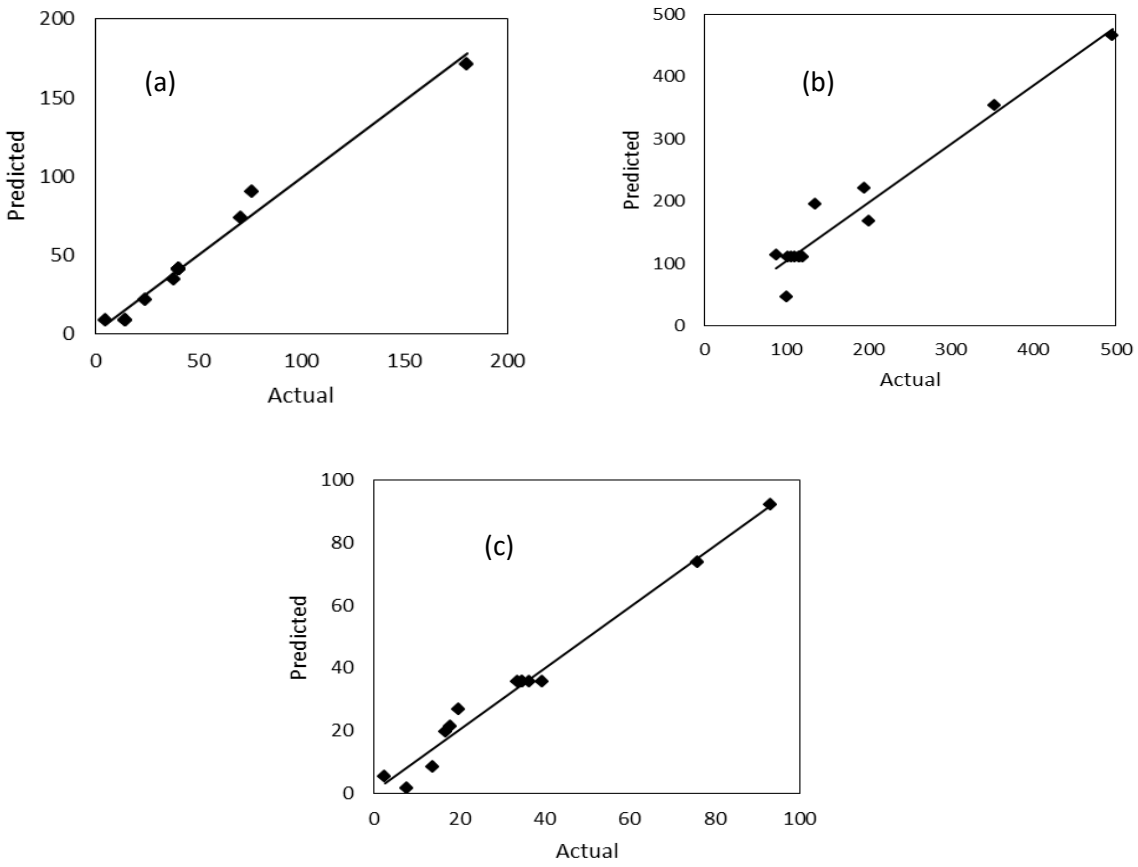

Figure 6-8: A plot of the predicted values from the models against the experimental values, (a) energy production by the anaerobic process, (b) UV photodegradation energy consumption and (c) Energy ratio.

Response surface plot depicting the effects of OLR_{AD} and HRT_{AD} on bioenergy production is shown in Figure 6-9a. The plots show that at low HRT_{AD} of 6 days the bioenergy production did not increase significantly with an increase in OLR_{AD}. Likewise, at low OLR 0.3 kg COD/m^3d the bioenergy production did not significantly increase with an increase in HRT_{AD}. However, at higher HRT_{AD} values there was a massive increase in bioenergy production with an increase in OLR_{AD}. Similarly, at higher OLR_{AD}, there was improved bioenergy production with an increase in HRT_{AD}.

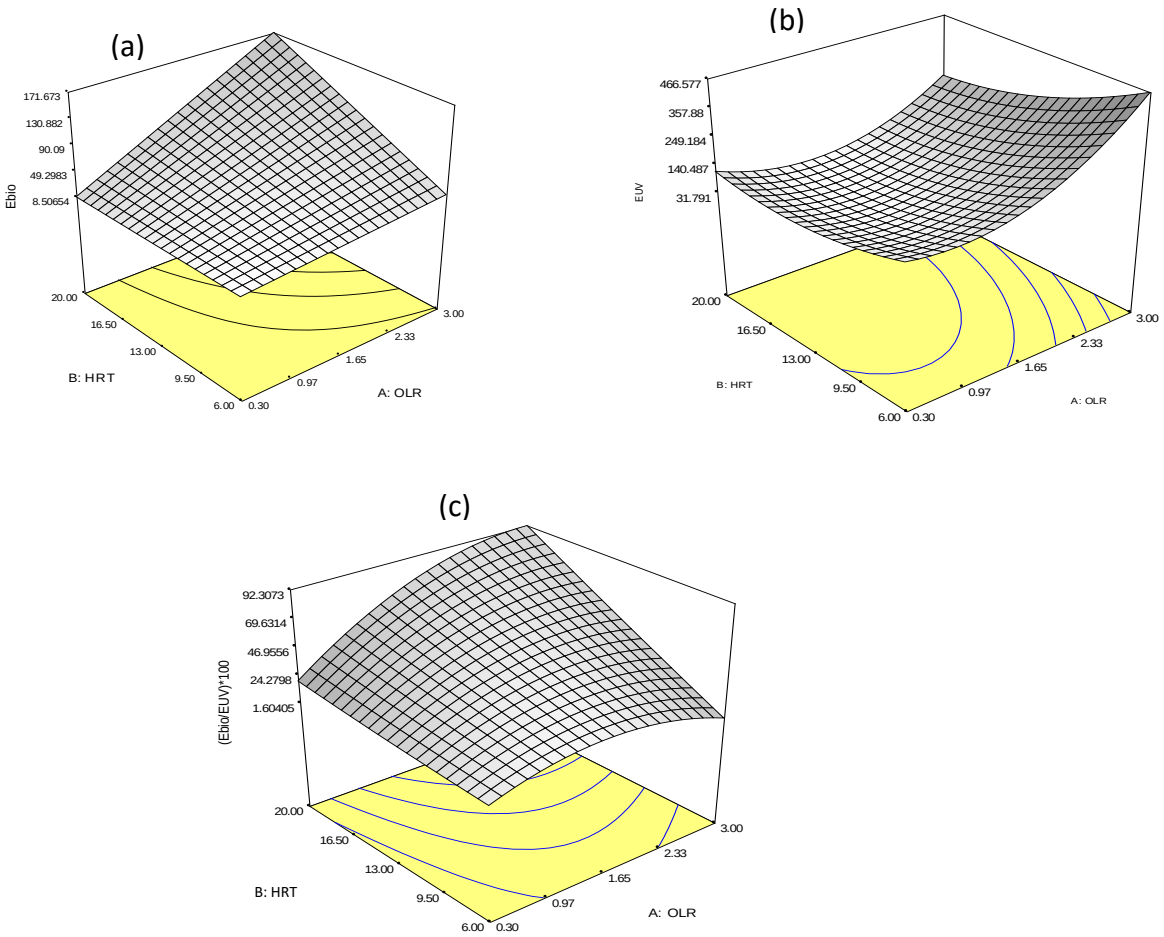

Figure 6-9: Response surface plot indicating the effects of OLR_{AD} and HRT_{AD} on (a) bioenergy production, (b) UV lamp energy consumption and (c) energy efficiency.

This was due to the fact that when OLR_{AD} was kept constant at high values (without shock loading) and operated at high HRT_{AD}, the reactor was able to handle effluent with higher concentration leading to higher biogas production per unit effluent volume than if operated at low OLR_{AD} or low HRT_{AD}. Moreover, at low HRT_{AD} the reactor experienced a lot of microbial washout. A similar trend has been reported for biogas production during anaerobic treatment of various industrial wastewater (Rastegar et al., 2011). The slight reduction in bioenergy production when HRT_{AD} was reduced at high and fixed OLR_{AD} could be attributed to the development of non-methanogens at these conditions (Zinatizadeh et al., 2010). The increased trend in bioenergy production with an increase in OLR_{AD} at fixed HRT_{AD} showed that the rate of substrate conversion to biogas increased with an increase in OLR_{AD} and this could be attributed to an increase in microbial community, due to an increase in available feed, which leads to reactor stability even at high OLR_{AD} in the range studied (Rastegar et al., 2011).

Alternatively, the observed increase in organic conversion rate to biogas with an increase in feed concentration could be attributed to the stability of the anaerobic fluidised bed reactor owed to immobilization of micro-organisms to small fluidised particles (Borja et al., 2004).

6.3.9 UV photodegradation energy consumption

The analysis of the interaction between the applied OLR_{AD} and HRT_{AD} in the bioreactor and the energy utilised by the UV lamp in photodegradation post-treatment was described by:

$$E_{UV} = 69.02 + 101.54A - 75.00B + 121.37A^2 + 52.07B^2 - 47.59AB \quad (10)$$

From the model the quadratic term of the OLR_{AD} had the strongest effect on the energy consumption of the photodegradation process as indicated by its high coefficient while the linear interaction between the OLR_{AD} and HRT_{AD} had the least effect as indicated by its low coefficient. Further, the linear term of OLR_{AD} and the quadratic terms of both OLR_{AD} and HRT_{AD} were additive to the response while the linear term of HRT_{AD} and the interaction between the two variables had a reducing effect to the response. The model depicts a convex shaped plot attributed to by the quadratic effect of OLR_{AD} (A) since the quadratic effect of HRT_{AD} (B) was not significant as shown by the ANOVA (Table 6-6). The quadratic model was validated by plotting predicted values against experimental values (Figure 6-8b); a straight line with R^2 value of 0.9418 was obtained indicating that the model accurately described the dependence of E_{UV} on OLR_{AD} and HRT_{AD}.

It is shown in Figure 6-9b that, generally, the energy required by the UV lamp for photodegradation post-treatment increased with an increase in OLR_{AD} at various $HRTs_{AD}$ studied. This was due to the fact that the AD effluent concentration increased with an increase in OLR_{AD} applied as depicted in Figure 6-2 (Wang & Wu, 2004) leading to high energy requirement for photodegradation post-treatment. At low OLR_{AD} (0.3 kg COD/m^3d) an increase in HRT_{AD} did not significantly affect the energy requirement due to low AD effluent concentration at low OLR_{AD}.

However, at high OLR_{AD} (3 kg COD/m^3d) there was a significant reduction in energy required with an increase in HRT_{AD} from 6 to 20 days due to low AD effluent concentration at high HRT_{AD} (Zinatizadeh et al., 2010). Generally, high HRT_{AD} ensures longer contact time between microbes and pollutants, leading to effective removal of biodegradable constituents. Thus the discharged AD effluent does not contain a lot of biodegradable constituents that could compete with the biorecalcitrant constituents during photodegradation process leading to high

efficiency. Moreover, operating an AD reactor at high HRT at fixed OLR_{AD} leads to more colour reduction due to the increased contact time between the reactants. Therefore, an AD effluent with low colour intensity can be degraded faster compared to an effluent with high colour intensity which causes light attenuation during photodegradation.

6.3.10 Energy ratio

A quadratic model in terms of coded factor which describes the relationship between overall energy efficiency of the integrated system and the variables was expressed as:

$$\beta = 46.64 + 17.31A + 26.28B - 18.01A^2 + 1.02B^2 + 19.07AB \quad (11).$$

This model suggests that the dependence of the response on the variables is described by a concave like curvature attributed to by the quadratic term of OLR_{AD} (A). The quadratic term of HRT_{AD} (B) did not considerably contribute to the curvature since it was not significant as shown in Table 6-6. A plot of the predicted values against the experimental values using the model is shown in Figure 6-8c where distribution of the data points along a line with a unit slope indicates the validity of the model.

In Figure 6-9c, at low HRT_{AD} (6 days), the energy ratio increased with an increase in OLR_{AD} up to an OLR_{AD} of 1.65 kg COD/m^3d, and then it reduced as OLR_{AD} was further increased to 3 kg COD/m^3d. This trend was partly due to the fact that at lower OLR_{AD} of 0.3 kg COD/m^3d the bioenergy production was low as compared to that at higher OLR_{AD} of 1.65 kg COD/m^3d (Rastegar et al., 2011) leading to a low energy ratio. At the same time, at high OLR_{AD} of 3 kg COD/m^3d, the colour intensity of the AD effluent was higher than that at OLR_{AD} of 1.65 kg COD/m^3d, therefore higher energy was required for photodegradation resulting in a decreased energy ratio. Due to these two pulling factors, best energy efficiency at low HRT_{AD} was attainable mid-way between low and high $OLRs_{AD}$, which was at 1.65 kg COD/m^3d. At high HRT (20 days) the energy efficiency increased with an increase in OLR_{AD} majorly due to an increase in bioenergy production per unit volume with an increase in OLR_{AD}. In a similar study of anaerobic digestion of wastewater, higher methane production per unit feed flow rate was recorded at high OLR_{AD} and high HRT_{AD} than at low OLR_{AD} and low HRT (Zinatizadeh et al., 2010). Moreover, high HRT_{AD} at high OLR_{AD} leads to more digestion efficiency therefore eliminating most biodegradable constituents that would otherwise compete with the recalcitrant component during photodegradation post-treatment.

An increase in HRT_{AD} at low OLR_{AD} did not significantly improve the energy efficiency. This was due to the fact that at low OLR_{AD} bioenergy production per unit feed volume was usually low irrespective of the HRT_{AD} applied under this study. Operating bioreactor at low OLR_{AD} and high HRT_{AD} is considered uneconomical since low organic load could be degraded within a short time. It therefore follows that there was no substantial difference in photodegradation energy requirement for effluent discharged by bioreactor operating at low OLR_{AD} at either low or high HRT_{AD} as shown in Figure 6-9b. In fact, operating a bioreactor at high HRT_{AD} and low OLR_{AD} can lead to cell death due to starvation.

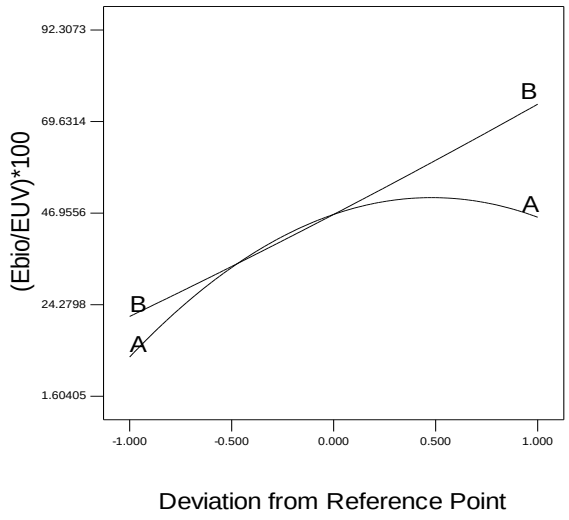

Figure 6-10: Perturbation plot for energy efficiency.

Perturbation, which indicates the deviation of the energy efficiency from the reference point caused by the variables, is shown in Figure 6-10. The reference point considered was at OLR of 1.7 kg COD/m^3d and HRT_{AD} of 13 days, which is the mid-point. Holding one factor constant at the mid-point while varying the other helps to compare the effect of the variables at a particular point. In Fig. 6, at the reference point, an increase in HRT_{AD} (B) led to an increase in energy efficiency. Similarly, an increase in OLR_{AD} led to an increase in efficiency up to a point where further increase in OLR_{AD} did not increase the efficiency. From the perturbation plot it could also be seen that the effect of OLR_{AD} was concave-like due to its significant quadratic term, in contrast, the effect of HRT_{AD} was linear due to its insignificant quadratic term (Table 6-6).

6.3.11 Electrical energy and carbon dioxide emission reduction analysis

The environmental sustainability of the integrated process was evaluated on the basis of the electrical energy generation from the bioemethane produced by the AD process and carbon dioxide emission reduction (CER) associated with the application of the generated electrical energy in the ensueing photodegradation process. The conditions for this study were OLR_{AD} of 3 kg COD/m^3d and HRT_{AD} of 6-20 days. The fixed OLR_{AD} of 3 kg COD/m^3d was chosen since it was the highest OLR_{AD} at which the bioreactor was still stable with a good performance. Assumed biomethane conversion efficiency of 45% to heat and 33% to electricity in a co-generation process was considered (Moraes et al., 2015). To estimate the CER, a base line emission factor, when electricity from national grid was applied, of 0.957 kg CO_2 equivalent/kWh of electricity generated was applied (Spalding-Fecher, 2011). The CER achieved by applying the electricity generated from the bioemethane was compared to the carbon emission (CE) when electricity from the grid was applied to power the UV lamp in the photodegradation post-treatment (Figure 6-11).

In Figure 6-11a and b, the electricity consumption of the photoreactor components (UV lamp and compressor), and the CE reduced with an increase in HRT_{AD} while the energy generation and the CER increased with an increase in HRT_{AD}. This was due to the fact that at low HRT_{AD} the effluent discharged by the AD process had a higher concentration or colour intensity than that at high HRT_{AD} and therefore demanded more electrical energy to drive the UV lamp for the photodegradation post-treatment. Moreover, there was low biogas production per unit feed volume at low HRT_{AD} compared to that at high HRT_{AD} leading to low electricity generation. In Figure 6-11a it was also found that the UV lamp was the most energy consuming component of the photoreactor as it constituted 80% of electricity requirement while the compressor used for mixing constituted the remaining 20%.

In Figure 6-11b the bioenergy application as electricity source for UV lamp led to CER of 57 kg CO_2e/m^3_{feed} corresponding to a 31% CER compared to the case when electricity from the grid was applied. The CER could go up to 134.7 CO_2e/m^3_{feed} or 72.5% if the heat produced was used for other activities in the process such as heating the digester. Yasar et al. (2015) applied a base line emission factor of 0.4829 kg CO_2/kWh and obtained a CER of about 55 kg CO_2e/m^3 when energy generated from anaerobic treatment of distillery effluent in an industrial scale was applied in the economy. Apart from the difference in the applied baseline emission factor, which varies significantly with regions (Spalding-Fecher, 2011), the CER values obtained by Yasar et al. (2015) were close to those of this study.

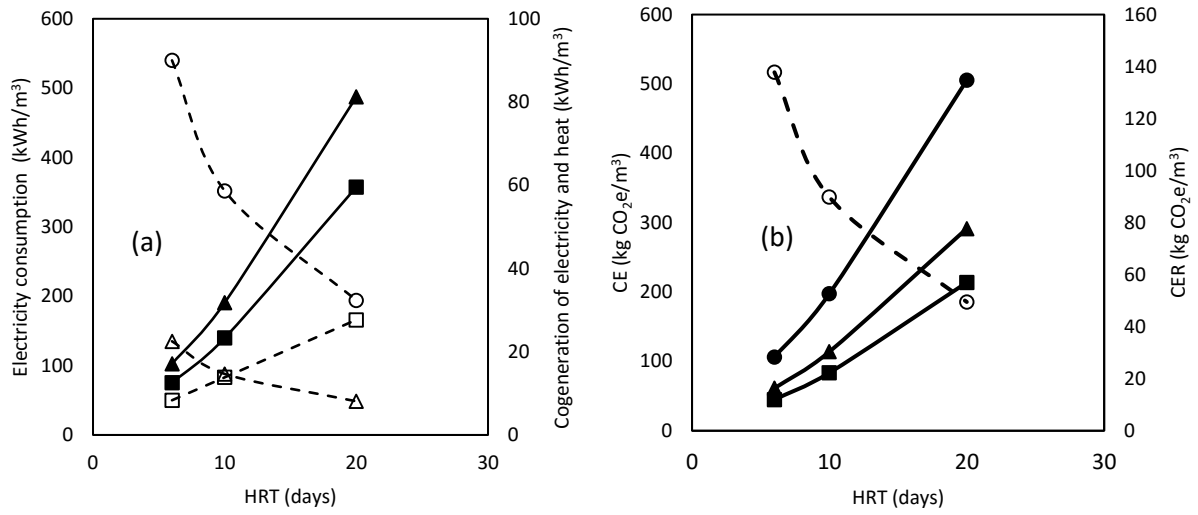

Figure 6-11: (a) Electricity consumption of: UV lamp (○), compressor used for mixing in the photoreactor (Δ), pump for the AD process (□); Electricity (■) and heat (▲) generated from biogas. (b) Carbon dioxide emission due to the electricity consumption by the UV lamp (○) and carbon dioxide emission reduction when biomethane was presumably applied as electricity source (■), as heat (▲) and a combination of electricity and heat (●).

It was observed, in Figure 6-11a, that increasing HRT_{AD} led to a reduction in electricity requirement of the photoreactor; in contrast, it led to an increase in electricity demand of the bioreactor. Economic analysis was used to investigate cost reduction by application of renewable energy in the integrated system at various HRT_{AD}.

6.3.12 Cost analysis of application of renewable energy in photodegradation

The possible cost reduction due to the application of electricity from biomethane to drive various components of the photoreactor was analysed by applying cost of electricity unit of 0.08 USD/kWh (Yasar et al., 2015). In Figure 6-12 the operation cost due to electrical consumption of the photoreactor components reduced with an increase in HRT_{AD} due to a reduction in colour intensity of the AD effluent with an increase in HRT_{AD}. However, the cost of operating the AD reactor increased with increased HRT_{AD} due to long digestion time. Considering the electricity requirement of the UV lamp (which is the major electric component of the photoreactor) and that of the AD unit, it could be considered that it was more economical to operate the integrated process at high HRT_{AD} than at low HRT_{AD} in this study. This is due to the fact that, although, increasing HRT_{AD} from 6 days to 20 days led to an increase in operational cost of the AD process, the increase was only 9 USD/m^3 compared to a reduction of 28 USD/m^3 for UV lamp operation cost when HRT_{AD} was increased from 6 days to 20 days. Besides, at high HRT_{AD} there was a better colour and TOC reduction than at low HRT_{AD}.

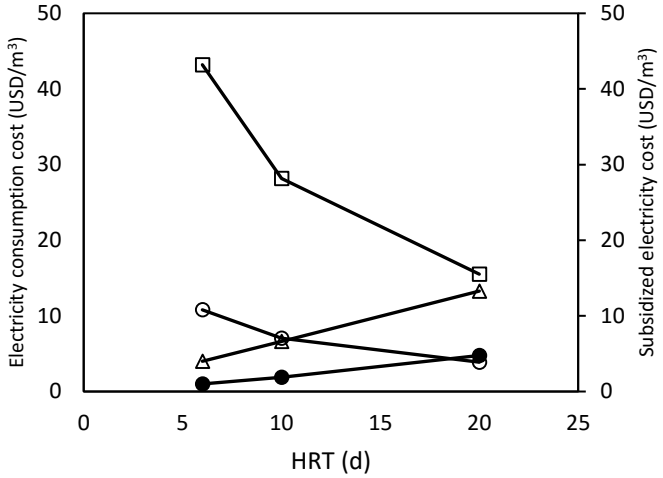

Figure 6-12: Electricity consumption cost of operating the photoreactor, UV lamp (□) compressor (Δ), electricity consumption for bioreactor (Δ) and the electricity cost subsidized by the application of bioenergy (●).

The possible cost subsidized by renewable energy applied in photodegradation could be 31% for the UV lamp at HRT_{AD} of 20 days while it was as low as 2% for low HRT_{AD} of 6 days. The low value at low HRT_{AD} was due to low bioenergy production coupled with a discharge of high colour intensity from the bioreactor which hindered photodegradation post-treatment. Generally, the electricity from biomethane could subsidize up to 24% of the total electricity cost for the photodegradation unit which corresponds to a cost reduction of USD 4.7/$m^3_{effluent}$. Further analysis showed that the electricity from the bioenergy can subsidize up to 12% of the global cost of operating an integrated AD – UV process. Fuess & Garcia (2015) reported a cost reduction of 5-15% when energy from distillery effluent is utilized in the distillation process.

Conclusion

The pollution removal and energy efficiency of an integrated anaerobic digestion (AD) and photodegradation treatment process for distillery effluent was studied. The interaction between the organic loading rate and hydraulic retention of the initial AD step on the efficiency of the combined process was modelled using response surface methodology (RSM). Kinetic analysis of the integrated system showed that high substrate utilization rate in the initial AD step was not additive to the rate of photodegradation post-treatment. However, substrate removal efficiency was a more significant indicator, as compared to substrate utilization rate, in predicting the performance of the post-treatment unit. The integrated process was found to be efficient in energy utilization as the renewable energy from the AD could supply up to 31% of

the electricity requirement of the UV lamp in the photodegradation process, leading to an operational cost reduction of USD 4.8/m^3 $_{effluent}$. As a result, the process led to environmental conservation as the carbon dioxide emission reduction when electricity from bioenergy was used to power the UV lamp, was 28.8 kg CO_2e/m^3. This led to reduction in carbon dioxide emission by 30% compared to when electricity from the grid was used to power the UV lamp. Therefore, the integrated process is suitable for the treatment of distillery effluent.

References

ACHARYA, B.K., MOHANA, S. & MADAMWAR, D. (2008). Anaerobic treatment of distillery spent wash - a study on upflow anaerobic fixed film bioreactor. *Bioresour. Technol.* 99. p.4621–6.

AL-MOMANI, F., TOURAUD, E., DEGORCE-DUMAS, J.., ROUSSY, J. & THOMAS, O. (2002). Biodegradability enhancement of textile dyes and textile wastewater by VUV photolysis. *J. Photochem. Photobiol. A Chem*. 153. p.191–197.

BAGHERI, M. & MOHSENI, M. (2015). Impact of hydrodynamics on pollutant degradation and energy efficiency of VUV/UV and H2O2/UV oxidation processes. *J. Environ. Manage.* 164. p.114–20.

BORJA, R., GONZALEZ, E., RAPOSO, F., MILLAN, F. & MARTIN, a. (2002). Kinetic analysis of the psychrophilic anaerobic digestion of wastewater derived from the production of proteins from extracted sunflower flour. *J Agric Food Chem*. 50. p.4628–4633.

BORJA, R., RINCÓN, B., RAPOSO, F., DOMÍNGUEZ, J.R., MILLÁN, F. & MARTÍN, A. (2004). Mesophilic anaerobic digestion in a fluidised-bed reactor of wastewater from the production of protein isolates from chickpea flour. *Process Biochem*. 39. p.1913–1921.

CHAUDHARI, P.K., MISHRA, I.M. & CHAND, S. (2007). Decolourization and removal of chemical oxygen demand (COD) with energy recovery: Treatment of biodigester effluent of a molasses-based alcohol distillery using inorganic coagulants. *Colloids Surfaces A Physicochem. Eng. Asp*. 296. p.238–247.

CHEN, Z.-B., CUI, M.-H., REN, N.-Q., CHEN, Z.-Q., WANG, H.-C. & NIE, S.-K. (2011). Improving the simultaneous removal efficiency of COD and color in a combined HABMR-CFASR system based MPDW. Part 1: optimization of operational parameters for HABMR by using response surface methodology. *Bioresour. Technol*. 102. p.8839–47.

DUERR, M., GAIR, S., CRUDEN, A. & MCDONALD, J. (2007). Hydrogen and electrical energy from organic waste treatment. *Int. J. Hydrogen Energy.* 32. p.705–709.

FERNÁNDEZ, N., MONTALVO, S., BORJA, R., GUERRERO, L., SÁNCHEZ, E., CORTÉS, I., COLMENAREJO, M.F., TRAVIESO, L. & RAPOSO, F. (2008). Performance evaluation of an anaerobic fluidized bed reactor with natural zeolite as support material when treating high-strength distillery wastewater. *Renew. Energy*. 33. p.2458–2466.

FUESS, L.T. & GARCIA, M.L. (2015). Bioenergy from stillage anaerobic digestion to enhance the energy balance ratio of ethanol production. *J. Environ. Manage*. 162. p.102–14.

HAMPANNAVAR, U. & SHIVAYOGIMATH, C. (2010). Anaerobic treatment of sugar industry wastewater by Upflow anaerobic. *Int. J. Environ. Sci*. 1. p.631–639.

KALAVATHI, D., UMA, L. & SUBRAMANIAN, G. (2001). Degradation and metabolization of the pigment—melanoidin in distillery effluent by the marine cyanobacterium *Oscillatoria boryana* BDU 92181. *Enzyme Microb. Technol*. 29. p.246–251.

MORAES, B.S., JUNQUEIRA, T.L., PAVANELLO, L.G., CAVALETT, O., MANTELATTO, P.E., BONOMI, A. & ZAIAT, M. (2014). Anaerobic digestion of vinasse from sugarcane biorefineries in Brazil from energy, environmental, and economic perspectives: Profit or expense? . 113. p.825–835.

MORAES, B.S., ZAIAT, M. & BONOMI, A. (2015). Anaerobic digestion of vinasse from sugarcane ethanol production in Brazil: Challenges and perspectives. Renew. Sustain. *Energy Rev*. 44. p.888–903.

OLLER, I., MALATO, S. & SÁNCHEZ-PÉREZ, J.A. (2011). Combination of Advanced Oxidation Processes and biological treatments for wastewater decontamination--a review. *Sci. Total Environ*. 409. p.4141–66.

RASTEGAR, S.O., MOUSAVI, S.M., SHOJAOSADATI, S.A. & SHEIBANI, S. (2011). Optimization of petroleum refinery effluent treatment in a UASB reactor using response surface methodology. *J. Hazard. Mater*. 197. p.26–32.

RINCÓN, B., RAPOSO, F., DOMÍNGUEZ, J.R., MILLÁN, F., JIMÉNEZ, A. M., MARTÍN, A. & BORJA, R. (2006). Kinetic models of an anaerobic bioreactor for restoring wastewater generated by industrial chickpea protein production. *Int. Biodeterior. Biodegrad.* 57. p.114–120.

SALAM, K.K., AGARRY, S.E., ARINKOOLA, A.O. & SHOREMEKUN, I.O. (2015). Optimization of Operating Conditions Affecting Microbiologically Influenced Corrosion of Mild Steel Exposed to Crude Oil Environments Using Response Surface Methodology. 7. p.68–78.

SANKARAN, K., PREMALATHA, M., VIJAYASEKARAN, M. & SOMASUNDARAM, V.T. (2014). DEPHY project: Distillery wastewater treatment through anaerobic digestion and phycoremediation - A green industrial approach. Renew. Sustain. *Energy Rev*. 37. p.634–643.

SATYAWALI, Y. & BALAKRISHNAN, M. (2008). Wastewater treatment in molasses-based alcohol distilleries for COD and color removal: a review. *J. Environ. Manage*. 86. p.481–97.

SHU, Z., BOLTON, J.R., BELOSEVIC, M. & EL DIN, M.G. (2013). Photodegradation of emerging micropollutants using the medium-pressure UV/H2O2 Advanced Oxidation Process. *Water Res*. 47. p.2881–9.

SPALDING-FECHER, R. (2011). What is the carbon emission factor for the South African electricity grid ? *J. Energy South Africa*. 22. p.8–12.

WANG, J.-L. & WU, L.-B. (2004). Wastewater treatment in a hybrid biological reactor (HBR): nitrification characteristics. *Biomed. Environ. Sci*. 17. p.373–379.

WILSON, P.C. (2013). Water Quality Notes : Alkalinity and Hardness 1 Ecological / Management. Univ. Florida, IFAS Ext. 1–6.

YASAR, A., AHMAD, N., CHAUDHRY, M.N., REHMAN, M.S.U. & KHAN, a. a a. (2007). Ozone for color and COD removal of raw and anaerobically biotreated combined industrial wastewater. *Polish J. Environ. Stud*. 16. p.289–294.

YASAR, A., AHMAD, N. & KHAN. (2006). Energy requirement of ultraviolet and AOPs for the post-treatment of treated combined industrial effluent. *Color. Technol*. 122. p.201–206.

YASAR, A., ALI, A., TABINDA, A.B. & TAHIR, A. (2015). Waste to energy analysis of shakarganj sugar mills; biogas production from the spent wash for electricity generation. *Renew. Sustain. Energy Rev*. 43. p.126–132.

ZINATIZADEH, A.A.L., PIRSAHEB, M., BONAKDARI, H. & YOUNESI, H. (2010). Response surface analysis of effects of hydraulic retention time and influent feed concentration on performance of an UASFF bioreactor. *Waste Manag*. 30. p.1798–1807.

Chapter 7

7 Conclusions and recommendation

7.1 Conclusion

The review of the available literature showed that there was a need for integrating anaerobic digestion (AD) with an appropriate treatment technique to remove both biodegradable and biorecalcitrant components of distillery effluent. This study found that it was efficient to integrate AD with UV photodegradation, as AD converted the biodegradable components, which formed about 90% of distillery effluent, into biomethane while photodegradation removed the colour-causing biorecalcitrant components which are majorly melanoidins. The study designed an integrated AD-UV treatment system consisting of both a fluidised bed anaerobic reactor and fluidised bed photoreactor. The aim of the study was to achieve effective pollution reduction at a reduced operational cost by estimating the cost reduction when electricity from biomethane, produced by the AD process, was used to operate the energy intensive UV photoreactor.

The optimal hydrodynamic conditions for the digester and the photoreactor were determined using an optical attenuation technique based on particle and gas distribution in the respective reactors. Best particle distribution in the bioreactor was found to be at superficial liquid velocity of between 0.6 cm/s and 0.75 cm/s. The radial bubble distribution in the photoreactor was found to vary with superficial gas velocity (U_g) and the reactor aspect ratio. The bubble trajectory was found to be spiral or zig-zag in nature attributed to large bubble size, which was ranging between 6 and 11 mm in diameter depending on the applied U_g. The optimal gas hold up and solid hold up for the photoreactor was found to be 0.077 and 0.003, respectively.

Kinetic analysis was applied to evaluate the stability and the performance of the fluidized bed anaerobic reactor at various (hydraulic retention time) HRT and (organic load rate) OLR. The degradation followed first order kinetics and fitted the Michaelis-Menten kinetic model for substrate utilization. The kinetic analysis further showed that about 10% of the TOC was non-biodegradable. It was then established that the non-biodegradable component was responsible for the dark-brown colour of the distillery effluent since anaerobic digestion resulted in low colour reduction but high TOC reduction. Therefore, there was a need to employ a post-treatment technology for the removal of the melanoidins. Further, it was found that biomass yield was 0.4658 g/g while endogenic micro-organisms' decay coefficient was 0.0293 which suggested that there was a need to install a sludge handling unit prior to the photodegradation post-treatment. This was due to fact that the suspended solid (sludge) could hamper the

efficiency of photodegradation due to increased light attenuation. The mean cell residence time (MCRT) or the sludge retention time (SRT) was found to be at least 2.5 times the HRT which indicated that the zeolite that was applied in the reactor led to effective separation between HRT and SRT, since zeolite retained the micro-organisms in the reactor.

A study on combined anaerobic digestion and photodegradation treatment of distillery effluent in batch fluidised bed reactors showed that anaerobic digestion as a single unit was efficient in TOC reduction but was ineffective in colour reduction while photodegradation was efficient in colour reduction but was less effective in TOC reduction. Thus, photodegradation post-treatment was effective for colour removal in anaerobically treated effluent. During photodegradation, nitrate (NO_3^-) and ammonium (NH_4^+) were formed indicating the degradation of the biorecalcitrant coloured melanoidins. This confirmed mineralization of nitrogen heteroatom within the melanoidin structure which when bonded to carbon, forms a chromophore. Subsequently, the degradation of carbon – nitrogen bond led to colour reduction through the breaking down of the chromophores.

The interaction between HRT_{AD} and OLR_{AD} of the initial AD step on the overall performance of the integrated process was modelled using response surface methodology (RSM). It was more efficient to operate the system at both high OLR_{AD} and HRT_{AD} since high OLR_{AD} led to high bioenergy production while high HRT ensured that the AD process discharged effluent with low concentration to the photoreactor resulting in low energy utilization in the photoreactor. It was found that the initial biological step removed about 90% of TOC and only about 50% of the colour while photodegradation post-treatment removed 98% of the remaining colour. Energy demand of the UV lamp was lowest at low OLR_{AD} irrespective of HRT_{AD}, with values ranging between 87 and 496 kWh/m^3. The energy analysis further showed that the electricity requirement of the UV lamp in photodegradation was 80% of the total energy requirement of a fluidised bed photoreactor while mixing consumed 20% of electricity. The AD process produced 59 kWh/m^3 of electricity which could supplement the electricity demand of the UV lamp by 30% leading to operation cost reduction of about USD 4.8/m^3. The presumed carbon dioxide emission reduction (CER), when electricity from bioenergy was used to power the UV lamp, was 28.8 kg CO_2e/m^3. Thus, the combined process was effective in pollutant removal at a reduced energy cost.

7.2 Recommendations

Research on improving the performance of the integrated process by employing a photocatalyst with enhanced activity is recommended. A photocatalyst, with high quantum efficiency, which can degrade the melanoidins at a more reduced time than TiO_2/SiO_2 catalyst, could result in reduced energy requirement and thus reduce the operational cost further. Furthermore, application of robust techniques such as computational fluid dynamic modelling for reactor design and operation can be employed to optimize the reactor operating conditions and this can lead to an increased reaction rate resulting in a reduction in reactor size and operation cost.

The performance of the UV photodegradation post-treatment was highly affected by the turbidity of the digester effluent and the sludge discharged from the bioreactor. This was due to the fact that turbidity and sludge particles led to light attenuation in the photoreactor. To mitigate this ozonation process, which is not affected by turbidity, should be studied as an alternative to UV photocatalysis. Moreover, ozononation is reported to be capable of solubilizing sludge. This again can eliminate the application of the sludge filtration unit. Finally, application of solar energy to drive photodegradation in the integrated process should be investigated. It can lead to remarkably improved energy efficiency and substantial improvement on reduction in carbon dioxide emission.

Appendix

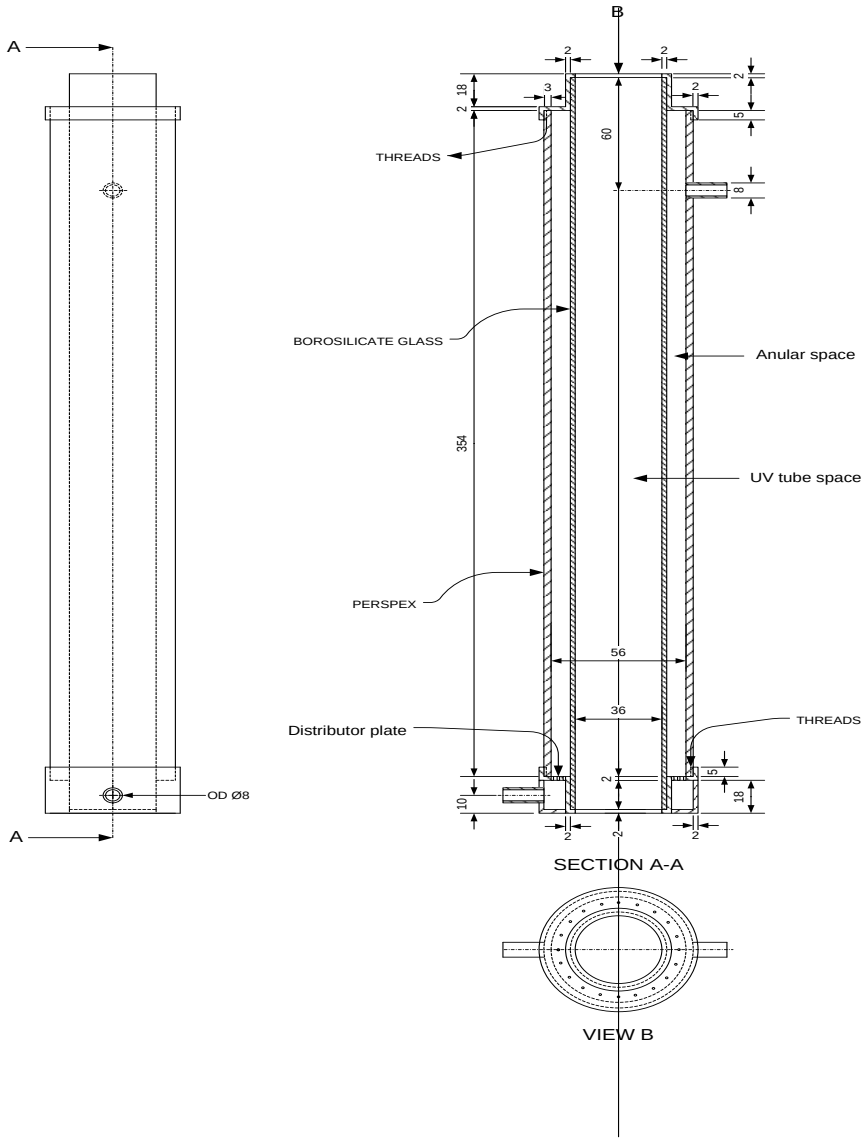

Figure A1: Photoreactor design.

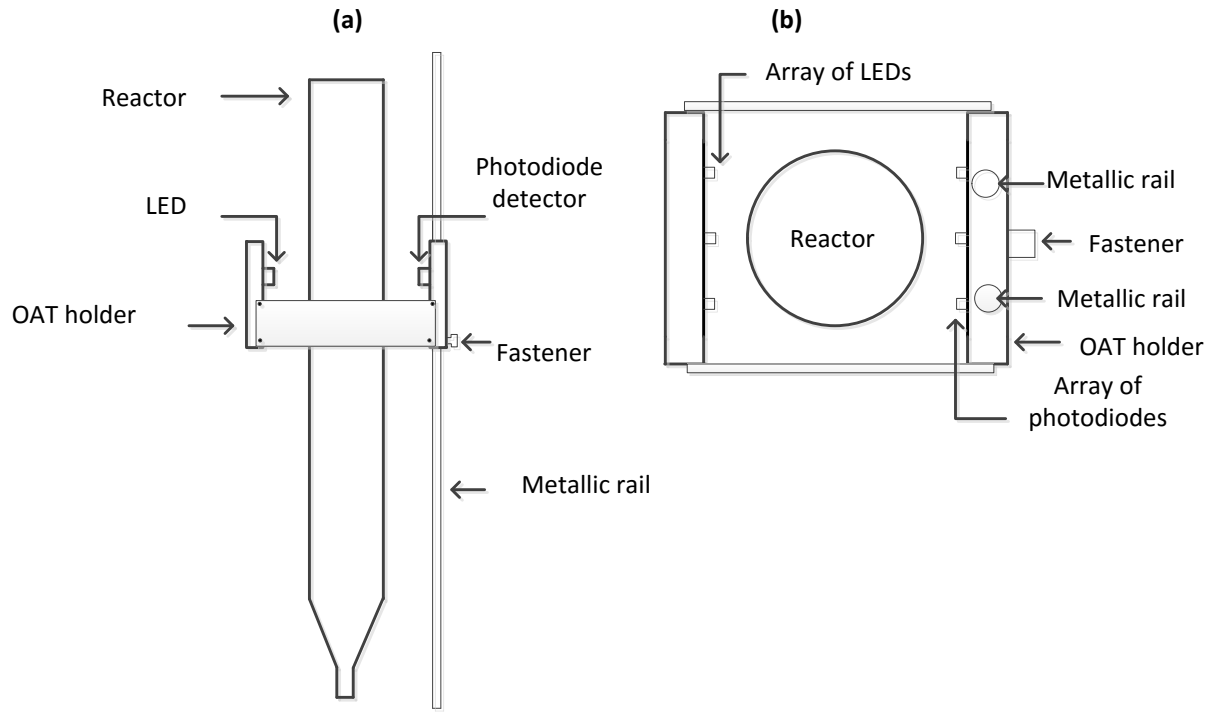

Figure A2: Reactor and OAT set up, (a) side view and (b) Top view.

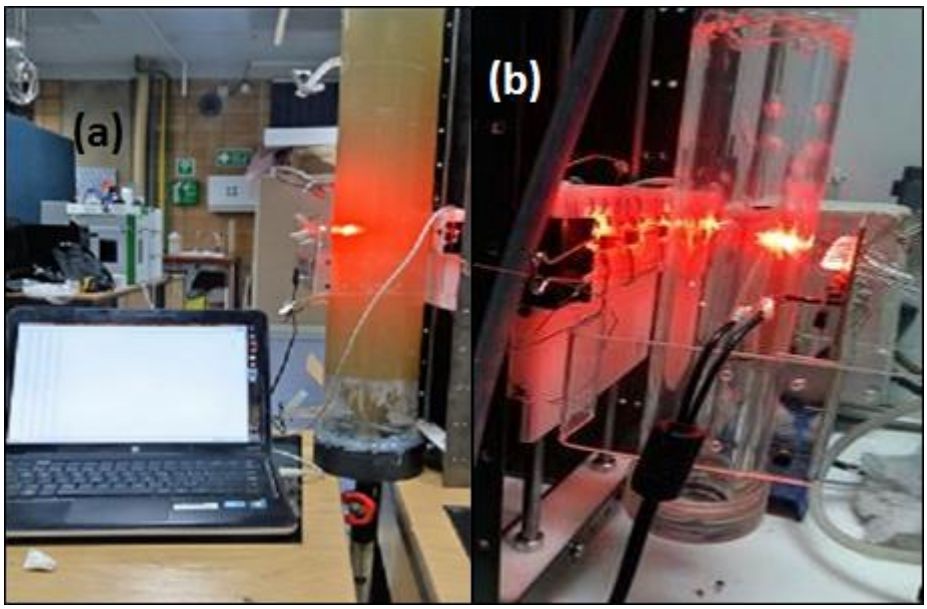

Figure A3: Picture of the reactor and OAT, (a) Bioreactor and (b) Photoreactor

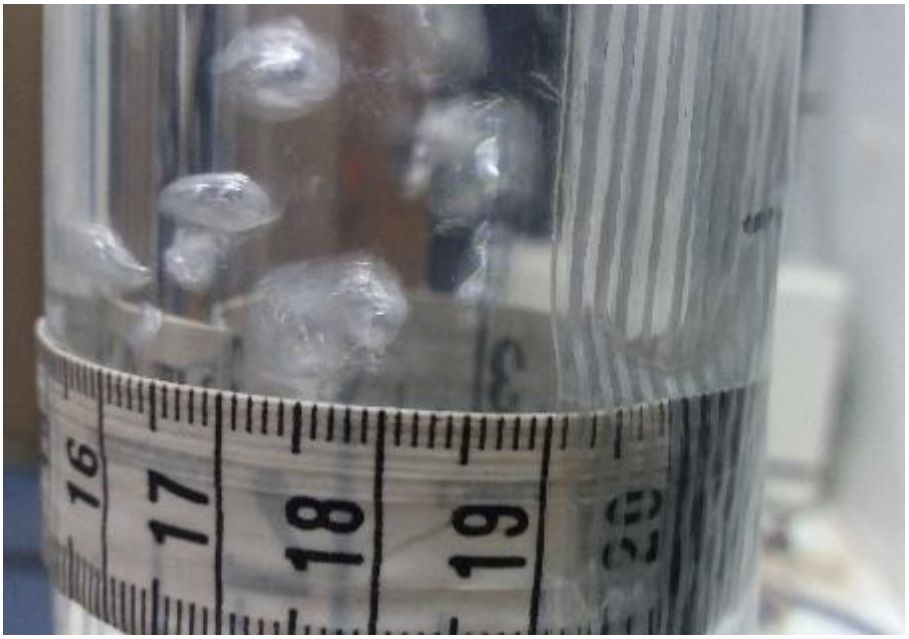

Figure A4: Bubble size estimation in the photoreactor.

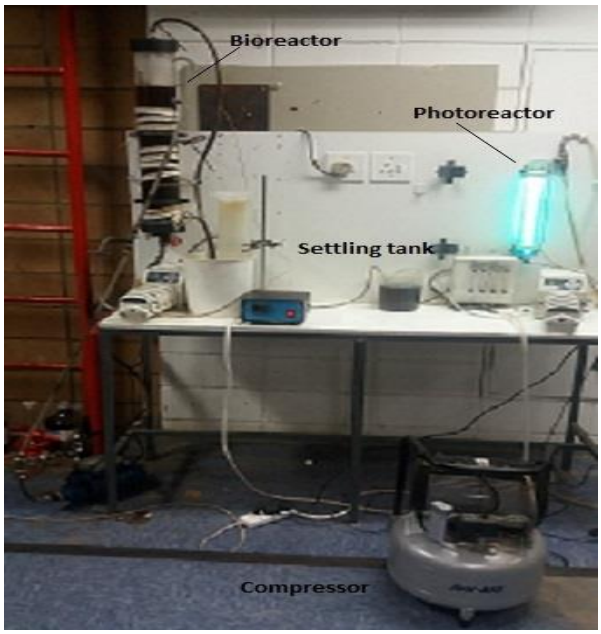

Figure A5: Integrated anaerobic digestion and photodegradation set-up.